國立臺灣大學生命科學院生化科學研究所

博士論文

Graduate Institute of Biochemical Sciences
College of Life Science
National Taiwan University

Doctoral Dissertation

酪氨酸磷酸水解酶 PTP52F 對於果蠅發育之重要性

Role of the midgut-enriched receptor protein tyrosine phosphatase PTP52F in *Drosophila melanogaster*

Abirami Santhanam

珊他那 阿逼拉米

指導教授：孟子青 博士與陳光超 博士

Advisors: Tzu-Ching Meng, Ph.D. and Guang-Chao Chen, Ph.D.

中華民國 101 年 7 月

July, 2012

Acknowledgements

I wish to express my gratitude first and foremost to my Mentor and advisor Dr.Tzu-Ching Meng, who enabled me to achieve my long time dream of getting a doctorate. Indeed it's my honor to be his student and his tutelage helped me to thrive in my PhD, and I am very thankful for his guidance. I would like thank him for all the support, patience, advices, confidence, friendship and freedom that he has provided me in these years. I have always admired the curiosity and cheerfulness in him to explore things. He definitely has inspired me and molded me in a right direction. I am amazed by his way of looking at all situations from the brightest side. His positive attitude has encouraged me a lot. Thank you also for the indirect instructions on how to prioritize in life. For this, I cannot thank him enough. I am forever grateful. Thank You!

I also wish to express my gratitude to my advisor Dr.Guang-Chao Chen who has always motivated me for the best. He always has driven me in right direction at times of trouble. I have learnt from him how to balance science and family life. Thank you very much for providing me such a great opportunity for learning.

Work would not have been as pleasant as now without the company of other members in our lab. Thank you very much for all your support. I am indeed thankful to you all for making our lab meeting presentations in English. I can understand the effort, practice and courage needed to do presentations in English, Thank you friends. Special thanks to you all for so many personal helps and special times with Siddharth.

Big thanks to all my friends outside the lab. You were the helping hands for us in many times of trouble. I can not forget our times of joy, happiness and sharing. I wish I can continue this friendship forever. I also wish that all my friends reap their harvests soon.

Very special thanks to Taiwan and its people. We loved this country because of this lovable and friendly people. Whenever we got a problem, many people helped voluntarily which reflected the attitude of the people. I have lot of good memories from Taiwan to cherish throughout my life time.

I am indeed grateful to my parents for their love, affection, patience and sacrifice. They are living for me and I am sure that they will be very proud for me now. I am the world for my father and mother and they live their life for me. I do not know how to thank them, Thank you mom and dad. I want to thank my beloved husband Mr.Rajasekaran who was always the support for me. The warmth under his shoulders has given me courage, support, love, affection and cheer. I may not be where I am without him. It is difficult to thank him for he is a part of me. Finally and importantly I would like to thank my darling son Siddharth whose smile always cheered me in times of my trouble. He is such a lovely and wonderful kid who loves me a lot no matter how little is the time I spend with him. Thank you dear. Also I wish to thank all my family for being a support to my parents.

I take this opportunity to express my gratitude to all whoever helped me to attain this degree. Last but not the least I want to thank the Almighty for guiding me in the right direction with right people around me.

ABSTRACT

In *Drosophila*, a number of cellular processes including proliferation and differentiation are regulated by protein tyrosine phosphatases (PTPs). However, to date the mechanisms by which PTPs regulate the developmental processes remain elusive especially in the case of receptor PTPs (RPTPs) which are involved in the regulation of axon guidance and synaptogenesis decisions in *Drosophila* embryos and larvae. To reveal the other potential functions we utilized systematic data mining approaches focusing on RPTP expression profiles during critical stages of development. This lead to the identification of a highly midgut enriched RPTP-the PTP52F especially in the larva-pupa transition during which the ecdysone action kicks in. Results from real-time PCR and cell based experiments confirmed RPTP52F as an ecdysone response gene. Genetic studies showed a critical role of PTP52F in midgut metamorphosis during larva pupa transition. Using a substrate-trapping strategy we identified, transitional endoplasmic reticulum ATPase94 (TER94), ortholog of human Valosin Containing Protein (VCP) as a bonafide substrate of PTP52F. Interestingly, tyrosine 800 of TER94 which is phosphorylated by Src kinase is targeted and dephosphorylated by PTP52F. We showed that PTP52F mediated dephosphorylation of TER94 could facilitate the ubiquitin mediated degradation of various proteins including *Drosophila* inhibitor of apoptosis1 (DIAP1) a key regulator controlling midgut cell death. In vivo evidences demonstrated that the forced expression of TER94 rescued the defect of midgut metamorphosis induced by knockdown of PTP52F, suggesting the importance of coordinated action between PTP52F and TER94. Our studies for the first time reveal a novel regulatory role of a RPTP that contributes to proper tissue organization of midgut formation in *Drosophila* metamorphosis.

Abbreviations

APF after pupa formation

BPF before pupa formation

ConA Concavalin A

DAPI 4,6-diamidino-2-phenylindole

DIAP1 *Drosophila* inhibitor of apoptosis protein-1

DN Dominant negative

EcR ecdysone receptor

ERAD endoplasmic reticulum associated degradation

GC gastric ceaca

IAM iodoacetamide

MG midgut

MS mass spectrometry

NGS Next Generation Sequencing

PF pupa formation

PNPP *p*-nitrophenyl phosphate

PTP Protein tyrosine phosphatase

RPTP Receptor protein tyrosine phosphatase

RT PCR reverse transcriptase polymerase chain reaction

SAP-1 Stomach cancer associated protein tyrosine phosphatase-1

TER94 Transistional endoplasmic reticulum 94

TUNEL Terminal deoxynucleotidyl transferase dUTP nick end labeling

VCP Valosin containing protein

TABLE OF CONTENTS

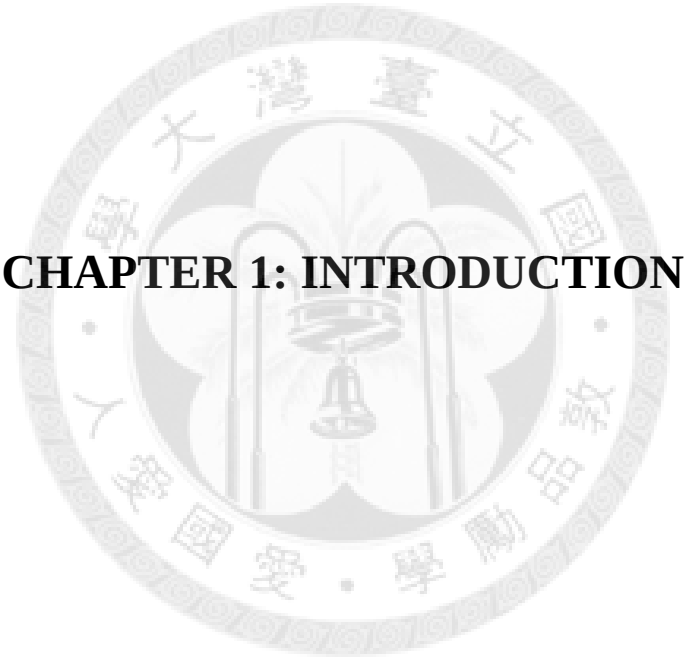

CHAPTER 1: INTRODUCTION

1.1 Protein tyrosine phosphatases

Reversible tyrosine phosphorylation is a very important post-translational modification. A diverse array of biological processes controlled by protein tyrosine phosphorylation and dephosphorylation in various metazoans are mediated by the coordinated action between protein tyrosine kinases (PTKs) and protein tyrosine phosphatases (PTPs) [1-3]. PTPs are encoded by the largest family of phosphatase genes. These enzymes are defined by the active-site signature motif HCX5R, in which the cysteine residue functions as a nucleophile and is essential for catalysis [4]. The classical PTPs include 21 transmembrane receptor like proteins (RPTPs) and 16 non transmembrane PTPs that have the potential to regulate signaling through ligand and substrate-controlled protein tyrosine dephosphorylation. Many of the RPTPs display features of cell-adhesion molecules in their extracellular segment and have been implicated in processes that involve cell–cell and cell–matrix contact. Of the 21 RPTPs in human, 12 possess a tandem arrangement of PTP domains in their intracellular segment. Most RPTPs contain two cytoplasmic catalytic domains, of which the membrane proximal domain D1 contains the majority of the activity while the membrane distal domain D2 exhibits little or no activity [5]. Nevertheless, the structural integrity of the D2 domain is important for the activity, specificity and stability of the RPTP as a whole [6]. Furthermore the D2 domain is important for protein–protein interactions that regulate RPTP dimerization [7]. The non-transmembrane PTPs are characterized by regulatory sequences that flank the catalytic domain and control activity either directly, by interactions at the active site that modulate activity, or by controlling substrate specificity (such as the interaction of PTP-PEST with p130cas [8] or STEP with the mitogen-activated protein kinase (MAPK) ERK17). These

non-catalytic sequences also control subcellular distribution, thereby indirectly regulating activity by restricting access to particular substrates at defined subcellular locations. The characterization of PTPs and their numerous substrates is of critical importance to our understanding of how the homeostasis of signal transduction is achieved. Over the last two decades, because of advances of biochemical, molecular and genetic approaches, the functions of many of the key players involved in this context, in particular PTKs, have been clarified [9, 10]. In contrast, our understanding of PTPs in the regulation of protein tyrosine phosphorylation-dependent signal transduction has lagged behind. Issues including substrate specificity as well as spatial and temporal control of cell signaling determined by PTPs remain elusive.

1.2 Substrate identification and functional characterization of PTPs

Since its development more than 15 years ago, the substrate trapping technique [11, 12] has been used to identify numerous bona fide and potential substrates of PTPs, significantly accelerating the biochemical characterization of these enzymes. The most fruitful method for finding substrates for both RPTPs and cytoplasmic PTPs has been the use of "substrate-trapping" mutants. The most effective substrate traps were devised by Tonks and coworkers, and are created by changing an invariant Asp (D) residue within the WPD loop to Ala (A) or by changing the invariable cysteine (C) in the signature motif to serine (S) [11]. This catalytic cysteine has an extremely low pK_a (4.5–5.5) and is unprotonated at intracellular pH. The unprotonated cysteine acts as a nucleophile, attacking the phosphorus center of the substrate, leading to a phosphoryl–cysteine intermediate (PTP–Cys–PO_3) and further release of the dephosphorylated substrate (S). Replacement of the catalytic site cysteine by a serine allows binding of the physiological

substrate to the mutant PTP but blocks the catalysis and a PTP– substrate intermediate is formed which leads to the stabilization of the enzyme–substrate interaction. The aspartate (D181 in PTP1B) in the invariant WPD loop serves at first as a general acid by protonating the leaving phenolic oxygen group from the substrate (P–O bond), whose event favors the expulsion of the dephosphorylated substrate from the catalytic site. The same aspartate is then postulated to serve as general base by reacting with a water molecule that will attack the Cys–PO_3intermediate, liberating free phosphate and regenerating the enzyme active. The D/A mutation acts as a substrate-trapping mutant first, because of the absence of its catalytic role and second, through the conformational change by flipping of the WPD loop that comes over the substrate and blocks it into the catalytic pocket, preventing its release. Mutation of the aspartate to alanine (D/A) also blocks the catalytic process and the PTP–D/A is almost completely catalytically inactive [12]. Substrate-trapping mutants expressed in cells often bind to a few phospho proteins, suggesting that PTPs exhibit high specificity in vivo [8].

Recently, studies have used specific PTP knockout mice to delineate their roles in developmental control and disease conditions. A few studies have clearly defined the critical role of some non-receptor PTPs, such as PTP1B in regulating insulin responsiveness [13, 14], leptin signaling [15-17] and breast tumorigenesis [18], T-Cell PTP (TC-PTP) in regulating T-cell signaling [19] as well as SHP-2, which participates in *H. Pylori*-induced gastric ulcer [20], Noonan syndrome [21] and LEOPARD syndrome [22, 23]. Genetic studies of other PTPs in mice, however, have encountered some difficulties, mostly due to the redundancy of multiple regulatory components in a given

signaling pathway. This problem was particularly prominent in the investigation of receptor PTPs (RPTPs). One such problem has been encountered in the genetic characterization for the functional role of R-PTPs belonging to the subtype R2A phosphatases [24]. Since the first knockout mouse model was generated, it has been suggested that PTP-sigma (PTP-σ) might participate in determining axon regeneration and extension [25]. However, detailed investigations found that the deletion of PTP-σ *per se* failed to produce an obvious phenotype during neuronal development [26], largely due to the functional compensation contributed by other R-PTPs in the same subtype. To date, it is clear that PTP-σ and PTP-delta (PTP-δ), both subtype R2A PTPs, compensate for each other in the control of neuronal development. Quantitative analyses have demonstrated that PTP-$\sigma^{+/-}$/PTP-$\delta^{-/-}$ and PTP-$\sigma^{-/-}$/PTP-$\delta^{+/-}$ mutants exhibit intermediate phenotypes in motoneuron survival and phrenic nerve branching, whereas no significant defect has been detected in either PTP-σ or PTP-δ single mutant [24]. These data suggest that more studies involving multiple knockouts in mice are needed to clarify the functional role of individual PTPs. Considering the complexity of functional compensation among mammalian PTPs, we proposed that other simpler model organisms might provide alternatives for genetically characterizing the PTPome.

1.3 *Drosophila* PTPome

Drosophila is an excellent model organism for investigating diverse tyrosine phosphorylation-dependent signaling pathways, which are regulated by many modulators exhibiting similar functions across species throughout evolution [27-29]. Its relatively simple genome allows the precise dissection of signaling networks without the genetic

redundancy-related complications often seen in mammalian genetic screenings [30-32]. Moreover, while there are a large number of classical PTPs in mammals (38 in humans), there are only fifteen putative *ptp* genes in the *Drosophila* genome (8 non-receptor PTPs and 7 R-PTPs). Several of the *Drosophila* PTPs have been classified as orthologs of human PTPs based on the similar sequence alignment between the two, suggesting evolutionarily conserved functions [33]. In fact, a number of early breakthroughs in functional characterizations of R-PTPs have been made in genetic studies of *Drosophila*, and all R-PTPs have been found to be involved in axon guidance during embryogenesis [34-37].

1.4 *Drosophila* RPTP and CNS development

Human RPTPs are classified into eight subfamilies based on their sequence and structural analysis including R1/6, R2a, R2b, R3, R4, R5, R7 and R8. Most RPTPs with the exception of R1 subfamily are implicated in regulation of neuronal adhesion and axon guidance during CNS development [38-40]. Redundancy and functional compensation of RPTPS hampered the characterization of specific functions of individual RPTPs. *Drosophila* RPTPs share homology with human RPTPs and their reduced complexity opened the gate for analysis of RPTPs involved in CNS development in a much faster way. To date six RPTPS have been identified and studied in *Drosophila* and they belong to the R2a and R3 subfamily [35]. In fact the first clue for the involvement of R2a subfamily members in CNS development was made from the exclusive expression of *Drosophila* R2a RPTPs in the CNS during periods of axon guidance and synaptogenesis. Five of the six *Drosophila* RPTPs (Dlar, DPTP69D, DPTP99A, DPTP10D, DPTP52F)

are expressed only in the CNS neurons in late embryos [35]. Much of the insights into the role of RPTPs in CNS development and axon guidance came from the mutant analysis of *Drosophila* RPTPs. Creating double and triple mutants to delineate the specific functions are much faster in *Drosophila* compared to the mammals. Phenotypes from the zygotic mutants from all the five RPTPS resulted in alterations in axon guidance or synaptogenesis [34, 35, 41, 42].

Mutations in the *Ptp69D* and *Dlar* genes produce distinct, partially penetrant motor axon guidance phenotypes, while *Ptp99A* mutations are silent except in *Ptp69D* mutant background [34]. RPTP mutant combinations suggests that each pathway decision uses a specific subset of the six RPTPs. RPTPs can exhibit functional redundancy, so that the loss of one does not produce a defect unless another RPTP is also absent, or competition, in which loss of one RPTP suppresses the phenotype produced by loss of another [24, 35]. Much of the studies in *Drosophila* RPTPs were done during the embryonic stage of development due to the limitation raised by the lethality of the mutants beyond this stage. Recently the results from the PTP4E/PTP10D double mutant phenotypes represent the first evidence of an essential role for RPTPs in epithelial organ development and this finding may have implications in mammals [42, 43]. The double mutants die as early larvae due to severe tracheal defects that would prevent larval respiration [43].

1.5 Ligands and substrates of *Drosophila* RPTPs

RPTPs use combinatorial controls to target their substrates, specifically by their tissue-/cell-specific expression, subcellular localization/compartmentalization, posttranslational modification, and/or specific interaction between PTP active sites and target sequences

[44]. Also the binding of ligands by extracellular domains affect the downstream signaling events [45]. The identification of RPTP ligands and substrates are key to the characterization of RPTPs but are hampered due to the lethality of mutants in the embryonic stage. Only one set of ligands has been identified thus far. These are the heparan sulfate proteoglycans Syndecan (Sdc) and Dallylike (Dlp), which bind to the Lar RPTP with nanomolar affinity and contribute to its functions in axon guidance and synapse growth [46, 47]. Similarly, little is known about substrate specificity in vivo. Lar can dephosphorylate the Enabled (Ena) protein, which regulates the growth cone cytoskeleton, and genetic interaction studies suggest that Ena may be an in vivo substrate for Lar [48]. The transmembrane protein gp150 can be dephosphorylated by Ptp10D in cell culture and intact fly larvae, but genetics has not provided evidence that Ptp10D and gp150 are in the same signaling pathway in vivo [49]. Cell surface receptor tartan has been identified as the substrate of PTP52F [50].

1.6 Goals of the current study

To date, the findings used to define the functional role of R-PTPs in axon guidance have been limited to embryogenesis. Other than this stage, it is not clear whether and how R-PTPs participate in the regulation of *Drosophila* development. Therefore, this study investigated potential R-PTP involvement in development beyond the embryonic stage. Systematic data mining of available microarray databases found PTP52F to be highly enriched in the midgut tissue of prepupal flies. Our genetic studies demonstrated that PTP52F plays a critical role in the control of *Drosophila* development during the larva-pupa transition. Knock down of PTP52F resulted in pharate adult phenotype as well as delay in the midgut metamorphosis. Since its expression comes along with the increase in

ecdysone pulse during larva-pupa transition, we hypothesized that PTP52F may be a regulator or effector of ecdysone signaling during metamorphosis and hence we focused on the molecular mechanisms by which PTP52F regulates the downstream signaling cascade. The insect molting hormone ecdysone triggers key metamorphic events during fly development [51, 52]. *Drosophila* midgut undergoes extensive metamorphosis during larva-pupa transition. A high titer of ecdysone pulse at the end of larva development signals puparium formation (PF) and triggers stage specific destruction of obsolete larval tissues including the midgut [53]. Destruction of midgut features the phenomenon of both apoptosis and autophagy including acridine orange staining, DNA fragmentation and caspase activation [54]. In the current study we have focused on the molecular mechanisms by which PTP52F acts as an accelerator of midgut metamorphosis. We identified a potential substrate of PTP52F in vitro and in vivo and correlated the kinase-substrate-phosphatase cascade to the control of midgut metamorphosis in fly during the PF stage of development.

CHAPTER 2: MATERIALS AND METHODS

2.1 Fly stocks

The following strains were obtained from various sources: OreR flies (Bloomington stock center), PTP52F knockdown line (3116, VDRC), PTP52F mutant lines - Ptp52F$^{18.3}$/CyO, P{ActGFP}JMR1, Ptp52F$^{8.10.3}$/CyO, P{ActGFP}JMR1 (Bloomington stock center), EcR^{225}/Cyo-4899, UAS-EcRB1-ΔC655.F645A-6869 (Bloomington stock center), TER94 dominant negative lines TER94 E2Q and TER94 K2A were kindly provided by Prof. TK.Sang [55]. *GAL4-UAS* system was used to generate progeny expressing the target gene in a tissue-specific pattern [56]. *Tubulin-gal4*, *GMR-Gal4* (Bloomington stock center), NP1-GAL4 (DGRC, Kyoto) were used to drive tissue specific over expression or knockdown. All flies were maintained and crosses performed at 25^{o}C except for T80-Gal4 crosses for which the temperature is shifted from 18^{o}C to 30^{o}C during second instar larvae stage.

2.2 In-gel phosphatase activity assay

In-gel phosphatase activity assay was performed as described in previous studies [57, 58]. The SDS gel was prepared with the ^{32}P-labeled substrate to obtain a gel solution of 1.5 X 10^{6} cpm/20 ml, equivalent to approximately 2μM pTyr. The fly lysates of specific stages were collected with lysis buffer containing 1% NP40 and stored at -80^{o}C. For each lane, 35μg of total protein was loaded. After electrophoresis, the gel was processed with various buffers sequentially for fixation, protein denaturation and renaturation. In the final step of renaturation, DTT (3mM) was included in the buffer for activation of PTPs in the gel. The dephosphorylation reaction was terminated by staining the gel with Coomassie blue. After destaining, the gel was dried and exposed to X-ray film.

2.3 Microarray and Next generation sequencing (NGS) data mining

For the expression profile of R-PTPome, we utilized the NGS data from modENCODE Temporal Expression Data through Flybase. The National Human Genome Research Institute (NHGRI) model organism ENCyclopedia Of DNA Elements (modENCODE) project provides the biological research community with a comprehensive encyclopedia of genomic functional elements in the model organisms *C. elegans* and *D. melanogaster* [59, 60]. The expression levels of transcripts from RNA-seq data were analyzed and difference in levels of expression was recorded. The tissue specific expressions of R-PTPs were found in Fly Atlas, which is the *Drosophila* gene expression atlas available online [61] (http:www.flyatlas.org). For the screening of PTPome during larva-pupa transition, we utilized microarray data from two studies [51, 62].

2.4 Generation of PTP52F antibody

A fragment of synthetic peptide from the intracellular domain of PTP52F (amino acids 1400-1417) was used as the peptide for antibody production. The epitope was selected based on the scores from an antigenicity prediction program. The rabbit antisera showing the specificity was further purified by affinity chromatography. The purified antiserum was used at a final dilution of 1:10000 for immunoblots and 1:1000 for immunofluorescence staining.

2.5 Cloning and expression of PTP52F, TER94, Src42A and DIAP1

cDNA sequence corresponding to full length PTP52F was obtained by reverse transcription of total mRNA from pupa formation stage of the fly. The full length WT and $C_{1290}S$ (CS) mutants were constructed with a hemagglutinin (HA) tag at the C

terminus and cloned into pAc5.1A (for protein expression in S2 cells) vector. Full length TER94-Flag and Src42A-Myc plasmids were constructed using the cDNA sequences obtained from reverse transcription of total RNA from PF stage of fly. All cDNAs were examined by sequencing. Full length DIAP1 construct was kindly obtained from Prof. Kai Zinn, CalTech.

2.6 Cell Culture, Transfection, and Immunoprecipitation and immunoblotting

Drosophila S2 cells were routinely maintained in Schneider's medium supplemented with 10% fetal bovine serum. For transient transfection with the PTP52F expression vector, S2 cells ($5x10^5$ cells/6 cm plate) were incubated with a mixture of plasmid DNA (5 μg/6cm plate) and Lipofectamine 2000 (Invitrogen), according to the manufacturer's instructions. For immunoprecipitation, the cells were lysed in buffer containing 50 mM Tris-HCl (pH 8.0), 1% Nonidet P-40, 150 mM NaCl, 2 mM Na_3VO_4, and protease inhibitors. An aliquot of total lysate (1 mg) was precleaned with protein G-Sepharose (GE Healthcare) for 30 min at room temperature followed by immunoprecipitation with anti-HA antibody (clone HA-7, Sigma) at 4 °C for 3h followed by the elution of the beads with 2X sample buffer. For immunoblotting, 35 μg of total protein was loaded with 2X sample buffer for each sample followed by gel running and blocking with primary antibody and secondary antibody. Rabbit anti-PTP52F antiserum and mouse anti-HA antibody (Sigma) was used in this study. DIAP1 antibody was kindly provided by Prof. Bruce Hay from CalTech, TER94 antibody from Prof. Dennis McKearin, HHMI. We used the ubiquitin antibody from Cell signaling for immunobloting. 8% SDS gel was

used for all immunobloting experiments except for ubiquitin for which 6% SDS gel was used.

2.7 Phosphatase activity assay

Assays were performed as previously described [63] with a few modifications. Briefly, S2 cells overexpressing HA-tagged PTP52F-WT or PTP52F-CS were harvested in lysis buffer HA-PTP52F was immunoprecipitated from an aliquot of total lysate (1.5 mg) by HA antibody. The immunocomplex was incubated in phosphatase activity assay buffer (50 mM Hepes, pH 7.5, 1% NP-40, 10 mM DTT, and 20 mM p-nitrophenyl phosphate). The reaction was carried out at 37 °C for 1h. After the reaction was terminated by 2 N NaOH, the phosphatase activity in the immunocomplex was measured by spectrometric analysis at 405 nm.

2.8 Extraction of RNA, cDNA Synthesis and RT-PCR

Total RNA was isolated from *Drosophila* tissue during different developmental stage using a Trizol reagent kit (Invitrogen, CA, USA) according to the manufacturer's instructions. The cDNA was synthesized from total RNA (~3μg) with Transcriptor reverse transcriptase (Roche Applied Science) using oligo (dT) primers according to the manufacturer's instructions. Initial screening of PTPs was carried out using reverse transcription PCR and the primers were designed spanning an intron to distinguish the product from genomic DNA and cDNA. The primer sequences are listed in Table-1.

2.9 Quantitative Real-Time PCR

The detailed screening of PTP52F mRNA expression levels during different stages of development were also quantified by real time PCR using a LightCycler instrument (Roche Applied Science) with the SYBR Green PCR Master Mix (Roche) in a one-step reaction according to the manufacturer's instructions. Primers were designed using the LightCycler Probe Design software 1.0 (Idaho Technology). The primer sequences used are listed below in Table-1. The melting curves and gel electrophoresis of the end products were obtained to confirm the PCR specificity and the correct size of the PCR band. The mRNA levels of target genes were normalized to the relative amounts of the housekeeping gene *rp49* using the second derivative maximum method provided by the Relquant software (Roche).

Table-1

Gene name	Primer sequence
Ptp52F forward	5′-ATTGTTCAAGTTACCCAGTTTCGCG-3′
Ptp52F reverse	5′-TTTTTGGGAGAGGGAATGGCG-3′
Ptp99A forward	5′-AGATGGTCTGGGACCACAATGC-3′
Ptp99A reverse	5′-GCAAGAGGCTTGGATTAGTATCGGT-3′
Ptpmeg forward	5′-ATCCACCACATGCAGTACTTGGC-3′
Ptpmeg reverse	5′-TAGCGGAAGATTGTTGATTGCGT-3′
myopic forward	5′-TATTTCCAGAAAGCTGAAACGGC-3′
myopic reverse	5′-CATAGCGTTCTCTCAGCTCTCCAT-3′;
CG7180 forward	5′-GTGAATGGAAAATCGAGGGAACG-3′

CG7180 reverse	5′-AGCACCACCCGATTGTAGTCATA-3′
Ptp52F forward (real time)	5′-ATACGCCCAGTGATGAAGTTAAG-3′
Ptp52F reverse (real time)	5′-ATCGAGTAGGCTTCTGCTTCCA-3′
rp49 forward (real time)	5′-TACAGGCCCAAGATCGTGAA-3′
rp49 reverse (real time)	5′-ACGTTGTGCACCAGGAACTT-3′

2.10 Mass spectrometry based substrate trapping

The WT form and CS/DA mutant form of full length PTP52F with HA tag in the c-terminus were used for substrate trapping. The full length constructs were ectopically expressed in the S2 cells and the lysates were collected using the NP-40 lysis buffer. The over expressed PTP52F was immunoprecipitated using the HA-agarose beads (sigma) from ~2mg of total lysate. In the meantime Kc-167 cells stimulated with 100 μM pervanadate for 30 minutes was lysed at 4^{o}C with buffer containing 20 mM Tris-HCl, pH 7.4, 100 mM NaCl, 10% glycerol, 1%Triton X-100, 5 mM iodoacetamide (IAA) and protease inhibitors. Excess IAA in the total lysates was neutralized by DTT and further removed by a PD-10 column. IAA was used to drive the irreversible inhibition of PTP active site. We avoided using orthovanadate since the trace of unbound orthovanadate may inhibit the immobilized PTP52F in the subsequent step of substrate trapping. The immobilized PTP52F is allowed to react with the pervanadate treated total lysates (~4mg) for three hours at 4^{o}C. To elute the potential substrates associated with PTP52F, beads were either boiled in SDS sample buffer or incubated with 10 μM sodium orthovanadate (Na_3VO_4) at room temperature for 10 min. Those eluted proteins were resolved in a SDS-PAGE gel and then subjected to immunoblotting with anti-pTyr antibody (4G10 from

Millipore) or subjected to silver staining for in-gel trypsin digestion followed by LC-MS/MS analysis. For in vivo substrate trapping, the full length PTP52F-WT and CS/DA were overexpressed, pulled down and checked for their specific association with endogenous TER-94.

2.11 In vivo substrate trapping from fly tissue

UAS-PTP52F –WT and *UAS- PTP52F-DA* transgenic lines were generated using full length plasmids with HA tag in the c-terminal by microinjection and their over expression was confirmed in western blot by cross with *Tubulin-Gal4* line. In order to do the *in vivo* substrate trapping we used the *NP1-Gal4* to drive the midgut specific overexpression of PTP52F-WT and PTP52F-DA. White pupa were collected from the two crosses and the total lysates was obtained by grinding the fly tissues with lysis buffer containing 20 mM HEPES (pH 7.5), 1% Nonidet P-40, 150 mM NaCl, 10 mM NaF, 10 mM $Na_4P_2O_7$, 10% glycerol and protease inhibitors. The PTP52F was pulled down using the HA-agarose beads for two hours at 4^oC. To elute the potential substrates associated with PTP52F, beads were either boiled in SDS sample buffer, were resolved in a SDS-PAGE gel and then subjected to immunoblotting with TER94 antibody (kindly provided by Prof. Dennis McKearin, Howard Hughes Medical Institute).

2.12 Immunofluorescence staining

S2 cells were plated and transfected as described above. After 48h of incubation, the cells were suspended and replated on Concavalin A (ConA) (0.5 mg/ml; C2010; Sigma) -coated glass coverslips and stained with anti-PTP52F antibody followed by Cy2-conjugated goat anti-rabbit IgG or (Jackson). For F-actin staining, cells were stained with

tetramethyl rhodamine isocyanate conjugated phallodin (Jackson). The samples were visualized using a Zeiss LSM 510 confocal microscope. Late third instar larval midguts were dissected in PBS and fixed im 4%paraformaldehyde for 30 minutes followed by, permeabilization with 0.3% Triton X-100 for 10 minutes. Blocking was done with 5% goat serum in 0.3% Triton X-100 and stained with either anti-PTP52F antibody or anti-DIAP1 antibody (kindly provided by Prof.Bruce Hay, Caltech) at 4^{o}C overnight followed by Cy3-conjugated goat anti-mouse IgG -(Jackson) according to the protocol described in a previous study [64]. The samples were visualized using a Zeiss LSM 510 confocal microscope.

2.13 Light Microscopy

Midguts from APF4H pupae were dissected in PBS and fixed in 4% Para formaldehyde for 20 minutes and were mounted and examined using Olympus-BX51 microscope. For each set 30 flies (n=30) were scored for the phenotype analysis.

2.14 TUNEL staining

Midgut tissue was dissected from different stages of third instar larvae and fixed in 4% paraformaldehyde in PBS for 30 min at RT. Samples were permeabilized in 100mM Sodium Citrate in PBTx (PBS + 0.1% Triton X100) at 37 ^{o}C for 30 min followed by the addition of TUNEL mix according to the manufacturer instructions (In Situ Cell Death Detection Kit, Roche) and incubated at 37^{o}C for 1hr on a humid chamber. Tissues were stained with DAPI before mounting and were mounted in 90% glycerol/PBS with 0.5% propyl gallate and TUNEL positive cells were detected by fluorescence microscopy (Olympus BX51).

CHAPTER 3: RESULTS AND DISCUSSION

3.1 Profiling of PTPs during Drosophila development by in-gel phosphatase activity assay

While individual PTPs have been implicated in the regulation of *Drosophila* development during embryogenesis, the expression and activity profile of PTPs at other developmental stages remain uncharacterized. Such data might provide more insight into the role of PTPs playing in the control of the developmental process. We used in-gel phosphatase activity assay to visualize the possible participation of PTPs at each developmental stage. This assay displays a diverse array of active PTPs in total extracts of cells and tissues according to the molecular weights of these phosphatases resolved by SDS-PAGE. As shown in Figure 1, the overall PTP activity in the embryonic stage was significantly higher than in other developmental stages, suggesting that rapid protein tyrosine dephosphorylation plays a critical role in signal transduction during this stage. We found the activity of many PTPs to be diminished during the larva-pupa transition, and increased slightly in adult flies (Fig. 1). Although some PTPs were visible in adult flies, their activity was far weaker than the activity of those in embryos (Fig. 1). The biological implication of such interesting observation requires further investigation. Nonetheless, it should be addressed that all phosphatases detected by this assay format are likely to be non-receptor PTPs due to the inherited limitation of this technique [57, 58]. Indeed none of *Drosophila* receptor PTPs (RPTPs), which run greater than 100 kDa in SDS-gels according to the theoretical calculation (www.uniprot.org), was unraveled by the in-gel phosphatase activity assay (Fig. 1). This may be due to the refolding problem since during the process of experimental procedure we do denaturation followed by renaturation and receptor PTPs might not have refolded properly and hence cannot have

their activity. Obviously, other methods are needed to collect information for profiling RPTPs at different stages of *Drosophila* development.

3.2 Data mining from modENCODE to depict the mRNA expression profiles of RPTPs during Drosophila development

Since the protein expression profiles of RPTPs were not available, we switched our focus to other information such as the mRNA level of these phosphatases over various developmental stages. Flybase provides modENCODE temporal expression data for each gene [59, 60] (www.modencode.org). Since this database shows the expression pattern of every gene throughout the development of flies, is easily accessed, we decided to perform data mining to profile RPTPs using already existing information embedded in the Flybase. We analyzed all RPTPs in the *Drosophila* genome, including dLAR, PTP4E, PTP10D, PTP52F, PTP99A, and PTP69D except dIA2, which is a naturally inactive phosphatase. We examined the mRNA levels of these R-PTPs at various developmental stages (the embryo, early and late third instar larva, white prepupa, pupa and adult). As seen in Figure 2, all R-PTPs except PTP52F were highly expressed during embryogenesis. PTP4E, PTP10D and PTP69D levels were particularly pronounced in embryos (Fig. 2A and 2B), suggesting they may play essential roles in the control of developmental events at this time. These findings are in agreement with those of two recent studies reporting that PTP4E, PTP10D and PTP69D act in coordination of axon guidance during embryogenesis and that they have redundant and compensating functions [42]. Perhaps the most interesting observation in the profiling was the gradually increased expression of PTP52F from the embryonic stage to the larva-pupa transition (Fig. 2A and 2B), at

which time metamorphosis begins and most larval tissues are readily remodeled for the development to adult flies [52]. The discovery that PTP52F is specifically expressed at this particular stage of development suggested that receptor PTPs may be involved in the control of metamorphosis, despite a very low activity of non-receptor PTPs being observed at this time of pupal formation (Fig. 1).

3.3 Tissue distribution of RPTPs during third instar larval stage

We wanted to examine the expression of RPTPs in various tissues of *Drosophila*, particularly focusing on the tissue distribution of PTP52F, which is highly expressed during larva-pupa transition (Fig. 2). We used data mining to profile the expression of R-PTPs in the third instar larval tissues including salivary gland, CNS, trachea, tubule, hindgut and midgut using the Fly Atlas database, which provides the most comprehensive collection of the mRNA level data on each gene in each tissue during III instar larva and adult stages of development [61] (www.flyatlas.org). Data were mined using three criteria: (1) mRNA SIGNAL, the abundance of mRNA; (2) mRNA ENRICHMENT, mRNA of the specific gene compared to total mRNA of the whole flies; and (3) the Affymetrix PRESENT CALL, the number of time a specific gene was detectably expressed out of four arrays being analyzed. To summarize our findings, we presented a simplified anatomy of the third instar larvae showing major tissues with relative expression levels of R-PTPs (Fig. 3). Four out of six RPTPs (dLAR, PTP4E, PTP99A and PTP69D) were detected in the CNS, suggesting they play important roles in the neuronal formation not only during embryogenesis but also at the beginning of metamorphosis. To our surprise, we found PTP52F to be exclusively expressed in gut tissues, and to be particularly enriched in the midgut (Fig. 3). Since this kind of tissue

distribution of RPTPs had never been recorded in flies, we hypothesized that PTP52F may have a specific roles in the regulation of gut tissue during larva-pupa transition. Thus, the remainder of the study was devoted to the characterization of PTP52F and the study of its potential involvement in *Drosophila* development.

3.4 PTP52F is highly enriched in midgut during larva-pupa transition

Based on our analysis from microarray and NGS data mining for *Drosophila* PTPs, we identified, *Ptp52F*, to have changed its expression pattern during larva-pupa transition. In order to confirm the microarray analysis, we did the RT- PCR during the developmental stages of the fly. We used the total RNA extracts from different stages of fly and probed the *Ptp52F* gene by PCR. The primers were designed to cover an intron so that the product from genomic DNA and cDNA can be distinguished based on the size. The RT-PCR results showed that *Ptp52F* is increased during larva-pupa transition (Fig. 4A). We further confirmed its expression pattern by real-time PCR (Fig. 4B). We found a sharp increase in *Ptp52F* RNA during the white pupa formation (PF) stage (Fig. 4B). We used the antibody that we generated to examine the expression of endogenous PTP52F in total protein extracts isolated from both WT and PTP52F knockdown (RNAi) flies at the third instar larval stage, when mRNA of PTP52F was robustly enriched (Figs. 2 and 3). As shown in Figure 4C, the specific band at ~200 kDa appeared only in the WT flies but not in the RNAi line, suggesting that endogenous PTP52F protein was indeed expressed during the larva-pupa transition. The excellent performance of this antibody indicated that we could use it to further characterize PTP52F in developing flies with various genetic backgrounds. The results of our data mining of the Fly Atlas (Fig. 3) suggested there would be a robust level of PTP52F protein in the prepupal midgut tissue. To find

out, we performed immunofluorescence staining with anti-PTP52F antibody. As shown in Figure 4D, there was a strong signal of PTP52F in the midgut of WT flies, suggesting a high level of mRNA at this developmental stage (Figs. 2 and 3) might lead to the enhanced expression of its protein in larval epidermal cells or adult epidermal progenitor cells, both which are major types of cells in the larval midgut [65]. Interestingly, the staining of PTP52F protein was highly enriched in the midgut but much weaker in the hindgut region (Fig. 4D), consistent with the information of its mRNA distribution provided by the Fly Atlas (Fig. 3).

3.5 PTP52F is an ecdysone response gene

Since the molting hormone ecdysone plays an important role during larva-pupa transition, we further checked the role of ecdysone in *Ptp52F* expression. We used an EcR heterozygous mutant to do the real-time PCR for *Ptp52F* and we found that inducible expression of *Ptp52F* during pupa formation is highly reduced in the EcR mutant compared to WT flies (Fig. 5A). We also found that the protein expression of PTP52F was also highly reduced in EcR mutant compared to the WT fly during the PF stage (Fig. 5B). Based on our previous studies we have identified some potential EcR response elements in the promoter region of *Ptp52F* [66]. Hence we used the Kc167 cells to do the ecdysone stimulation in-vitro. Kc167 cells were stimulated with ecdysone for different time points from 0-24 hours. Even though we see little increase in the early time points, the inducible expression of PTP52F was very clear at 24 hrs confirming the role of ecdysone in the inducible expression of PTP52F (Fig. 5C). Taken together the results from our studies and also from previous studies from Thummel's lab [51] clearly show

that PTP52F is an ecdysone response gene and it is increased during the PF stage in the fly during which the ecdysone pulse is high.

3.6 PTP52F mutants show delay in midgut metamorphosis

Based on our earlier studies we already confirmed that the PTP52F is highly enriched in the midgut during the larva-pupa transition. Ecdysone triggers and directs metamorphosis during the pre-pupal and pupal transitions. Ecdysone binds to EcR and activates a set of early response genes triggering tissue specific responses during metamorphosis [65]. The midgut is one of the major tissues that undergo extensive metamorphosis under ecdysone stimulation during larva-pupa transition. Since *Ptp52F* is highly enriched in the midgut and is an ecdysone response gene, we next asked whether PTP52F have any functional role in midgut metamorphosis. First we did the immunofluorescence experiment to analyze the inducible expression of PTP52F in midgut during larva-pupa transition. Our data showed that the PTP52F was increased during PF and APF-2h compared to <5h BPF (Fig. 7A). We also noticed that PTP52F is highly enriched in the gastric ceaca of the midgut which will be destroyed by cell death during metamorphosis. As shown by earlier studies the midgut will undergo cell death during metamorphosis and its size is highly condensed during APF-4h compared to PF or <5H BPF and this process is shown in representative images in Fig. 6. We can also notice that the gastric ceaca is completely destructed at APF-4h. EcR, the key mediator of ecdysone action is known to regulate midgut metamorphosis. Mutation or loss of function of EcR results in the delay of midgut metamorphosis. The size of midgut still does not condense at APF-4h and has been shown by Thummel's group [67]. Our results also shows that the over expression of dominant negative EcR lead to a delay in midgut metamorphosis and hence we can see

the gastric ceaca at APF-4h compared to the control (Fig. 7B upper panels). Correlating to its inducible expression the PTP52F-KD lines as well as the PTP52F-CS mutant lines (loss of phosphatase activity) showed a delay in the midgut metamorphosis (Fig. 7B middle panels). Also we have checked the midgut metamorphosis in transheterozygous mutants, and all the trans-heterozygous mutants show delayed gastric ceaca degradation compared to the heterozygous lines (Fig. 7B lower panels). Whole length of the gut in KD and mutant line is longer than the control. Gastric ceaca is also seen clearly compared to the control. We used gastric ceaca as an indicator to show the delayed metamorphosis of the gut. This phenotype clearly suggests that the ecdysone induced PTP52F is involved in regulation of midgut metamorphosis. The protein levels of EcR and PTP52F showed the corresponding increase and decrease according to the lines used representing the degree of knockdown and over expression in Fig. 7C.

3.7 Ectopically expressed PTP52F is an active, plasma membrane-localized phosphatase

We performed sequence analysis on the full-length cDNA of *Ptp52F* gene that we cloned from flies and found it to be identical to the one published previously [45]. As shown in Figure 8A, the PTP52F protein contains a putative signal sequence, six fibronectin type III repeats, a single transmembrane segment, and a single phosphatase domain in the intracellular region. We generated an antibody specifically targeting the C-terminal tail outside of phosphatase domain (Fig. 8A). This antibody recognized the wild type (WT) phosphatase ectopically expressed in *Drosophila* S2 cells (Fig. 8B). We noticed that the full-length PTP52F ran as a single band at a higher position (~200 kDa) than the

predicted size (~160 kDa) in SDS-gels (Fig. 8B), suggesting the occurrence of post-translational modifications. The phosphatase activity of the WT form of PTP52F, but not the $C_{1290}S$ (CS) mutant form, was confirmed by the typical PNPP assay (Fig. 8C). To examine the subcellular localization of PTP52F, we performed immunofluorescence staining with anti-PTP52F antibody together with F-actin co-staining in S2 cells attached to the lectin ConA substrate. When spreading on the ConA-coated surface, cortical actin structure in S2 cells would be concentrated at the cell periphery, thus allowing us to determine the leading edge of plasma membrane as demonstrated in our previous study [68]. Using F-actin staining as the guidance, we have observed that the ectopically expressed WT form of PTP52F was highly enriched near plasma membrane (Fig. 8D). Considered together, these findings suggest that PTP52F acts as an active form of receptor tyrosine phosphatase.

3.8 VCP/TER94 is a potential substrate of PTP52F and is also involved in midgut metamorphosis

We next wanted to know how the PTP elucidates its role in gut metamorphosis. We first wanted to identify some potential substrates of PTP52F that may be involved in this process. Substrate trapping by trapping mutants whose active site signature motif is mutated to trap the substrate is a well-established technique used to identify potential substrates of PTPs [11]. As established in our previous studies we used substrate trapping combined with mass spectrometry to identify the target substrates of PTP52F [68, 69]. In the current study, we used the full length PTP52F –WT vs. PTP52F CS/DA mutant (in which the signature motif cysteine (C) and WPD loop aspartate (D) are mutated) to do

the trapping experiment rather than the truncated form used in previous studies [50, 68]. Also we used the S2 cells to over express the full length WT and CS/DA PTP52F rather than the bacterial expression system. This ensured the usage of full length receptor PTP for trapping experiment. We used S2 cells to ectopically express large amount of PTP52F because for the easiness of handling S2 cells compared to KC cells which are very loosely attached. Since Kc167 cells can express endogenous PTP52F, we thought it is relevant to use it to get the substrate pool for trapping rather than S2 cells which do not express endogenous PTP52F. The over expressed PTP52F – WT and CS/DA in S2 cells were pulled down by IP and the pulled down beads were incubated with the pervanadate (PTP inhibitor) treated lysates from Kc167 cells. Then the beads were washed for several times and eluted with 5 mM orthovanadate which serves as a competitive inhibitor to release the bound substrates from the active site. A part of the eluted fraction was used for probing with anti-pTyr antibody and the remaining fraction was used for the MS-analysis. As expected the anti-pTyr blot showed that more substrates are eluted from PTP52F –CS/DA mutant compared to the WT (Fig. 10A left panel). We went for the MS analysis of all the 11 bands identified in sypro ruby staining. The detailed results of the MS analysis are attached at the Appendix-I. Since a band around 100-kDa showed a significant contrast between PTP52F-WT and CS/DA and that band was identified as TER94 by MS-analysis (Fig.10A right panel), we further want to characterize and confirm its identity. TER94 is the fly ortholog of human Valosin containing protein (VCP). We first confirmed that TER94 indeed can be tyrosine phosphorylated by pervanadate stimulation (Fig. 10B). This was followed by an in vitro dephosphorylation assay to show that TER94 was dephosphorylated by PTP52F-WT significantly compared

to the PTP52F-CS mutant (Fig. 10C). This was followed by the in vitro substrate trapping to validate TER94 as the potential substrate of PTP52F (Fig. 10D). Further we also did an in vivo trapping assay in the endogenous TER94 was trapped by the over expressed PTP52F-CS mutant in S2 cells (Fig. 10E). We also generated transgenic fly lines over expressing PTP52-WT and PTP52-DA form with a HA tag in the C-terminus. We utilized these fly lines to overexpress PTP52F specifically in the midgut using the *NP1-Gal4* driver. White pupae at the PF stage were collected and lysates were used for substrate trapping. A detailed description is available in the materials and method section. The results show the trapping of endogenous TER94 by PTP52F-DA mutant (Fig. 10F). Together these data showed that TER94 is indeed a bona fide substrate of PTP52F both in vitro and in vivo. Since we know that knockdown of PTP52F leads to delayed migut metamorphosis, we further checked the involvement of TER94 in this phenomenon. When we over expressed TER94 in flies, the metamorphosis was not affected and when we cross this fly with *Ptp52F* RNAi line, we found that the delay in metamorphosis is not seen further and was rescued suggesting that TER94 may be involved in the midgut metamorphosis regulation pathway of PTP52F (Fig. 10G).

3.9 Src42A is the upstream kinase of TER94

VCP the human ortholog of TER94 was shown to be tyrosine phosphorylated by Src kinase [70, 71]. Also based on the sequence comparison between VCP and TER94 shows 87% identity and the C-terminal tyrosine residue phosphorylated by Src kinase in VCP is highly conserved in TER94 (Fig. 11A). Based on the conserved motif analysis and software anslysis, Src kinase was the most predicted kinase for Y-800 (Fig. 11B).

Drosophila melanogaster has two *c-src* homologs (*src64B* and *src42A*) and one *csk* homolog, with a high degree of homology to their mammalian counterparts [72, 73]. Since Src42A was the closest ortholog of human c-src [73], we continued with Src42A for our study. Wild-type Src overexpressed in Schneider 2 cells is shown to be phosphorylated at additional tyrosines outside of the C-terminus. These tyrosines correspond to the major in vitro autophosphorylation sites. Overexpression of wild-type Src significantly increased the phosphorylation of numerous Schneider cell (S2) proteins on tyrosine, while expression of catalytically inactive mutants of Src has no such effect. Thus, in contrast to the repression of src family kinase activity in fibroblasts, Src is catalytically active when overexpressed in Drosophila cells, perhaps because of substoichiometric C-terminal tyrosine phosphorylation [74]. Since it is known that full length Src kinase is active in S2 cells we used the full length src42A in our cell based experiments. Based on our results we confirmed src42A can phosphorylate TER94. Also we identified Y-800 as the specific target of tyrosine phosphorylation (Fig. 11C and 11D). In order to confirm that PTP52F can also work on the same site of tyrosine phosphorylation, we carried out a substrate trapping experiment involving PTP52F, Src kinase and TER 94 and the results clearly show that src mediated pY of TER94 was targeted for dephosphorylation by PTP52F (Fig. 11E).

3.10 Src42A may not be the substrate of PTP52F

We also used the substrate trapping technique to investigate whether the kinase Src42A was also regulated by PTP52F. As shown in Fig. 12, Src42A was not associated with the DA mutant form of full length PTP52F when both proteins were ectopically expressed in

S2 cells whereas the endogenous TER94 was seen trapped by the DA mutant in the same experimental setup. This experiment clearly shows that Src kinase 42A was not regulated by PTP52F in context of ectopic expression in Kc167 cells.

3.11 PTP52F dephosphorylates TER94 Tyr(Y)-800 under ecdysone stimulation both *in vitro* and *in vivo*

Since we see the inducible expression of PTP52F under ecdysone stimulation, we checked the tyrosine phosphorylation of TER94 under this condition. We used the over expression of TER94 in Kc167 cells with ecdysone stimulation for different time points from 0- 24 hours. The TER94 phosphotyrosine levels were too low to detect even after pull down. Hence we co expressed Src and TER94 and followed the ecdysone stimulation. The appropriate amount of Src necessary for co expression was determined in a separate dose dependent experiment (data not shown). We used the minimal amount of Src for co expression below which TER94 cannot be phosphorylated. Our results showed that TER94 tyrosine phosphorylation was reduced at 24H of ecdysone treatment during which the endogenous PTP52F is inducibly expressed. We also noticed that under PTP52F-KD, the tyrosine phosphorylation of TER94 is not reduced compared to the mock (Fig. 13A). These results showed that inducibly expressed PTP52F can reduce the TER94 tyrosine phosphorylation under ecdysone stimulation. To further check this *in vivo*, we used the fly lysates from TER-WT over expression lines and checked the tyrosine phosphorylation status of TER94 during larva-pupa transition. As shown in Figure 13B the endogenous PTP52F was increased during 2H-APF and a corresponding decrease in TER94 tyrosine phosphorylation was noticed. Together these results show that TER94 can be

dephosphorylated by PTP52F under a physiological stimulus. Also these results demonstrate that TER94 tyrosine phosphorylation is modified *in vivo* in flies under physiological conditions.

3.12 TER94 tyrosine phosphorylation regulates its function in degradation of ubiquitinated substrates

Earlier studies have concluded that VCP is an integral component of ERAD and cellular stress pathways induced by the unfolded protein response and may be central to the efficacy of substrates that target the ubiquitin-proteasome pathway [75, 76]. Preliminary studies by other groups have shown that VCP tyrosine phosphorylation regulates its activity during ERAD [71, 76]. Hence in our current study we checked the effect of TER94 tyrosine phosphorylation on its potential to degrade ubiquitinated proteins. We used the Kc cells to check the effect of TER94 pY on total ubiquitination. Co expression of TER94 with PTP52F and Src was used to modulate the TER94 pY status. To our surprise we found that dephosphorylated TER94 i.e. TER94 co expressed with PTP52F showed the decreased total ubiquitin when compared to the phosphorylated TER94 i.e. co expressed with Src (Fig. 14A). The rescue experiment in which we knock down the endogenous TER94 followed by over expression of TER94-WT alone or with PTP52F/Src also reflected the similar results in which TER94 co expressed with PTP52F showed the highest rescue effect in terms of total ubiquitin (Fig. 14B). The total ubiquitination is lowest in the lane in which TER94 is co expressed with PTP52F suggesting that TER94 is more effective in degrading ubiquitinated proteins when it is in the dephosphorylated form (Fig.14B). We also wanted to check the effect of YF mutation

on TER94 function and we carried out a rescue experiment using the TER-WT and TER-YF. The results showed that TER94-YF is not so effective in the rescue compared to the TER-WT (Fig. 14C). Similar results were also obtained in the Immunofluorescence based rescue experiments (Fig. 14D), the ubiquitin levels are higher in cells expressing TER-YF compared to the cells expressing TER-WT. The YF mutant is similar to phosphorylated TER94 in terms of rescue. Taken together these results showed that TER94 in a dephosphorylated form with tyrosine residue at 800^{th} position is more effective in degrading ubiquitinated proteins. We also checked the effect of YF mutation on midgut metamorphosis. We have generated transgenic lines of Drosophila expressing either TER94-WT or TER94-YF mutant form. We see a delay in gastric ceaca degradation in TER94-E2Q (dominant negative form of TER94) flies and also in TER94-YF mutant flies showing the necessity for effective degradation of ubiquitinated proteins during metamorphosis (Fig. 14E). This observation is also supported by the earlier studies that characterized the tissue specific gene expression and ecdysone regulated genomic networks in *Drosophila*. In this study midgut is one of the tissue chosen to study the ecdysone network during metamorphosis and it shows that transcripts encoding proteasome components increase during the ecdysone pulse that triggers the onset of cell death in larval cells in an ecdysone dependent manner [65]. The previous study together with our results shows that proteasome mediated ubiquitin degradation is important during midgut metamorphosis.

3.13 TER94-dependent degradation of the apoptosis inhibitor DIAP1 is regulated by TER94 phosphorylation status

Drosophila inhibitor of apoptosis (DIAP1) is required to block premature cell death during larval development delaying death until its effect is overcome by the death activator genes *reaper (rpr)* and *head involution defective (hid)* [64, 77]. Knockdown of DIAP1 during third instar larva is leading to premature larva midgut cell death [64]. Our immunofluorescence data from midgut during larva-pupa transition also show the time dependent reduction of DIAP1 during metamorphosis (Fig. 15A). Recent studies from other group have also shown that TER94-dependent DIAP1 degradation is required for proper neuronal remodeling and apoptosis [78]. Through the already available knowledge we know that DIAP1 is one of specific substrates of TER94 mediated degradation. Using our model we wanted to check whether TER94 tyrosine phosphorylation is involved in regulating DIAP1 degradation. First we checked the amount of ubiquitinated DIAP1 in a over expression system in Kc cells in which DIAP1 and TER94 were co expressed with either PTP52F or Src. Ectopically expressed DIAP1 was immunoprecipitated using the HA tag and checked for ubiquitination levels. Our results show the effective degradation of DIAP1 co expressed with PTP52F whereas TER94-YF and TER-94 with Src shows higher levels of ubiquitinated DIAP1 correlating to its reduced degradation (Fig. 14A). TER94-QQ is used as a dominant negative form of TER94 showing the highest accumulation of ubiquitinated DIAP1 (Fig. 14A). We also checked the endogenous levels of DIAP1 under different conditions of TER94 over expression in Kc cells. The results show low levels of DIAP1 when TER94 is co expressed with PTP52F suggesting that dephosphorylated TER94 is more efficient in degrading DIAP1 (Fig. 15B). We also

checked the endogenous DIAP1 in midgut tissue in wild type flies during larvae pupa transition (Fig. 16A) which shows the gradual decrease of DIAP1 from BPF to 2H-APF. We see the accumulation of DIAP1 in TER94-QQ as well as PTP52F-KD flies in 2H-APF compared to the control flies (Fig. 16B). This result clearly correlates the delayed gastric ceaca degradation in these flies to the accumulated DIAP1 levels. Together these results demonstrate that TER94 phosphorylation is temporally and spatially regulated by PTP52F for timely midgut metamorphosis.

3.14 Delay in midgut metamorphosis is due to reduced cell death revealed by TUNEL staining

Since we noticed a reduced degradation of DIAP1 in PTP52F-KD flies, we hypothesized a corresponding delay in cell death involved in gastric ceaca degradation. In order to confirm this, we did the TUNEL staining in the midgut tissue during metamorphosis. First we checked the cell death using TUNEL staining in the WT flies. Cells that undergo cell death are marked by the TUNEL positive nuclei (bright red dots in the nuclei). Our results show that cell death is increased during PF and APF-2H compared to <5H-BPF (Fig. 17A). Once we confirmed this we checked the cell death in the midgut tissue of PTP52F-KD flies. The results showed that cell death is delayed in PTP52F trans-heterozygous flies compared to the heterozygous control flies represented by the less dense TUNEL positive cells in PTP52F trans-heterozygous flies (Fig. 17B). We have also checked the total ubiquitin profiles from midgut of PTP52F-KD flies during metamorphosis. These results together with the DIAP1 staining (Fig. 16B) suggest that the delayed gastric ceaca degradation in PTP52F mutant flies is due to the decreased cell

death which in turn is due to the accumulation of DIAP1. Finally all these results together showed that PTP52F mediated TER94 dephosphorylation is involved in the degradation of DIAP1 leading to cell death.

3.15 Summary

RPTPs play major roles in growth and development. *Drosophila* has so far served as a simple and excellent model organism for elucidating the functions of RPTPs. So far all the functions attributed to *Drosophila* RPTPs are related to CNS development. Since the complexity of RPTPome is highly reduced in *Drosophila* we proposed that RPTPs may have major roles in development other than that in CNS. Based on our micro array data mining approach we identified PTP52F to be highly enriched in the midgut during third instar larva. We confirmed the inducible expression of PTP52F in midgut during larva-pupa transition under ecdysone stimulation. We also found that knockdowm of PTP52F leads to delayed midgut metamorphosis. Further based on our results we identified TER94 as a potential in vivo and in vitro substrate of PTP52F. We have identified a possible mechanism by which PTP52F can play role in midgut metamorphosis and thereby in fly development. PTP52F mediated dephosphorylation of TER94 can lead to the effective degradation of DIAP1 leading to spatially controlled midgut metamorphosis in fly. Our study for the first time demonstrates a developmental role of a RPTP other than the CNS development and also more than the embryonic stage of development. The results of our study are summarized in Fig. 18.

3.16 Discussion

Data accumulated so far have suggested that the involvement of *Drosophila* RPTPs is mostly in neural-specific functions [34, 45, 50]. Essentially nothing was known about the functions for *Drosophila* RPTPs outside the nervous system until a very recent finding that demonstrated the role of PTP4E and PTP10D in determination of tracheal tube geometries in embryos [43]. However, it must be noticed that, no matter what origin of cell type or what signaling pathway was discussed so far, the functional role of RPTP was only shown in *Drosophila* embryos mostly due to the lethality of RPTP mutant flies during embryonic development. In the current study, PTP52F was found by data mining to be specifically enriched in the midgut during the larva-pupa transition, a finding we confirmed through genetic manipulation combined with immunoblotting and immunofluorescence approaches. Thus, we were able to show for the first time that an endogenous RPTP protein is highly expressed outside the nervous and tracheal systems at a developmental stage other than embryos.

The involvement of PTP52F in midgut metamorphosis is a spatially and temporally controlled event. Since TER94 pY is controlled by Src kinase and PTP52F, we checked the expression profile of Src 42A. It is present in high levels in all tissues and increased during early third instar and late white pupa wheareas PTP52F increased during late third instar larva and early white pupa showing the elegant spatial and temporal control of the signaling cascade that is up regulated during metamorphosis. The midgut metamorphosis during larva pupa transition involves the crucial regulation of many such events including the degradation of DIAP1 as well as inhibition of DIAP1 synthesis to activate apoptosis [64, 77, 79]. We have identified the novel role of an RPTP during the crucial stage of

development showing the importance of tyrosine phosphorylation signaling during development. There may be further unidentified roles of RPTPs in development that need to be analyzed.

The latest version of computational and bioinformatics analysis defined PTP52F as an unclassified member in the PTP super family without a clear ortholog in humans [33]. However, based on the sequence of full-length PTP52F clones obtained by us and by Zinn's group earlier report [33, 45], we propose that the classification of *Drosophila* RPTPs be revised. Apparently PTP52F contains only one catalytic domain in the intracellular region instead of two tandem putative phosphatase domains, as suggested previously [45]. The overall layout of PTP52F architecture composed of multiple fibronectin repeats, a single transmembrane segment plus a single phosphatase domain (Fig. 8A) re-classifies this phosphatase as a member belonging to the subtype R3, together with PTP4E and PTP10D in the *Drosophila* PTP family (Fig. 19). Thus, the earlier study, which defined PTP52F as an unclassified phosphatase, should be modified. As shown in Fig. 19A, there are three *Drosophila* RPTPs and six human RPTPs in the subtype R3. Obviously, it is difficult to classify the ortholog pair merely based on the sequence alignment. Other important criteria, such as the regulatory role in evolutionarily conserved signaling pathways or the tissue-specific expression profile of RPTPs across species must be taken into consideration. Recently, PTP10D and PTP4E were regarded as the functional orthologs of human density-enriched PTP-1 (DEP-1) due to their similar expression in epithelial cells and their shared ability to down-regulate receptor tyrosine kinases-mediated signaling [43]. Following the same principle of consideration, we

propose that PTP52F might be the functional ortholog of human and mouse stomach-associated PTP-1 (SAP-1) (Fig. 19B). Accumulated data clearly show that mammalian SAP-1 is exclusively expressed in gastro intestinal epithelial cells [80], similar to the midgut-enriched expression of PTP52F in flies. It has been proposed that the inactivation of AKT and ILK by SAP-1 contributes to SAP-1 induced apoptosis [81, 82]. In the current study we have dissected the role of PTP52F in apoptosis through TER94 mediated DIAP1 degradation suggesting the regulatory role of PTP52F in apoptosis. Such a specific expression profile and functional co relation of both PTP52F and SAP-1 suggests that they may regulate evolutionarily conserved signaling pathways in the gut tissue.

In conclusion, data shown in the present study suggest that endogenous *Drosophila* RPTPs act in the developmental control outside the nervous and tracheal systems and also beyond the early embryonic stage and thus potentially play an indispensable role in the regulation of metamorphosis. Our study has opened a new avenue for understanding the role of *Drosophila* RPTPs that may mediate signal transduction during development and other biological processes in areas beyond our current knowledge.

CHAPTER 4: FUTURE STUDIES

4.1 Future directions

To date, our understanding of PTP52F in regulation of signal transduction is limited, largely due to the lack of knowledge about substrates and signaling pathways regulated by this phosphatase. A recent study showed that Tartan, a transmembrane protein, is a candidate substrate of PTP52F [50]. Genetic experiments further illustrate that both PTP52F and Tartan act synergistically in pathways of motor axon guidance in embryos [50]. Tartan was also detected in tracheal tissue [83]. However, nothing is known about the distribution or potential functions of Tartan in midgut of larva and pupa. Based on the data mining we found that tartan is highly expressed in CNS rather than the midgut and hence this may not be a potential candidate of PTP52F in the midgut. Therefore, it is difficult to predict whether the phenotype of pharate adult lethality seen in the PTP52F knockdown flies is due to the mechanism identified in our study or it was influenced by the deregulation of Tartan or other yet-to-be-identified substrates of PTP52F. Further investigations are required to delineate the molecular basis for PTP52F-mediated regulation of signaling pathways. Nonetheless, it is interesting to point out that the pharate adult phenotype revealed by the ablation of PTP52F has also been reported in some mutants of ecdysone response genes [65, 84], including ecdysone receptor (EcR) [85], a key mediator of metamorphosis during the transformation from larva to pupa. The similarity of phenotype suggests a possibility that PTP52F may participate in ecdysone-mediated signal transduction. Indeed our preliminary data support a genetic interaction between EcR and PTP52F. Based on these observations, we hypothesized that *Ptp52F* might be a downstream gene transcriptionally regulated by EcR. As a typical steroid hormone receptor, EcR recognizes specific consensus motifs on the promoter region of

effector genes (47). We therefore analyzed 2 kb region upstream of the first exon of *Ptp52F* gene to search for potential ecdysone response elements using the software **NubiScan-2.0** (http://www.nubiscan.unibas.ch/), which is an *in silico* tool that helps predict nuclear receptor binding sites. Based on the analysis, two possible ecdysone response elements with high scores were identified (Fig. 20A). Importantly, the sequences of these elements are similar to the consensus motif shown in the known EcR-regulated genes (Fig. 20B). Also we have identified that the ecdysone mediated increase of endogenous PTP52F was not seen in the EcR heterozygous mutant fly. Our cell based experiments also show the ecdysone mediated inducible expression of PTP52F. Together these results suggest that *Ptp52F* may be a downstream gene of ecdysone action. It is interesting to note that some of the steroid hormone mediated disorders in humans are correlated to expression levels of certain PTPs. A recent study by Lessard et al., have shown that PTP1B is increased in response to androgen in androgen receptor positive cells implicating a role for PTP1B in prostate cancer [86]. Our study in *Drosophila* shows a positive relation between ecdysone and PTP52F during a developmental process and may also be involved in pathological conditions which need to be analyzed further. We also did a preliminary microarray data mining to evaluate the overall role of PTPs during larva-pupa transition [51, 62]. Based on the results we choose five PTPs for further analysis including PTP52F (Fig. 21). The preliminary results show that more PTPs other than PTP52F are regulated during larva pupa transistion which needs to be analysed further.

The whole body knockdown of PTP52F leads to pharate adult phenotype (Fig. 22) in which the adult flies die inside the pupa cage during eclosion. This data suggests that

PTP52Fhave more essential functions in development including midgut metamorphosis. The other roles of PTP52F have to be studied further. Based on our micro array analysis PTP52F seems to be highly enriched in midgut during the adult stage of the fly as well (Fig 23). The role of PTP52F in adult development also needs to be analyzed further. A systems biology based approach may be used in future to identify the tissue specific and stage specific functions of PTP52F in which *in vivo* substrate trapping can be carried out using tissue specific and stage specific methods to identify spatial and temporally controlled functions of PTP52F.

CHAPTER 5: FIGURES

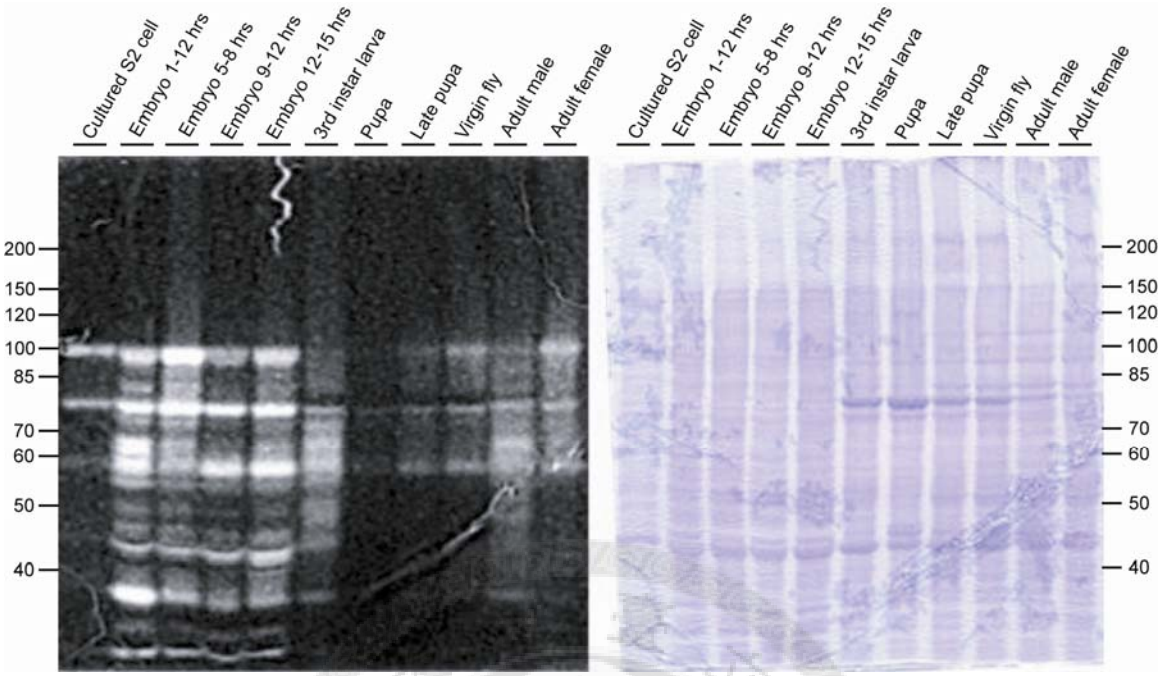

Figure 1. In-gel assay reveals the dynamic change of PTP activity in multiple stages during *Drosophila* development

The total protein extracts (35 μg each) were collected from the whole fly at various developmental stages as indicated, and then applied to a SDS-gel cast in the presence of radioisotope-labeled PTP substrate. Left panel, upon the complete process with the denaturation and renaturation buffers, the gel was exposed to an X-ray film for the visualization of PTPs. The clear zones shown in each lane represent the activity of phosphatases according to their molecular weights resolved by SDS-PAGE. Right panel, the Coomassie blue staining of the same gel indicates an equal amount of protein extract loaded in each lane.

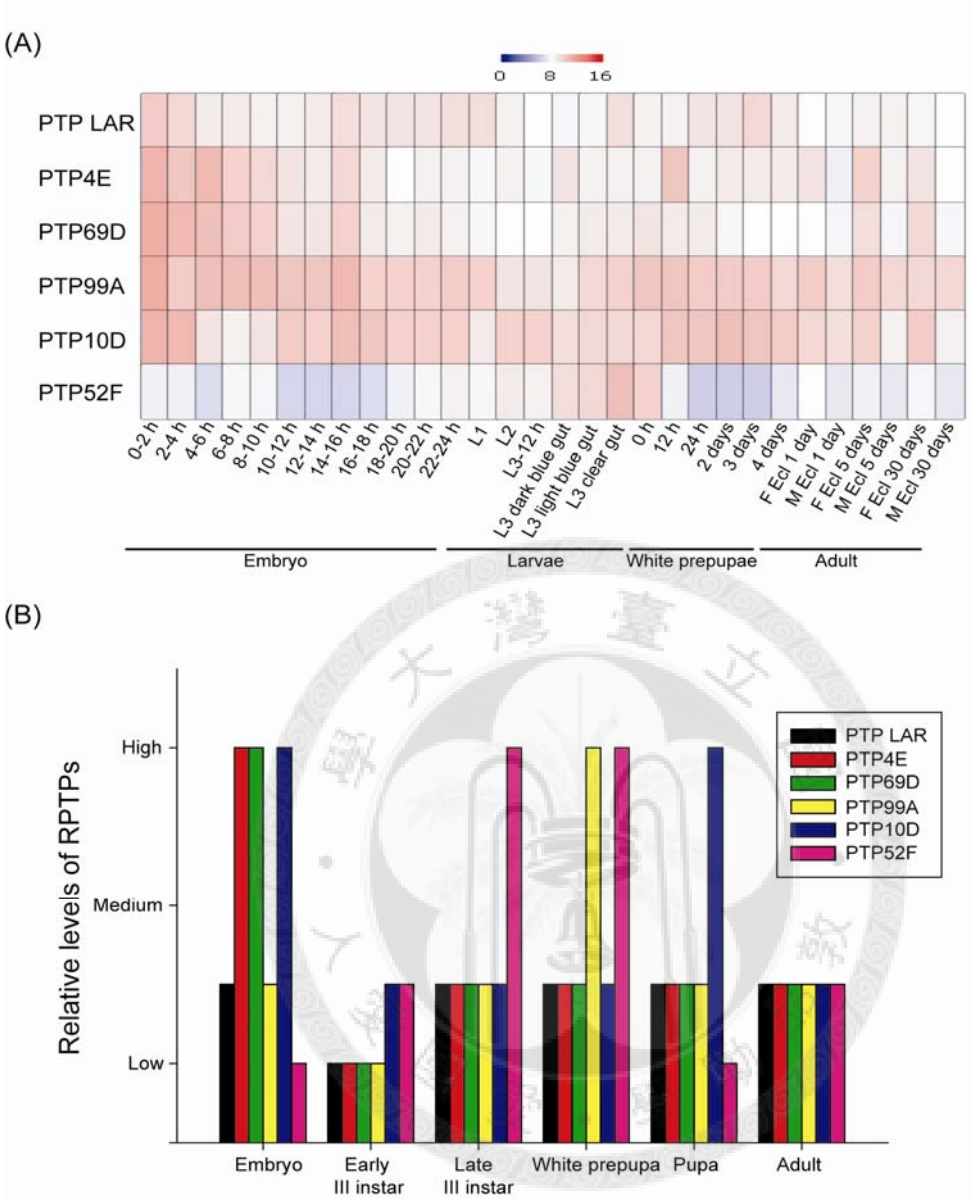

Figure 2. Data mining reveals the mRNA expression profile of R-PTPs in multiple stages during *Drosophila* development

The mRNA levels of six *Drosophila* R-PTPs at various developmental stages were obtained from the modENCODE Temporal Expression Data of the Flybase. (A) Heat map showing relative changes in R-PTP expressions following the onset of embryogenesis until adult. The heat map scale indicates the relative fold expression of genes within this group as log2 of the actual value. (B) A simple graphical representation of the heat map for easy visualization. Note that PTP52F and PTP99A were expressed in relatively high levels during the larva-pupa transition.

(A)

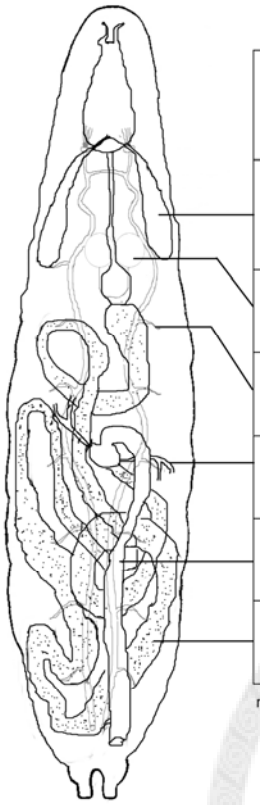

Tissue	mRNA level					
	PTP LAR	PTP4E	PTP69D	PTP99A	PTP10D	PTP52F
Salivary gland	--	+	+	--	--	--
CNS	++	+	+++	++++	--	--
Trachea	--	+++	--	+	+	--
Tubule	--	--	+	--	--	--
Hindgut	--	++++	--	--	+	+
Midgut	--	--	--	--	--	+++

mRNA level scale : <50 = -- ;100-199 = +; 200-299 = ++; 300-399 = +++; 400-499 = ++++; >500 = +++++

Figure 3. Tissue distribution of R-PTPs during third instar larval stage

Diagram on the left panel shows the major tissues that are undergoing metamorphosis during the transformation from larva to pupa. The relative mRNA level of each R-PTP in these tissues obtained from the Fly Atlas is shown on the right panel. For the purpose of easy visualization, the numerical value of mRNA expression has been converted into a scale of enrichment indicated by the "+" sign. Note that PTP52F was specifically enriched in the midgut.

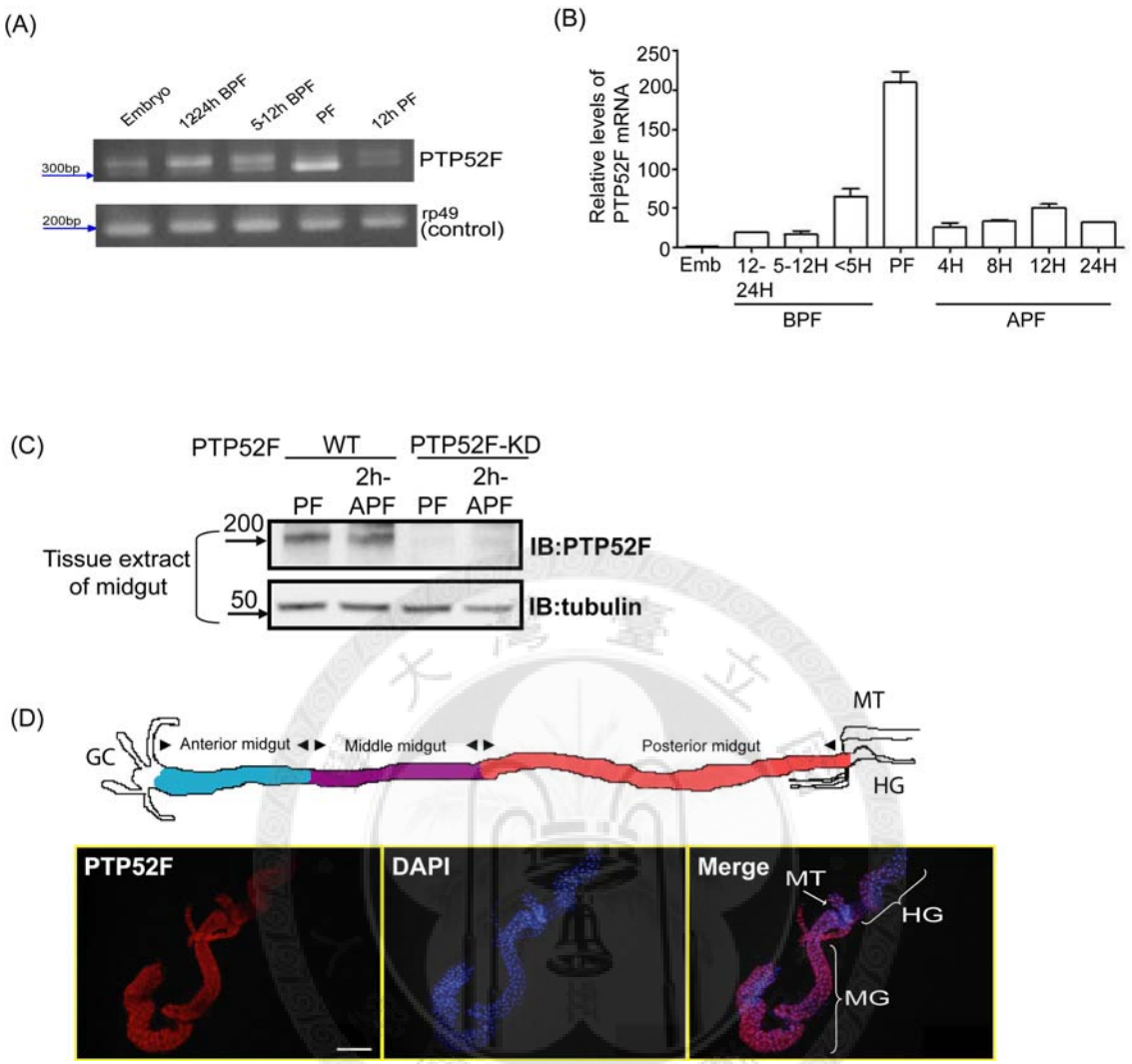

Figure 4. PTP52F is highly enriched in midgut during larva-pupa transition

(A) RT-PCR results showed the increase of *Ptp52F* during the PF stage of development. *rp49* is used as the loading control. (B) Q-PCR results also show the increase of *Ptp52F* during the PF stage of development. (C) The immunoblot of PTP52F from the WT and RNAi flies clearly shows the specificity of the antibody that we have generated for PTP52F. (D) Shows the immunofluorescence staining of PTP52F in the fly midgut with the upper panel showing the anatomy of fly gut. PTP52F is specifically expressed in the midgut and cannot be detected in the hind gut.

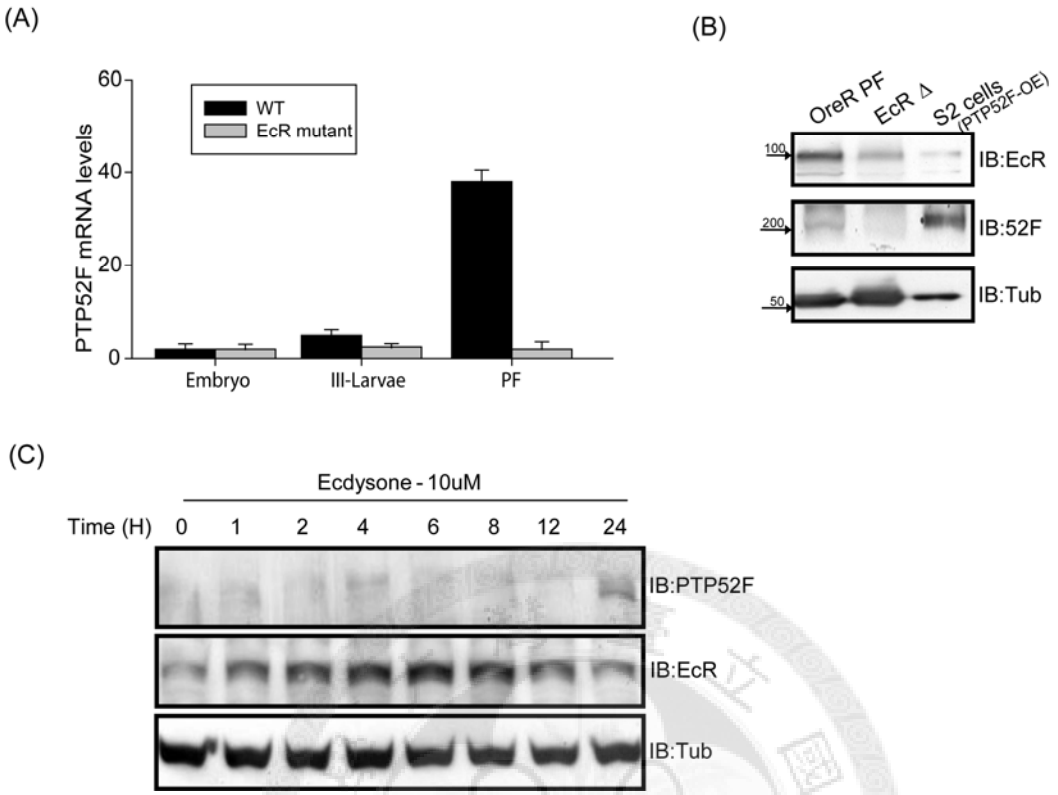

Figure 5. PTP52F is an ecdysone response gene

(A) Real time PCR shows the significant increase of *Ptp52F* in WT fly whereas the EcR heterozygous mutant (4899) cannot show the increase in *Ptp52F* transcript level. The total mRNA was collected from fly tissues during different developmental stages and were used for the Real time PCR analysis. (B) Western blot results show the ecdysone receptor mutant flies do not have comparable amount of endogenous PTP52F when compared to the WT flies. (C) Kc 167 cells were treated with ecdysone for the indicated time and checked for the endogenous PTP52F. Immunoblot results show the ecdysone dependent increase of endogenous PTP52F in cultured Kc167 cells especially at 24H.

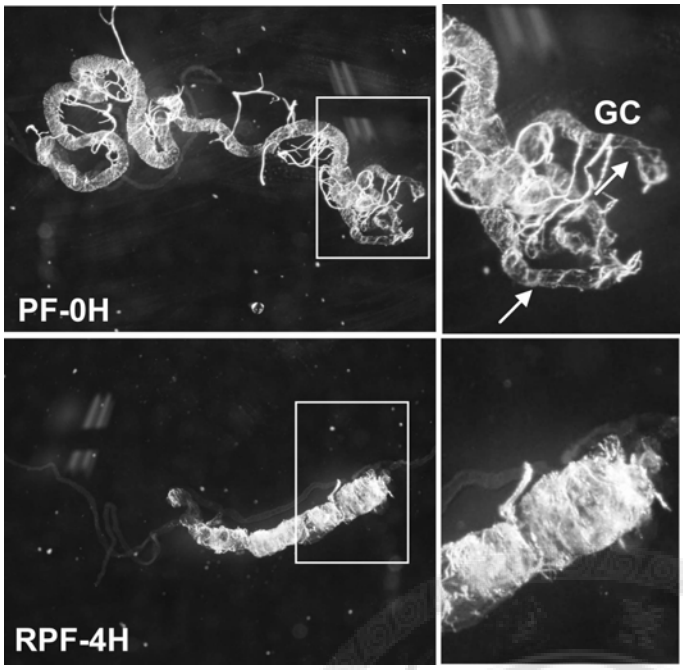

Figure 6. The *Drosophila* midgut undergoes extensive metamorphosis during larva-pupa transition. The midgut undergoes extensive cell death to destruct the larval tissue and regenerate into an adult tissue during larva-pupa transistion. At PF the midgut is highly extended with prominent gastric ceaca. They undergo cell death and become condensed losing its projections at APF- 4H. The zoom in view shows the degradation of gastric ceaca from PF to APF- 4H.

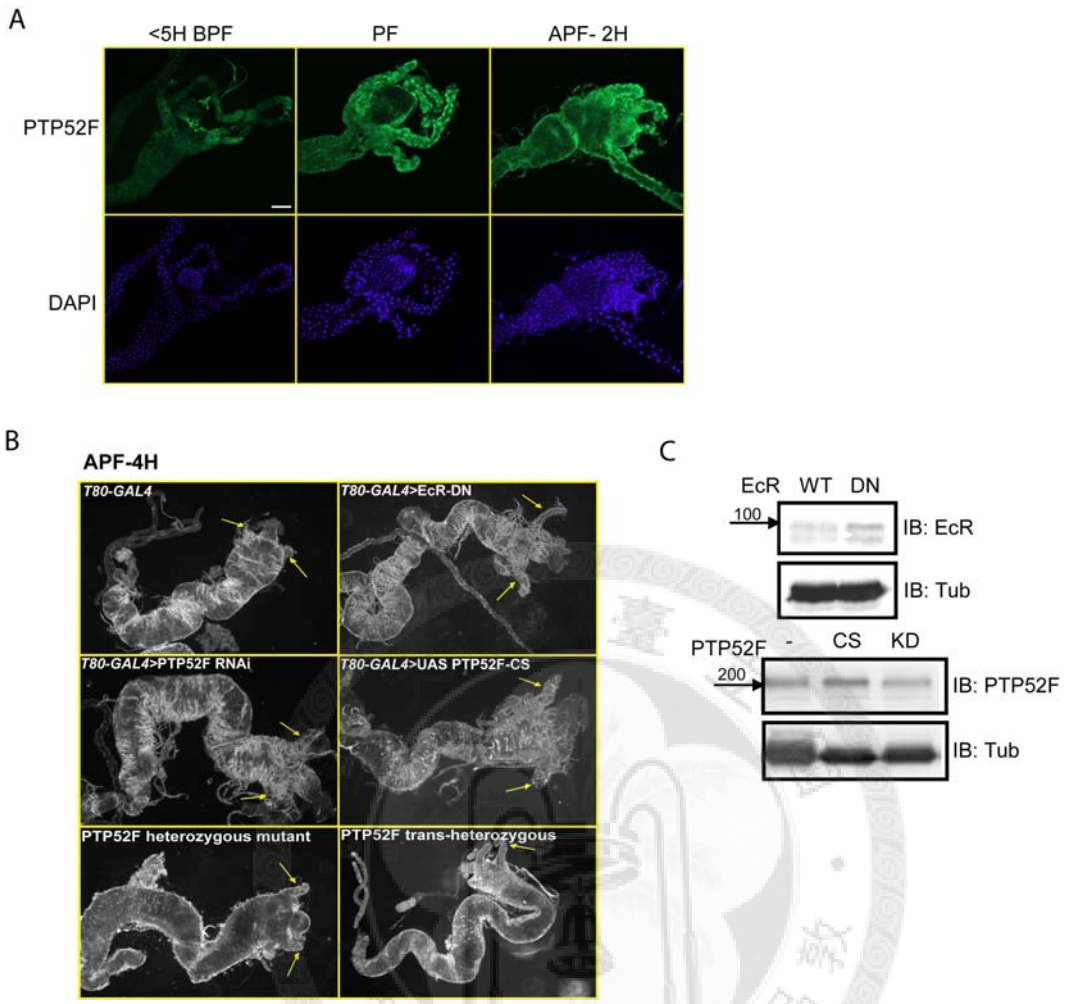

Figure 7. PTP52F is involved in midgut metamorphosis. (A) Midgut was isolated and stained for immunofluorescence as described in materials and methods. The immuno fluorescence data showed the time dependent increase in the levels of endogenous PTP52F (green) in the midgut. The picture shows the close view of gastric ceaca, a part of the midgut that will undergo extensive metamorphosis during larva-pupa transition. (B) Over expression of EcR –DN form results in delayed midgut metamorphosis. At APF-4hrs the gastric ceaca is usually processed from the gut in the WT flies, whereas in the EcR-DN flies they are still seen at APF-4H showing the involvement of ecdysone response in midgut metamorphosis. Knock down of PTP52F and over expression of PTP52F-CS (functionally inactive phosphatase) also resulted in delayed midgut metamorphosis suggesting its involvement in the process. (C) Immunoblot to show the over expression and knockdown of PTP52F and also to show the over expression of EcR-DN.

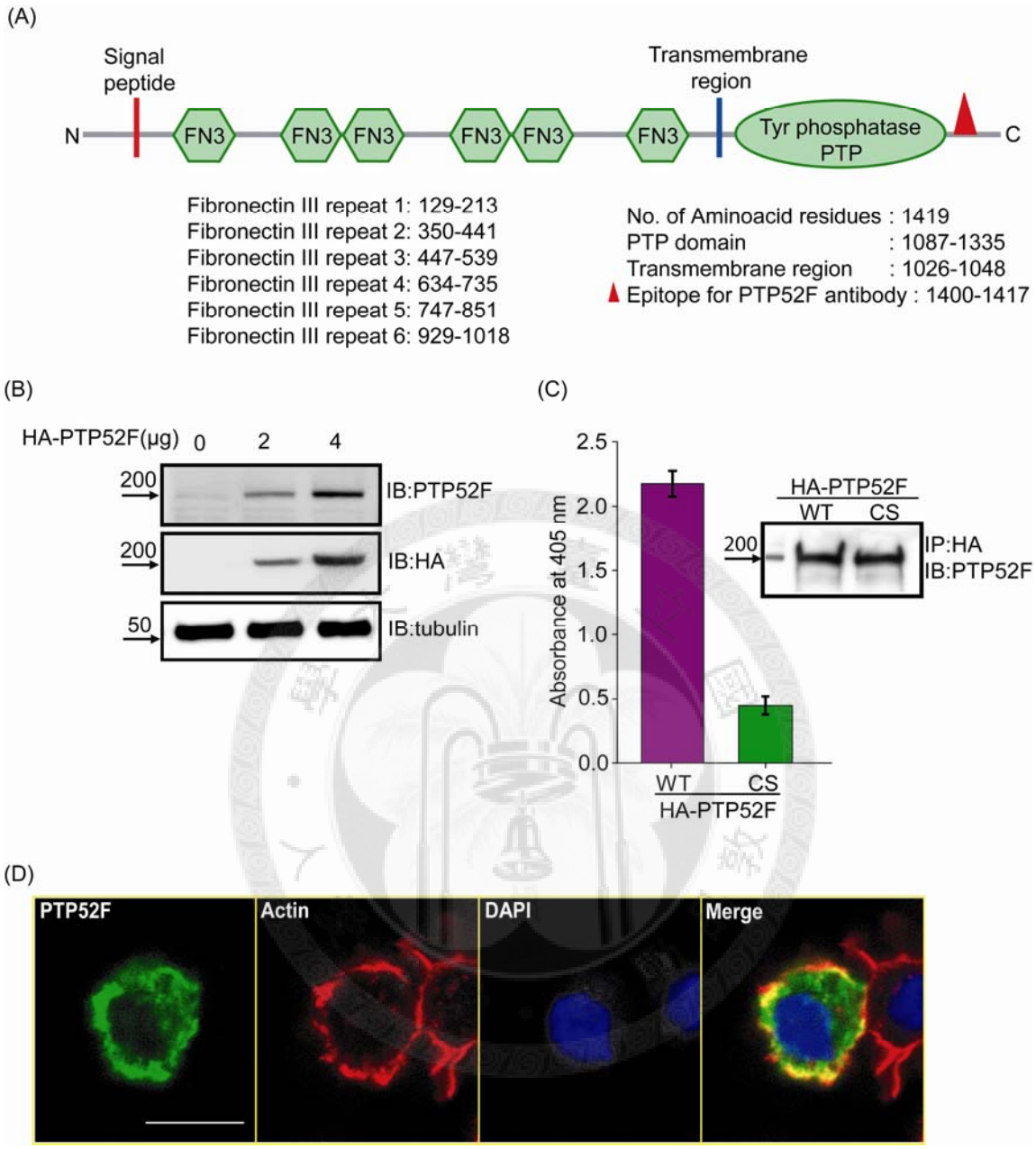

Figure 8. Characterization of PTP52F as an active phosphatase located in cell periphery

(A) The layout of fibronectin III repeats (FN3) and a phosphatase domain in the basic architecture of full-length PTP52F. The motif used as the epitope for antibody generation on the C-terminal region is marked. (B) Various amounts of plasmid were used for expressing the WT form of HA-tagged PTP52F in S2 cells. Aliquots of total lysates were subjected to immunoblotting with anti-PTP52F antibody and anti-HA antibody. (C) The HA-tagged WT form and $C_{1290}S$ mutant form (CS) of full-length PTP52F were expressed

in S2 cells, and then purified by immunoprecipitation with anti-HA antibody. Equal amounts of both WT and CS mutant forms of immunoprecipitated PTP52F were subjected to the phosphatase activity assay using pNPP as a substrate. The inset summarizes the results of immunoblotting with anti-PTP52F antibody. Similar levels of immunoprecipitated PTP52F were used for the activity assay. (D) The WT form of PTP52F was expressed in S2 cells. The subcellular localization of PTP52F was then examined in ConA-coated coverslips by immunofluorescence staining with anti-PTP52F antibody. Co-staining with cortical F-actin showed the clear localization of PTP52F in cell periphery. Bar 10μm.

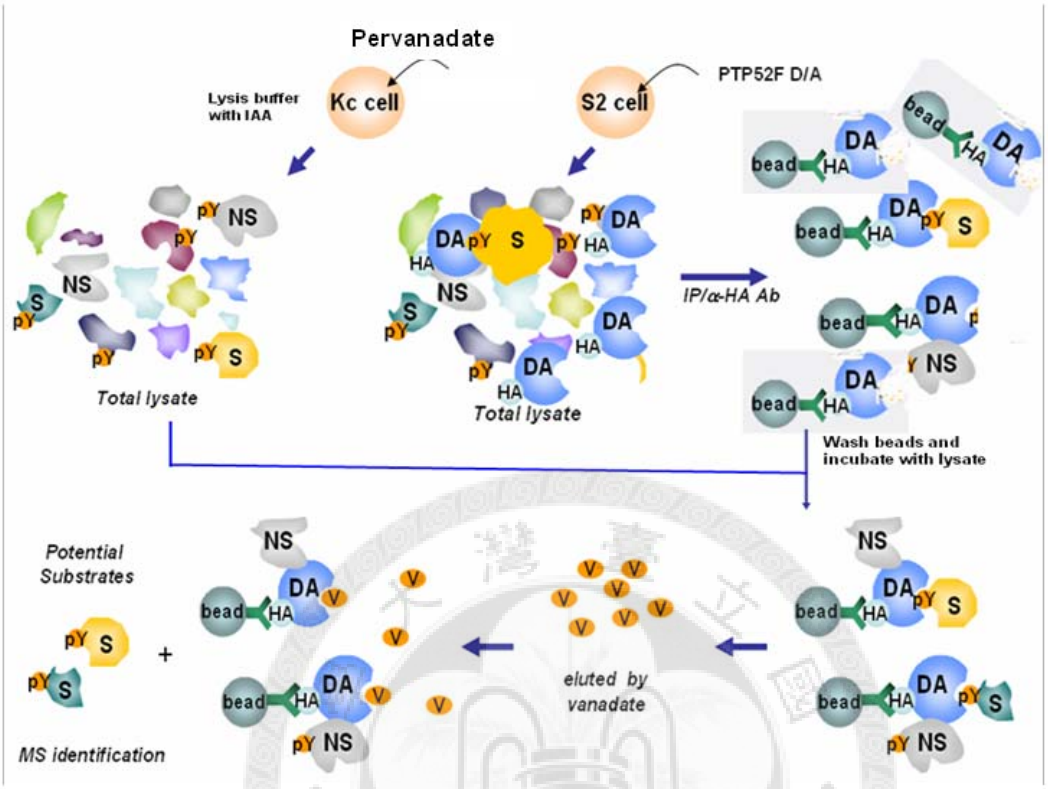

Figure 9. Strategy for MS-based substrate trapping

The work flow of large-scale substrate trapping experiment using pTyr subproteome as a source for identifying potential substrates of PTP. AS described in material and methods PTP52F was ectopically expressed in S2 cells and KC167 cells were used as the substrate source. Kc cells were stimulated with pervanadate and total lysates was collected in the presence of IAA to reversibly inactivate the PTPs. In the meantime ectopically expressed PTP52F-WT and PTP52F-CS/DA mutants were IP from S2 cell lysates and allowed to treat with the substrate source from Kc cells .The specific substrates from the trapping mutants were eluted by the competitive inhibition through vanadate. NS-nonspecifically associated proteins, S-potential substrate, V-vanadate, DA-DA mutant form of PTP52F, HA-HA tag of PTP52F protein. Figure modified from [69].

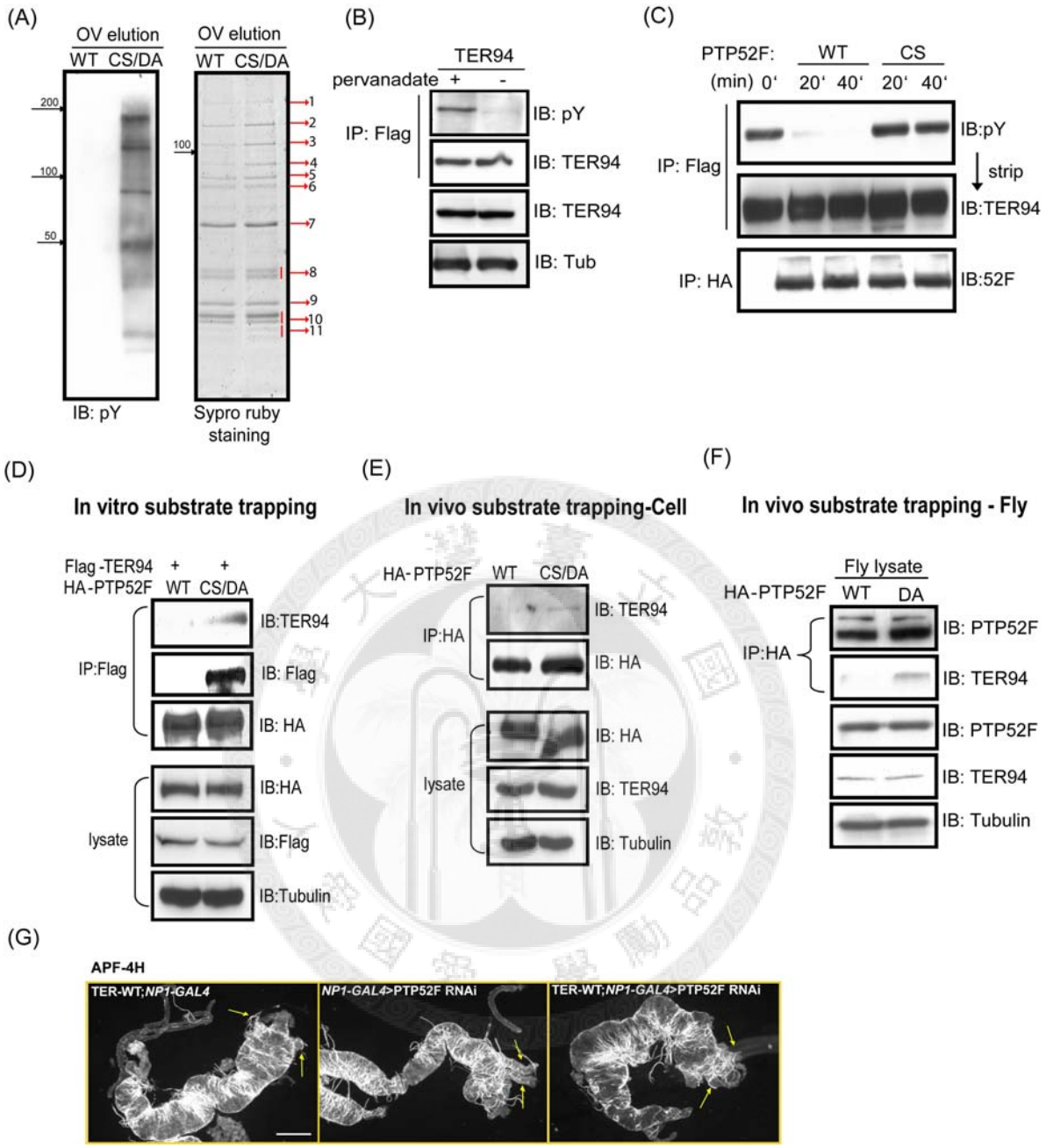

Figure 10. VCP/TER94 ,a potential substrate of PTP52F is also involved in midgut metamorphosis (A) The substrate trapping experiment was carried out as shown in the figure 9 and the IP pull was used for western blot (left panel) and mass spectrometry (right panel) analysis. The pY blot shows the significant trapping of tyrosine phosphorylated proteins by C/S mutant compared to the WT whereas in the sypro ruby staining a band around 90kDa showed significant difference between WT and trapping mutant. Eventhough we analysed all the eleven bands, we proceeded for further

confirmation experiments with band 4 which was identified as TER94. (B) In S2 cells ectopically expressed TER94 treated with pervanadate can be significantly tyrosine phosphorylated. (C) TER94 can be dephosphorylated in vitro by PTP52F-WT and not by the C/S mutant. 40 min showed the complete dephosphorylation. (D) In vitro substrate trapping by PTP52F specifically for TER94. (E) In vivo substrate trapping in which the endogenous TER94 was trapped by PTP52F. Both C and D showed that TER94 can be only trapped by PTP52F-C/S mutant. (F) The delay in midgut metamorphosis in PTP52-KD flies was partially rescued by TER-WT.

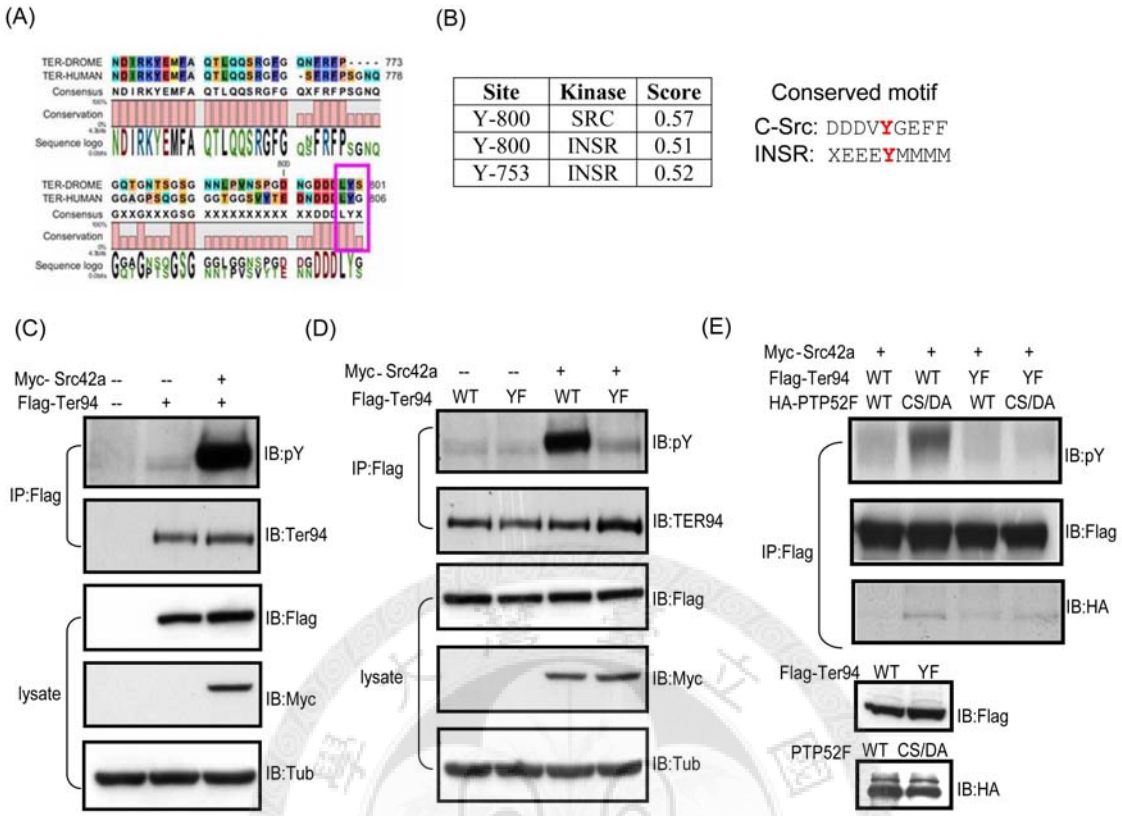

Figure 11. Src 42A is the upstream tyrosine kinase to phosphorylate TER 94 at Y-800. (A) The sequence alignment between TER-94 and VCP (human ortholog of TER94) showed 87% sequence similarity and the c- terminal tyrosine residue that is tyrosine phosphorylated in VCP is also conserved in TER94. (B) Software prediction and conserved motif analysis for possible tyrosine kinase of TER94. (C)Based on the prediction and conserved motif analysis, co- expression of TER94 with Src42A significantly increased the pY of TER94 (left panel). (D)Also the site directed mutagenesis of Y-800 significantly decreased the tyrosine phosphorylation of TER94 by Src kinase suggesting Y-800 as the major site of kinase and phosphatase activity (right panel). (E) Specific substrate trapping experiment for TER94 in which the tyrosine phosphorylation was stimulated by ectopically expressed Src42A rather than pervanadate. The results show that the TER94 phosphorylated by Src can be trapped by PTP52F.

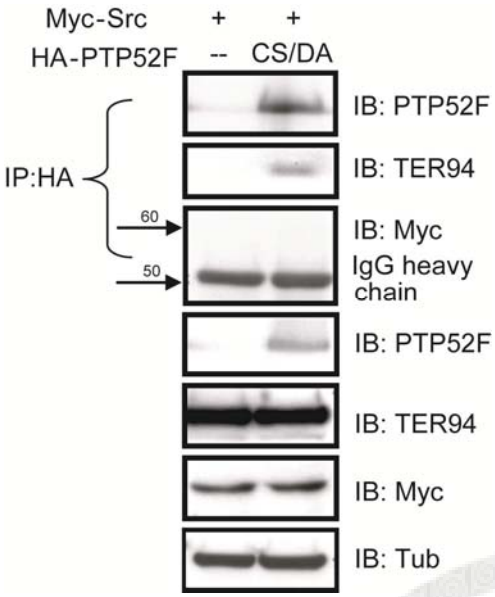

Figure 12. Src42A may not be the substrate of PTP52F

We used the Kc cell to ectopically express PTP52F and Src42A and then collected lysate to check the interaction or association between PTP52F and Src. The specific substrate trapping experiment for Src clearly showed that the PTP52F trapping mutant was not able to trap ectopically expressed Src42A in our system; in the meantime PTP52F can trap the endogenous TER94.

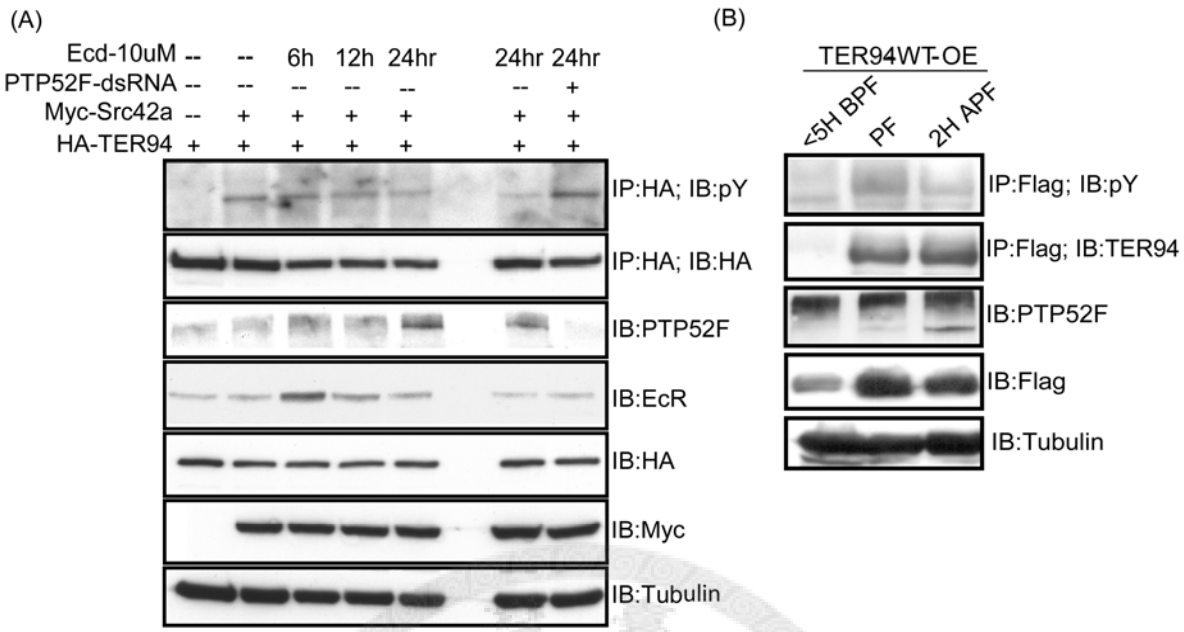

Figure 13. PTP52F dephosphorylates TER94 Tyr(Y)-800 under ecdysone stimulation both in vitro and in vivo (A) Kc cells stimulated with ecdysone for different time points were checked for the change in pY status of TER94 as well as endogenous PTP52F. The immunoblot result shows the change in the TER94 pY, at 24hr the endogenous PTP52F is inducibly expressed leading to the decrease in TER94 pY. (B) The TER94 pY from TER94 over expressing flies showed an increase during PF followed by a decrease at APF-2hr corresponding to the increase in PTP52F.

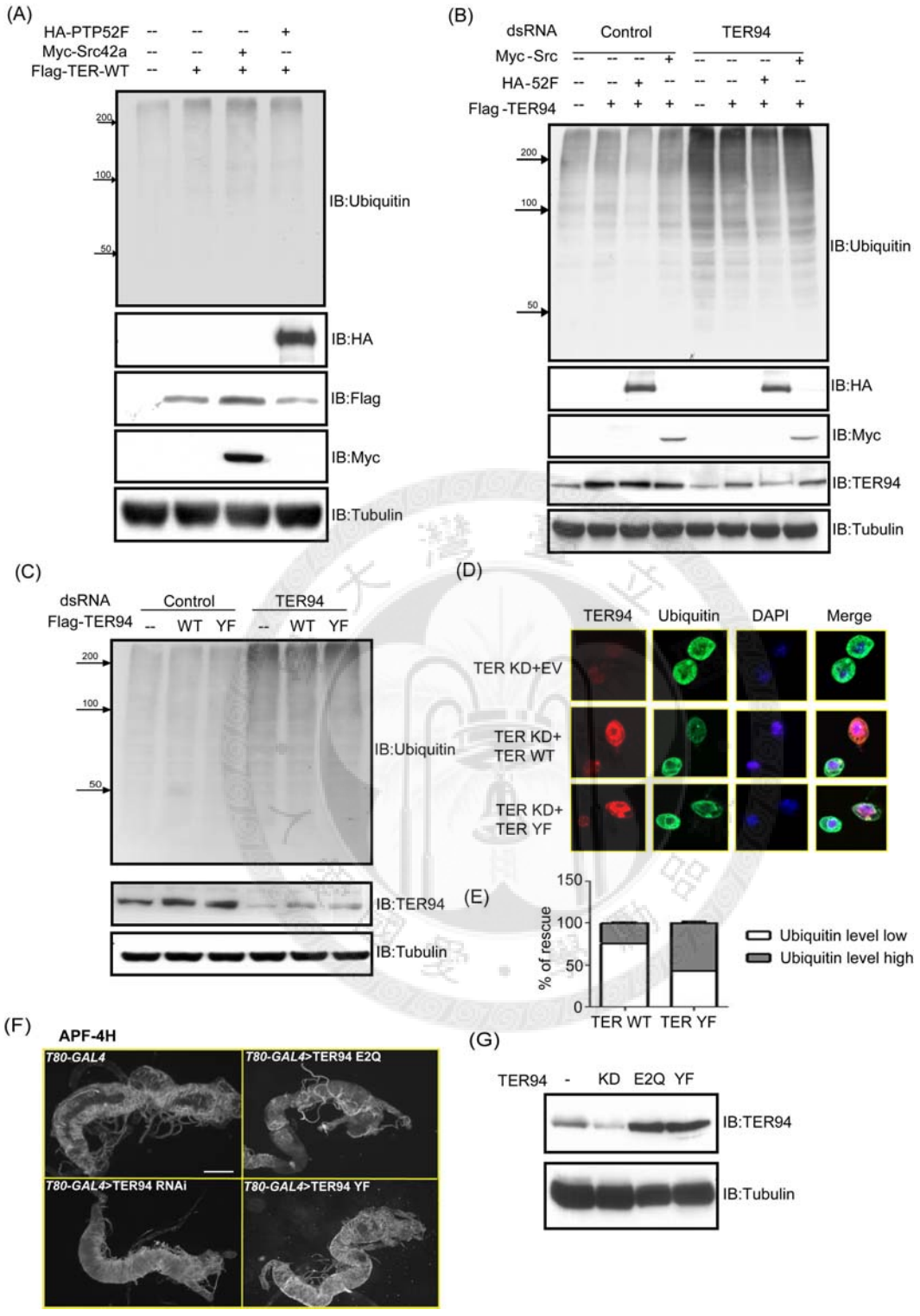

Figure 14. TER94 pY affects its function in ubiquitin-proteasome mediated protein degradation and midgut metamorphosis. (A) The total ubiquitin profile from Kc cells under different conditions of over expression of TER94. TER94 co expressed with

PTP52F shows the lowest ubiquitin accumulation. (B) The total ubiquitin profile under TER94 knockdown followed by rescue with TER94.TER94 knockdown increases the total ubiquitin and rescue effect was best when TER94 was co expressed with PTP52F. (C) Total ubiquitin profile under knockdown of TER94 followed by rescue with TER 94-WT and YF. The rescue is better with WT compared to YF mutant. (D) Similar experiment done to check the ubiquitin levels by immuno fluorescence. The results showed that tyrosine Y-800 is important for the function of TER94. (E) The graph represents the quantitative analysis of the immuno fluorescence data. Totally four hundred cells were counted and classified based on their ubiquitin intensity and TER94 over expression. **(**F)The knockdown of TER94 or the over expression of either TER94 dominant negative or YF mutant results in the delayed midgut metamorphosis as shown by the intact gastric ceaca compared to the control fly. (G) The immuno blot shows the knockdown and over expression of TER94 compared to the control.

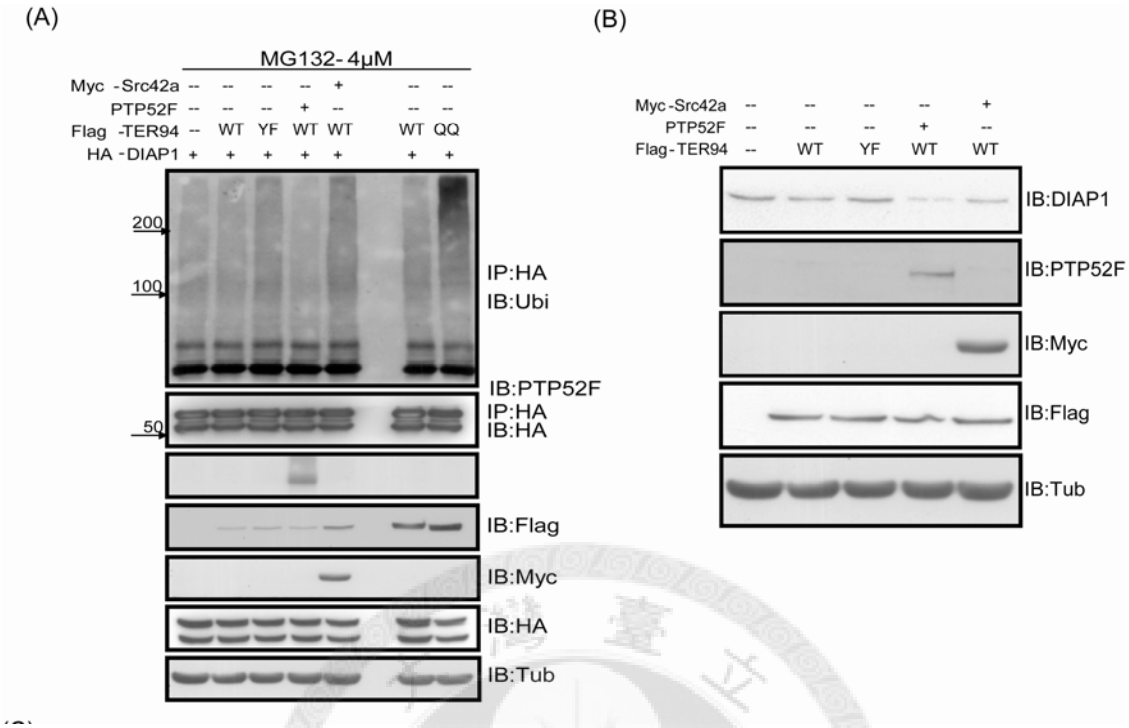

Figure 15.DIAP1 is a specific substrate of TER94 whose degradation is affected by the pY status of TER94 (A) Immuno blot to check the endogenous DIAP1 under different conditions of co expression of TER94. TER94-YF and TER94 co expressed with Src shows the increased accumulation of endogenous DIAP1 compared to TER-WT or TER-WT with PTP52F. (B) Kc cells over expressed with DIAP1 and TER94, the total lysate was used for IP of DIAP1 and checked for the ubiquitin. TER94 –QQ served as a negative control showing the highest levels of accumulation of ubiquitinated DIAP1. Dephosphorylated TER94 shows the lowest accumulation of ubiquitinated DIAP1 suggesting its effective degradation.

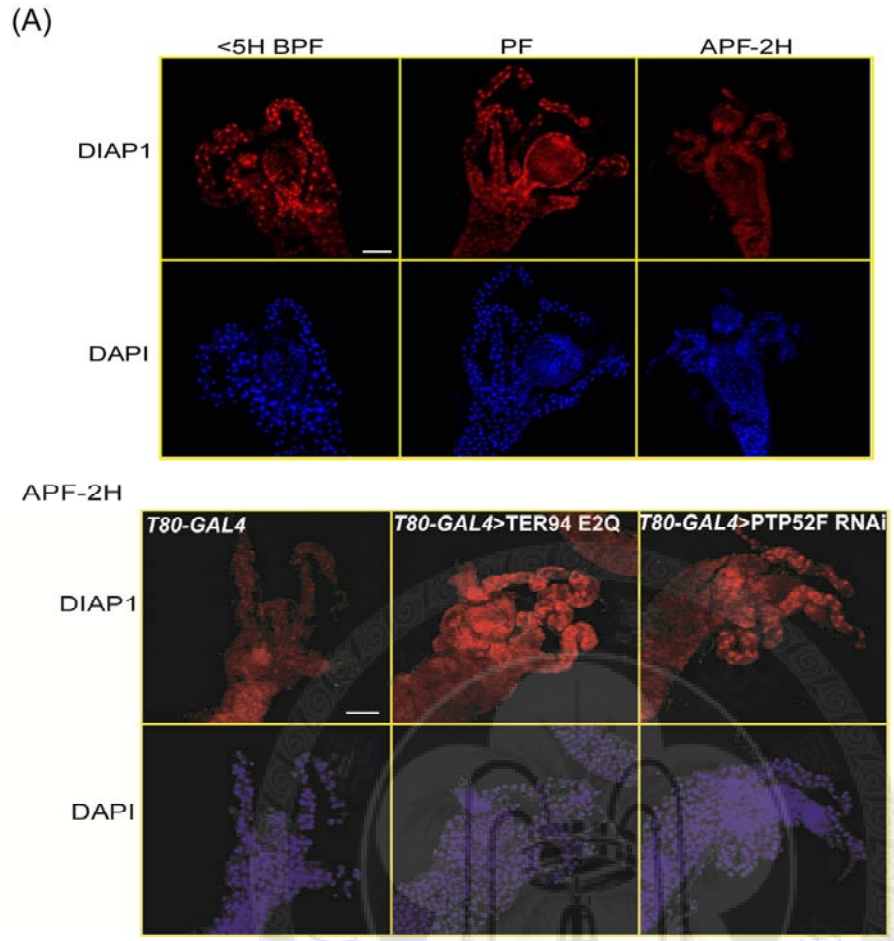

Figure 16. DIAP1 staining in midgut during larva-pupa transition in control flies

(A) Midguts were isolated from third instar larva to PF stages as described in materials and methods and used for DIAP1 immunostaining. Endogenous DIAP1 was rapidly degraded during larva- pupa transition. At APF-2H the endogenous DIAP1 is mostly degraded compared to the PF. (B) At APF -2H we checked the endogenous DIAP1 in TER94-DN flies and PTP52F knockdown flies. DIAP1 was still accumulated in the midgut in TER94-DN over expression and PTP52F knockdown flies compared to the control.

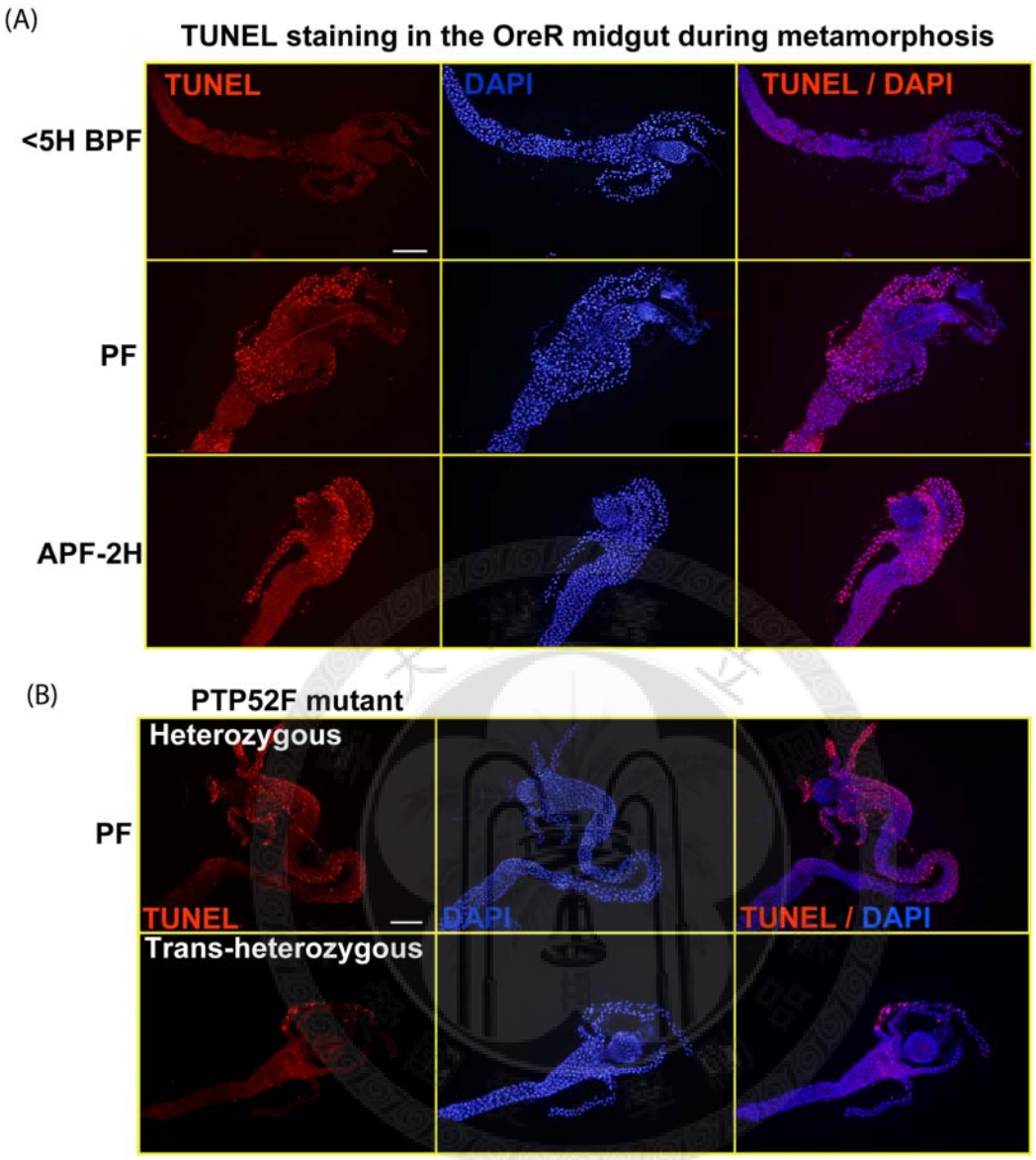

Figure 17.TUNEL staining shows cell death delay in PTP52F knockdown flies. (A) TUNEL staining was used to demonstrate the cell death during midgut metamorphosis. TUNEL staining in the midgut during larva pupa transition shows the gradual increase of positive TUNEL nuclei indicating the increase in cell death during larva-pupa transition in control flies. (B) TUNEL staining showed very few TUNEL positive nuclei in PTP52F trans-heterozygous mutant flies corresponding to the delayed cell death in PTP52F mutant flies compared to the PTP52F heterozygous mutant flies.

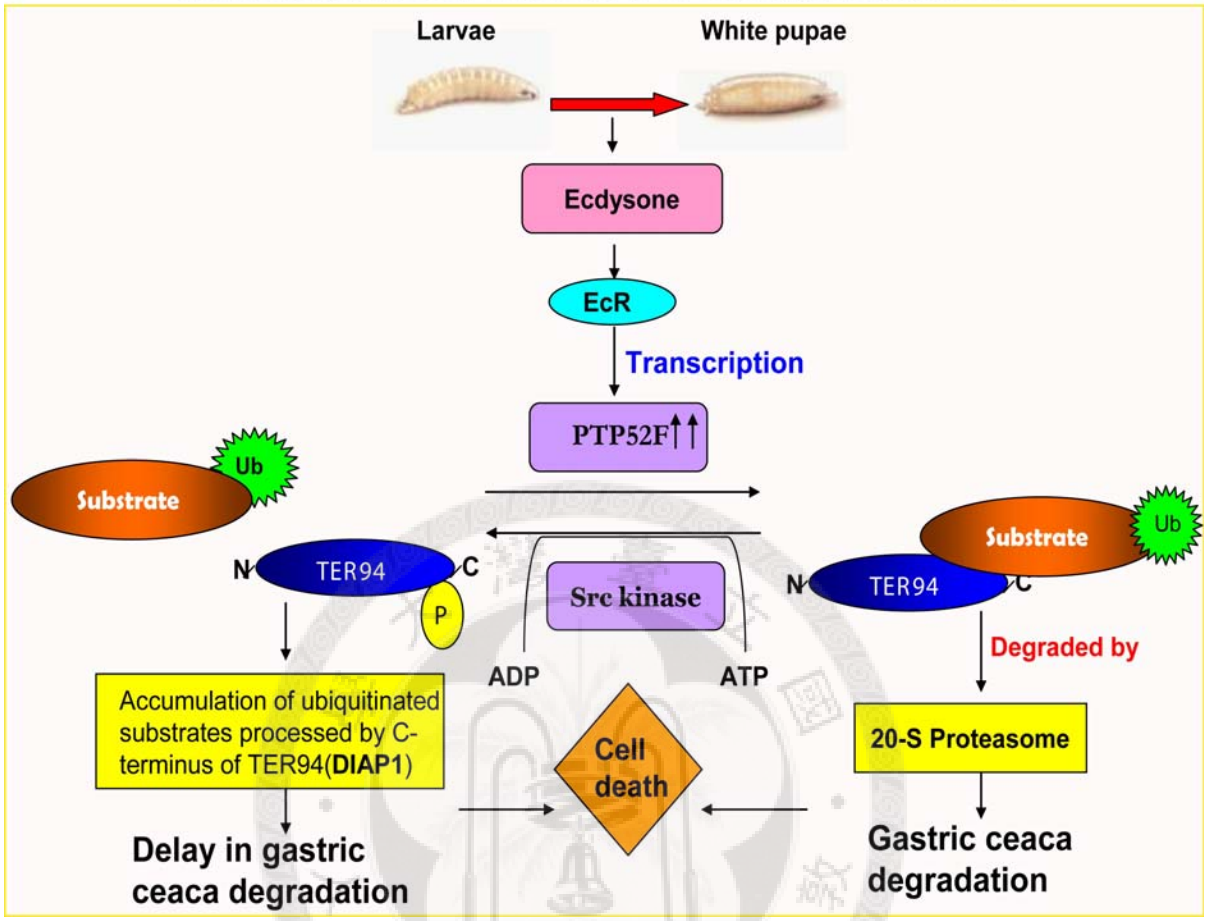

Figure 18. Proposed pathway through which PTP52F can mediate midgut metamorphosis.

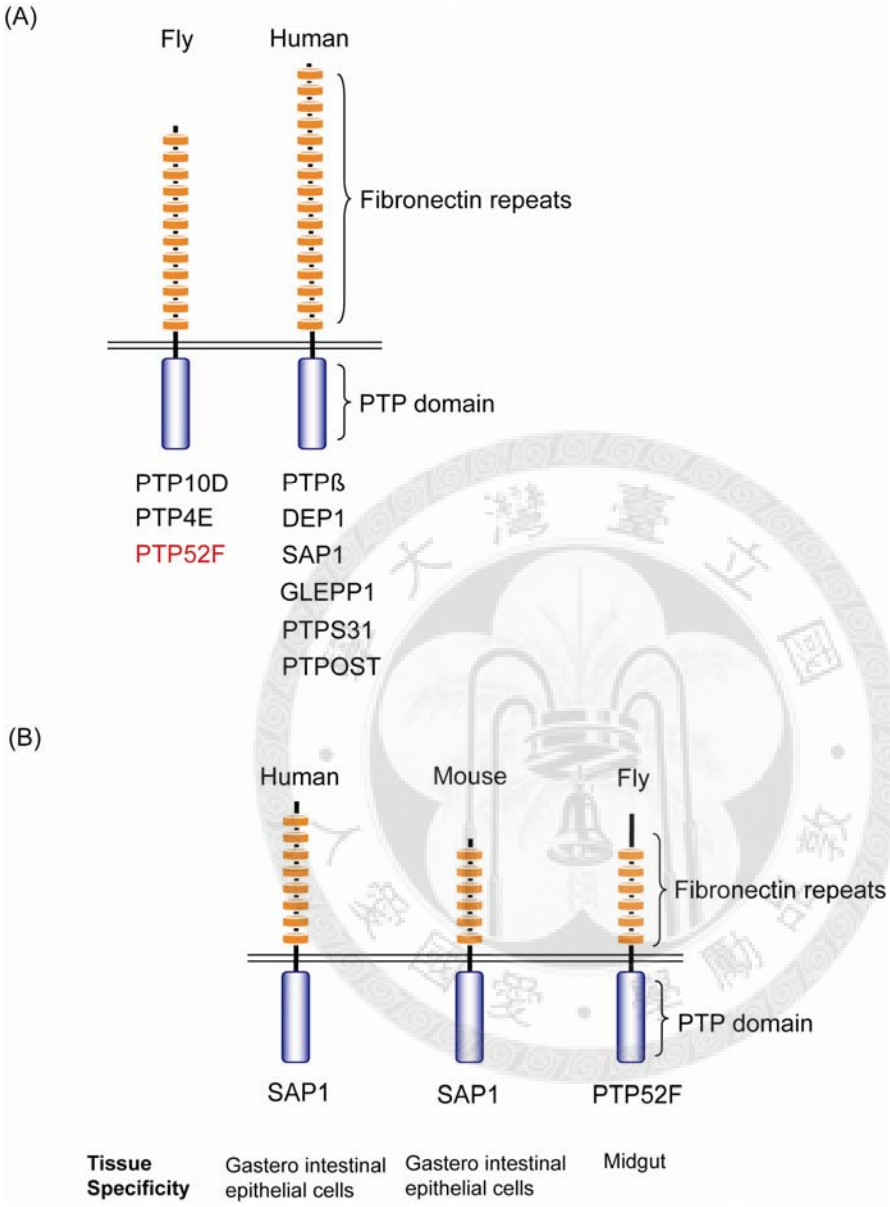

Figure 19. Reclassification of PTP52F as a member of subtype R3 PTPs

(A) Sequence analysis suggests that PTP52F, together with PTP10D and PTP4E, belongs to the subtype R3 in the PTP super family. There are six members of human R-PTPs in this subtype. (B) A proposed model showing that PTP52F might be the functional ortholog of human and mouse SAP-1.

(A)

AATTTTAAATGGTTTTGGGTGGGCGTGAGAGCGAGATAGTTGGCAAGGGG
CATAGACCAGGGCTGCAACGAACACACACACACACACAGTAAGGTCTTGA
ATTTTAAGGATCTTTCTCTTCCTCTCACTCCCCCTTTCGTTTGAATTCGC
TTGCTTATTCTCTCTCTCCCGCTCTGGCAAACAGACCTTGCACTTGCCTT
TGCTTGTTTATTTGCGTGTTTCATTGATTAGCACACACTCACACACGCGC
CGGCGAGCAAATGCAATTGCAATTTCAAGTGCAAAAAGAGAGAGGAAAAA
GGAAAACAATAGCCAAAAAAGCTT**TGAACTCCAGCTTTAACCC**CACGACG
GGCATCGAATGCAGGGACTAACCGTTAAGTGCCGAGACTTTTTGCTTTGC
CTTTCTTTAACCCACTGCTGGAAACGTGCAAAAAGCTCGTCACTAGATAA
TAGAAACAATTTGCAGTGTCAGGAGCGCTTTCCACACATTCTGGGAAATC
GCAACGGGTCTTGAATATCTAAAAGAATGCCGCAGCAAAAAAGCCCAAAA
CGGAAAACTGTAAAAAAAAAACAAAAACAACTACACAAGCACAACGAAGA
AAATAAAACGAGATTTCTTGTGCATTGGCAGAACTGGTTTGCCCAGTAAT
AGGTGTTGTTGGCCTATGGGGGAACGGGAAGTACATATATGCAAGGAATC
GGCCAGTTCGGGGACTCGACTTGGCTAAAAATCGATCAATTCTACTTTTG
GCGAGGGGGAGGACTCCAAACATGCGCGAAAATCCACAGACATCGTCACT
CGCACACACACACACACTCGCGCACGCACACCAACGCACTCGATGTGTCA
TCGCTTTCTGGTGGTTGTAAATAAAATGTAATCATAGTTCGTTTCTCCAC
TTATTTACTGATCGTCTTTTTGTTCAACACACTACTTTTTTTTGTGCATAA
TTTGCATAACTCTTTCGCTTGTTTTTTCATTCTCTTTTCAATAACAAACA
CAATAACAACAACAGTTTGAACGAAAATACTGTTACGACGGCCATCTTGG
ATAGAGAGAGGGGGCCAAGAGAAAGAAATGTCCCAAAGGCAATATGCATA
ATGGGGAAAAAGGACAAATATCCAAGCGCACATATAGTATATTATATTTT
CCGACTCCAACCGACATGCTTGGTACATAATGCGCGAACTAACACTTTGC
CATTGGCAGTTTTGTACATATGACGTTTTTTTTTCTTCATTTCTCCCAAT
AGCCCATTACACGGGTTGGTTGCGAAAAATCCATTTTGCTTGGGTGTTCT
ATTTACAACGCGGCGACTCGGTGTTTGTTCTTATTATGCAGCGAACGTTA
CTTACAACAATTTAGTATTTCATATATTTATAATTACGCTTATTTATTTA
TGTTTAATCGAAATATACGAAAAGAATTACGCAGAAAAGTGACGAGCGGA
CGAAAATGCTTCGATTAGTG**TGACCGCAGTGGAAGCAGCTCA**AAAAACAT
CACGGGACTATCGATGACAGCGATTAGCTATCGATGTGACTAGGAATGTA
GAAAAATGTTAATAAAAATATGTATAATAACTTCTAAATACTTTTTATAT
CTTATATAAGACCTAAGGACTGAAACCATTGAGTAAAGAACGAGTTGCCA
TAACTTAAGCCCTACTTCCATGCAAGCGCAGTGTGAACAGCTTAAAAAAT
TGGCGCGCTATTTAAAATGCTGATAAGGAAATGGACCTTCGTCAGCTTTT
TTTTTGCGGAACCACAACGCCTATCCGTGAGTGAACAAAATGGGTTTCCA
ATTATTTATGCCATATAAGTATTGCTATTTATTTATAACACATCCCAATT
CGATAGTCAACACTGCAGTTTGCTAATTGTAAACCGACTTTGTTGTTATC
TTACACACACATTCGCGATGGGAGTAAACTTTCCTTATCACCGCTCACAC
AGCGCCAGAACACAACACAACCGATTTATGGAGTGCTCCCTTTGGCGCTC
AGTATTCGAGAATCGCTCAGCGGAAACGGTTATTAGTTTACTGATTTTCG
GGCGACACACACACATTCGTTATTCATAGTTGGTGCGCCCAAATATTCGC
GAAACAGCAACAACAATTAGCAACCATCTGTCACCTGTGAGTGCAGCGTA

(B)

Consensus motif of steroid hormone response element

PuG(G/T)TCA (Xn) PuG(G/T)TCA - Direct (DR)
TGA(A/C)CPy (Xn) PuG(G/T)TCA - Everted (ER)

5'-**TGAACT**ccagctt**TAACCC**-3' -Predicted steroid hormone response element-1
5'-**GGGTTA**aagctgg**AGTTCA**-3' -Reverse complementary of response element-1 (DR)
5'-**TGACCG**cagtggaagc**AGCTCA**-3' - Predicted steroid hormone response element-2 (ER)

Figure 20. Identification of potential ecdysone response elements in the promoter region of *Ptp52F* gene

(A) The sequence shown indicates the -2 kb region upstream from the first exon (bold with underline) of *Ptp52F* gene. The sequence of this region was subjected to the analysis for the potential ecdysone response elements using the **NUBIScan 2.0** software

(http://www.nubiscan.unibas.ch/). This *in silico* tool predicts nuclear receptor response elements. We used the FXR-38 matrix algorithm for the analysis because this matrix includes EcR along with other farnesoid hormone receptors. When a threshold of 0.5 was used, more than 60 hits were obtained. Hence,the stringency was further increased until the threshold reached to 0.7, at which only two possible elements were reported and are marked in the sequence (bold, underline with gray highlight). (B) Sequence comparison of the potential ecdysone response elements in *Ptp52F* gene with the consensus steroid hormone response motifs. As shown, the reverse complementary sequence of the predicted ecdysone response element-1 identified in *Ptp52F* gene is highly similar to the direct repeat (DR), whereas the predicted ecdysone response element-2 is similar to the everted repeat (ER).

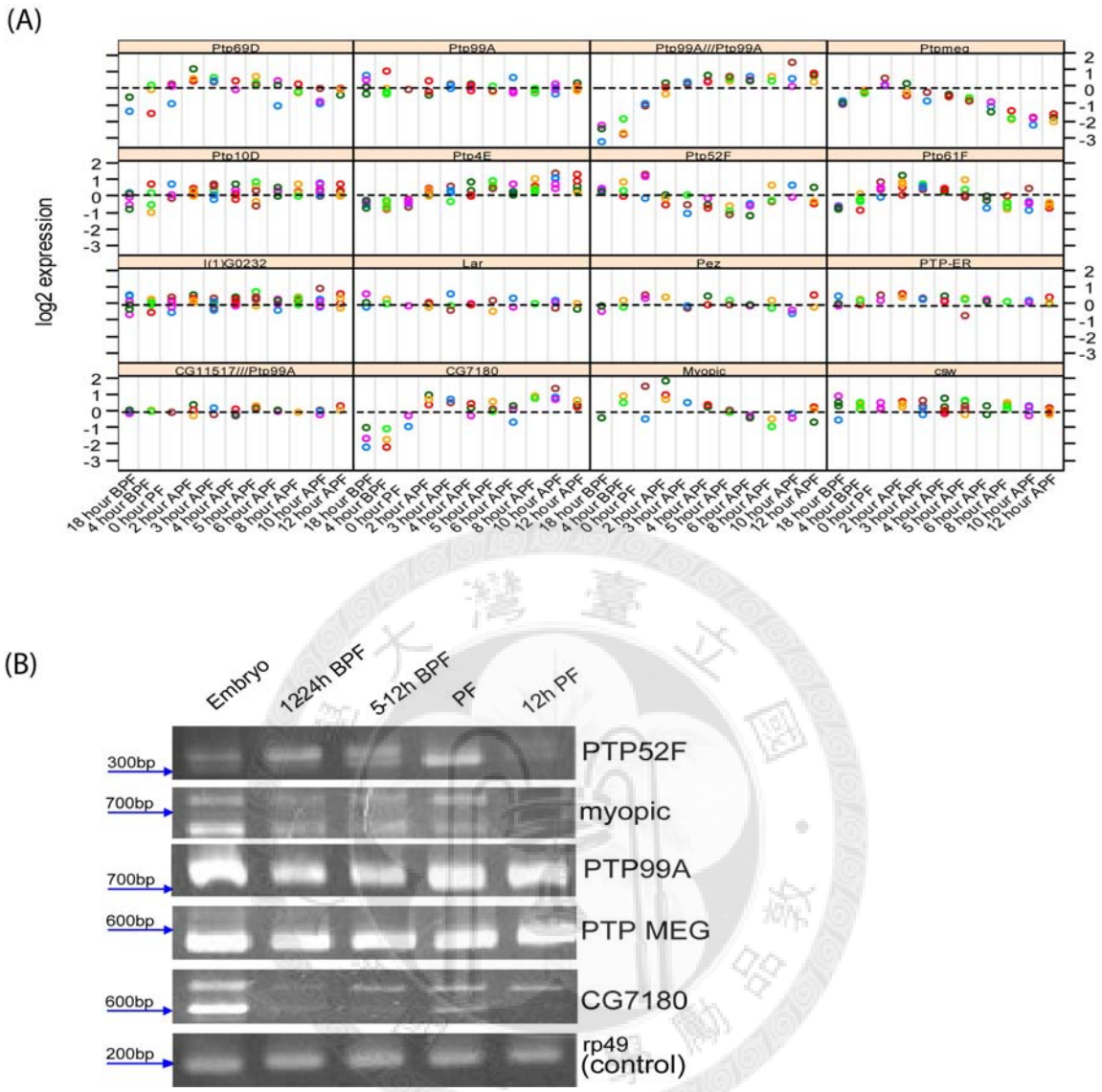

Figure 22. Microarray datamining of PTPs during larva-pupa transistion

(A) Microarray datamining of PTPs during larva-pupa transistion showed significant changes in five PTPs including PTP52F, PTP99A, PTP MEG, myopic and CG7180. (B) RT-PCR analysis for five PTPs based on the micro array data mining. PTP52F showed a significant increase during larva-pupa transition. All primers were designed to differentiate products from genomic DNA and cDNA.

(A)

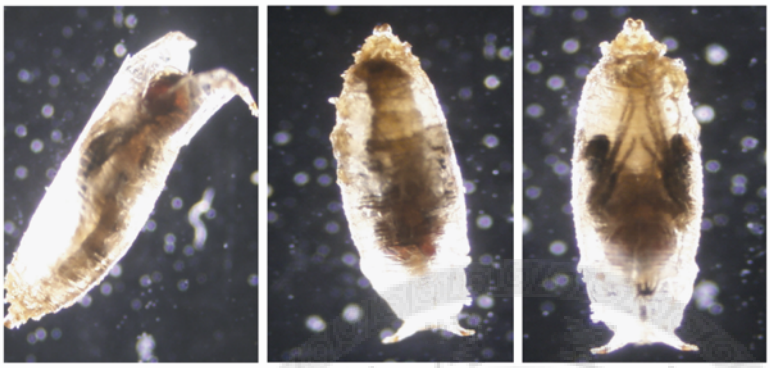

(B)

Analysis of lethality in *Tubulin-Gal4*>PTP52F-KD (n = 200)

Stage	Percentage
Early Pupa	17
Pharate adult	53
Die during eclosion	17
Eclose and die	13
Total	100

Figure 22. Ablation of endogenous PTP52F via RNAi led to pupal lethality

(A) The pharate adult phenotype was observed when endogenous PTP52F expression was knocked down by the *Tubulin-Gal4* driver. (B) The table summarizes the lethal phase analysis of PTP52F knockdown flies. Note that over than 50% of flies died as pharate adults. Most flies developed until the pupal stage but then died due to eclosion failure. Only a small fraction of flies (13%) died upon the completion of eclosion.

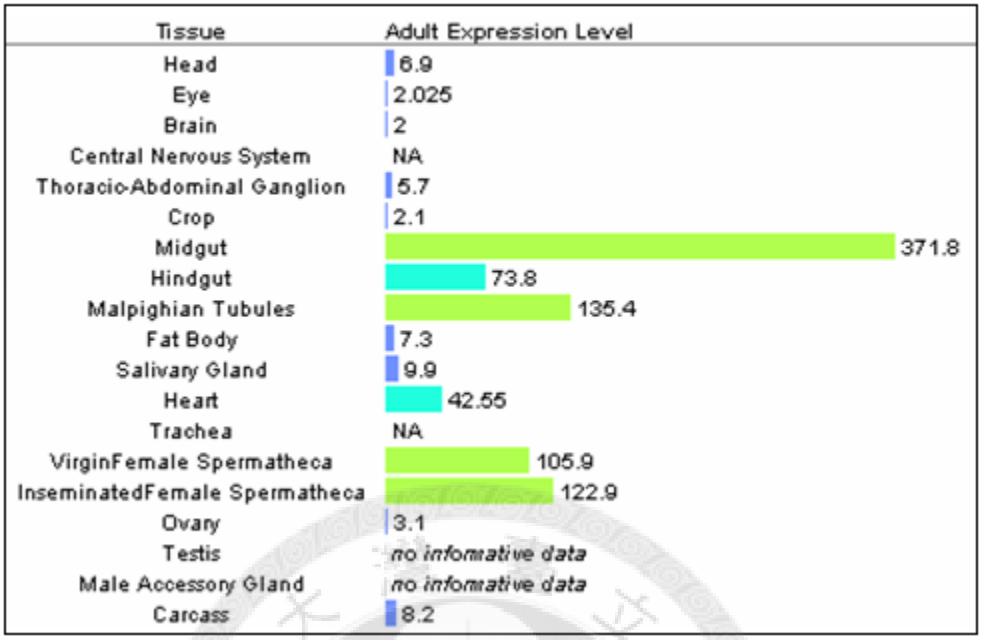

Figure 23. PTP52F is highly expressed in the midgut in adult flies

We also analysed the levels of PTP52F in different tissues in adult flies. It is seen from the data that PTP52F is highly enriched in the midgut, malphigian tubules and not in the CNS. This suggests more functions for PTP52F in the adult midgut.

CHAPTER 6: REFERENCES

1. Lemmon, M. A. & Schlessinger, J. (2010) Cell signaling by receptor tyrosine kinases, *Cell.* **141**, 1117-34.

2. Tonks, N. K. (2005) Redox redux: revisiting PTPs and the control of cell signaling, *Cell.* **121**, 667-70.

3. Schlessinger, J. (2000) Cell signaling by receptor tyrosine kinases, *Cell.* **103**, 211-25.

4. Neel, B. G. & Tonks, N. K. (1997) Protein tyrosine phosphatases in signal transduction, *Current opinion in cell biology.* **9**, 193-204.

5. Tonks, N. K. (2006) Protein tyrosine phosphatases: from genes, to function, to disease, *Nature reviews Molecular cell biology.* **7**, 833-46.

6. Streuli, M., Krueger, N. X., Thai, T., Tang, M. & Saito, H. (1990) Distinct functional roles of the two intracellular phosphatase like domains of the receptor-linked protein tyrosine phosphatases LCA and LAR, *The EMBO journal.* **9**, 2399-407.

7. Blanchetot, C., Tertoolen, L. G., Overvoorde, J. & den Hertog, J. (2002) Intra- and intermolecular interactions between intracellular domains of receptor protein-tyrosine phosphatases, *The Journal of biological chemistry.* **277**, 47263-9.

8. Garton, A. J., Burnham, M. R., Bouton, A. H. & Tonks, N. K. (1997) Association of PTP-PEST with the SH3 domain of p130cas; a novel mechanism of protein tyrosine phosphatase substrate recognition, *Oncogene.* **15**, 877-85.

9. Lahiry, P., Torkamani, A., Schork, N. J. & Hegele, R. A. (2010) Kinase mutations in human disease: interpreting genotype-phenotype relationships, *Nature reviews Genetics.* **11**, 60-74.

10. Rikova, K., Guo, A., Zeng, Q., Possemato, A., Yu, J., Haack, H., Nardone, J., Lee, K., Reeves, C., Li, Y., Hu, Y., Tan, Z., Stokes, M., Sullivan, L., Mitchell, J., Wetzel, R., Macneill, J., Ren, J. M., Yuan, J., Bakalarski, C. E., Villen, J., Kornhauser, J. M., Smith, B., Li, D., Zhou, X., Gygi, S. P., Gu, T. L., Polakiewicz, R. D., Rush, J. & Comb, M. J. (2007) Global survey of phosphotyrosine signaling identifies oncogenic kinases in lung cancer, *Cell.* **131**, 1190-203.

11. Flint, A. J., Tiganis, T., Barford, D. & Tonks, N. K. (1997) Development of "substrate-trapping" mutants to identify physiological substrates of protein tyrosine

phosphatases, *Proceedings of the National Academy of Sciences of the United States of America.* **94**, 1680-5.

12. Blanchetot, C., Chagnon, M., Dube, N., Halle, M. & Tremblay, M. L. (2005) Substrate-trapping techniques in the identification of cellular PTP targets, *Methods.* **35**, 44-53.

13. Elchebly, M., Payette, P., Michaliszyn, E., Cromlish, W., Collins, S., Loy, A. L., Normandin, D., Cheng, A., Himms-Hagen, J., Chan, C. C., Ramachandran, C., Gresser, M. J., Tremblay, M. L. & Kennedy, B. P. (1999) Increased insulin sensitivity and obesity resistance in mice lacking the protein tyrosine phosphatase-1B gene, *Science.* **283**, 1544-8.

14. Klaman, L. D., Boss, O., Peroni, O. D., Kim, J. K., Martino, J. L., Zabolotny, J. M., Moghal, N., Lubkin, M., Kim, Y. B., Sharpe, A. H., Stricker-Krongrad, A., Shulman, G. I., Neel, B. G. & Kahn, B. B. (2000) Increased energy expenditure, decreased adiposity, and tissue-specific insulin sensitivity in protein-tyrosine phosphatase 1B-deficient mice, *Molecular and cellular biology.* **20**, 5479-89.

15. Cheng, A., Uetani, N., Simoncic, P. D., Chaubey, V. P., Lee-Loy, A., McGlade, C. J., Kennedy, B. P. & Tremblay, M. L. (2002) Attenuation of leptin action and regulation of obesity by protein tyrosine phosphatase 1B, *Developmental cell.* **2**, 497-503.

16. Myers, M. P., Andersen, J. N., Cheng, A., Tremblay, M. L., Horvath, C. M., Parisien, J. P., Salmeen, A., Barford, D. & Tonks, N. K. (2001) TYK2 and JAK2 are substrates of protein-tyrosine phosphatase 1B, *The Journal of biological chemistry.* **276**, 47771-4.

17. Zabolotny, J. M., Bence-Hanulec, K. K., Stricker-Krongrad, A., Haj, F., Wang, Y., Minokoshi, Y., Kim, Y. B., Elmquist, J. K., Tartaglia, L. A., Kahn, B. B. & Neel, B. G. (2002) PTP1B regulates leptin signal transduction in vivo, *Developmental cell.* **2**, 489-95.

18. Julien, S. G., Dube, N., Read, M., Penney, J., Paquet, M., Han, Y., Kennedy, B. P., Muller, W. J. & Tremblay, M. L. (2007) Protein tyrosine phosphatase 1B deficiency or inhibition delays ErbB2-induced mammary tumorigenesis and protects from lung metastasis, *Nature genetics.* **39**, 338-46.

19. Wiede, F., Shields, B. J., Chew, S. H., Kyparissoudis, K., van Vliet, C., Galic, S., Tremblay, M. L., Russell, S. M., Godfrey, D. I. & Tiganis, T. (2011) T cell protein

tyrosine phosphatase attenuates T cell signaling to maintain tolerance in mice, *The Journal of clinical investigation.* **121**, 4758-74.

20. Higashi, H., Tsutsumi, R., Muto, S., Sugiyama, T., Azuma, T., Asaka, M. & Hatakeyama, M. (2002) SHP-2 tyrosine phosphatase as an intracellular target of Helicobacter pylori CagA protein, *Science.* **295**, 683-6.

21. Tartaglia, M., Mehler, E. L., Goldberg, R., Zampino, G., Brunner, H. G., Kremer, H., van der Burgt, I., Crosby, A. H., Ion, A., Jeffery, S., Kalidas, K., Patton, M. A., Kucherlapati, R. S. & Gelb, B. D. (2001) Mutations in PTPN11, encoding the protein tyrosine phosphatase SHP-2, cause Noonan syndrome, *Nature genetics.* **29**, 465-8.

22. Sun, W., Shen, Y. H., Qi, D. W., Xiang, Z. H. & Zhang, Z. (2012) Molecular cloning and characterization of Ecdysone oxidase and 3-dehydroecdysone-3alpha-reductase involved in the ecdysone inactivation pathway of silkworm, Bombyx mori, *International journal of biological sciences.* **8**, 125-38.

23. Stewart, R. A., Sanda, T., Widlund, H. R., Zhu, S., Swanson, K. D., Hurley, A. D., Bentires-Alj, M., Fisher, D. E., Kontaridis, M. I., Look, A. T. & Neel, B. G. (2010) Phosphatase-dependent and -independent functions of Shp2 in neural crest cells underlie LEOPARD syndrome pathogenesis, *Developmental cell.* **18**, 750-62.

24. Uetani, N., Chagnon, M. J., Kennedy, T. E., Iwakura, Y. & Tremblay, M. L. (2006) Mammalian motoneuron axon targeting requires receptor protein tyrosine phosphatases sigma and delta, *The Journal of neuroscience : the official journal of the Society for Neuroscience.* **26**, 5872-80.

25. Thompson, K. M., Uetani, N., Manitt, C., Elchebly, M., Tremblay, M. L. & Kennedy, T. E. (2003) Receptor protein tyrosine phosphatase sigma inhibits axonal regeneration and the rate of axon extension, *Molecular and cellular neurosciences.* **23**, 681-92.

26. Sapieha, P. S., Duplan, L., Uetani, N., Joly, S., Tremblay, M. L., Kennedy, T. E. & Di Polo, A. (2005) Receptor protein tyrosine phosphatase sigma inhibits axon regrowth in the adult injured CNS, *Molecular and cellular neurosciences.* **28**, 625-35.

27. Bartscherer, K., Pelte, N., Ingelfinger, D. & Boutros, M. (2006) Secretion of Wnt ligands requires Evi, a conserved transmembrane protein, *Cell.* **125**, 523-33.

28. Muller, P., Kuttenkeuler, D., Gesellchen, V., Zeidler, M. P. & Boutros, M. (2005) Identification of JAK/STAT signalling components by genome-wide RNA interference, *Nature.* **436**, 871-5.

29. Puig, O., Marr, M. T., Ruhf, M. L. & Tjian, R. (2003) Control of cell number by Drosophila FOXO: downstream and feedback regulation of the insulin receptor pathway, *Genes & development.* **17**, 2006-20.

30. Bier, E. (2005) Drosophila, the golden bug, emerges as a tool for human genetics, *Nature reviews Genetics.* **6**, 9-23.

31. Kaletta, T. & Hengartner, M. O. (2006) Finding function in novel targets: C. elegans as a model organism, *Nature reviews Drug discovery.* **5**, 387-98.

32. Reiter, L. T., Potocki, L., Chien, S., Gribskov, M. & Bier, E. (2001) A systematic analysis of human disease-associated gene sequences in Drosophila melanogaster, *Genome research.* **11**, 1114-25.

33. Andersen, J. N., Del Vecchio, R. L., Kannan, N., Gergel, J., Neuwald, A. F. & Tonks, N. K. (2005) Computational analysis of protein tyrosine phosphatases: practical guide to bioinformatics and data resources, *Methods.* **35**, 90-114.

34. Desai, C. J., Krueger, N. X., Saito, H. & Zinn, K. (1997) Competition and cooperation among receptor tyrosine phosphatases control motoneuron growth cone guidance in Drosophila, *Development.* **124**, 1941-52.

35. Johnson, K. G. & Van Vactor, D. (2003) Receptor protein tyrosine phosphatases in nervous system development, *Physiological reviews.* **83**, 1-24.

36. Van Vactor, D. (1998) Protein tyrosine phosphatases in the developing nervous system, *Current opinion in cell biology.* **10**, 174-81.

37. Van Vactor, D., O'Reilly, A. M. & Neel, B. G. (1998) Genetic analysis of protein tyrosine phosphatases, *Current opinion in genetics & development.* **8**, 112-26.

38. Lamprianou, S. & Harroch, S. (2006) Receptor protein tyrosine phosphatase from stem cells to mature glial cells of the central nervous system, *Journal of molecular neuroscience : MN.* **29**, 241-55.

39. Paul, S. & Lombroso, P. J. (2003) Receptor and nonreceptor protein tyrosine phosphatases in the nervous system, *Cellular and molecular life sciences : CMLS.* **60**, 2465-82.

40. Sun, Q., Bahri, S., Schmid, A., Chia, W. & Zinn, K. (2000) Receptor tyrosine phosphatases regulate axon guidance across the midline of the Drosophila embryo, *Development.* **127**, 801-12.

41. Desai, C. J., Gindhart, J. G., Jr., Goldstein, L. S. & Zinn, K. (1996) Receptor tyrosine phosphatases are required for motor axon guidance in the Drosophila embryo, *Cell.* **84**, 599-609.

42. Jeon, M., Nguyen, H., Bahri, S. & Zinn, K. (2008) Redundancy and compensation in axon guidance: genetic analysis of the Drosophila Ptp10D/Ptp4E receptor tyrosine phosphatase subfamily, *Neural development.* **3**, 3.

43. Jeon, M. & Zinn, K. (2009) Receptor tyrosine phosphatases control tracheal tube geometries through negative regulation of Egfr signaling, *Development.* **136**, 3121-9.

44. Tonks, N. K. & Neel, B. G. (2001) Combinatorial control of the specificity of protein tyrosine phosphatases, *Current opinion in cell biology.* **13**, 182-95.

45. Schindelholz, B., Knirr, M., Warrior, R. & Zinn, K. (2001) Regulation of CNS and motor axon guidance in Drosophila by the receptor tyrosine phosphatase DPTP52F, *Development.* **128**, 4371-82.

46. Fox, A. N. & Zinn, K. (2005) The heparan sulfate proteoglycan syndecan is an in vivo ligand for the Drosophila LAR receptor tyrosine phosphatase, *Current biology : CB.* **15**, 1701-11.

47. Johnson, K. G., Tenney, A. P., Ghose, A., Duckworth, A. M., Higashi, M. E., Parfitt, K., Marcu, O., Heslip, T. R., Marsh, J. L., Schwarz, T. L., Flanagan, J. G. & Van Vactor, D. (2006) The HSPGs Syndecan and Dallylike bind the receptor phosphatase LAR and exert distinct effects on synaptic development, *Neuron.* **49**, 517-31.

48. Wills, Z., Bateman, J., Korey, C. A., Comer, A. & Van Vactor, D. (1999) The tyrosine kinase Abl and its substrate enabled collaborate with the receptor phosphatase Dlar to control motor axon guidance, *Neuron.* **22**, 301-12.

49. Fashena, S. J. & Zinn, K. (1997) Transmembrane glycoprotein gp150 is a substrate for receptor tyrosine phosphatase DPTP10D in Drosophila cells, *Molecular and cellular biology.* **17**, 6859-67.

50. Bugga, L., Ratnaparkhi, A. & Zinn, K. (2009) The cell surface receptor Tartan is a potential in vivo substrate for the receptor tyrosine phosphatase Ptp52F, *Molecular and cellular biology.* **29**, 3390-400.

51. Beckstead, R. B., Lam, G. & Thummel, C. S. (2005) The genomic response to 20-hydroxyecdysone at the onset of Drosophila metamorphosis, *Genome biology.* **6**, R99.

52. Talbot, W. S., Swyryd, E. A. & Hogness, D. S. (1993) Drosophila tissues with different metamorphic responses to ecdysone express different ecdysone receptor isoforms, *Cell.* **73**, 1323-37.

53. Lee, C. Y., Cooksey, B. A. & Baehrecke, E. H. (2002) Steroid regulation of midgut cell death during Drosophila development, *Developmental biology.* **250**, 101-11.

54. Thummel, C. S. (2001) Steroid-triggered death by autophagy, *BioEssays : news and reviews in molecular, cellular and developmental biology.* **23**, 677-82.

55. Chang, Y. C., Hung, W. T., Chang, H. C., Wu, C. L., Chiang, A. S., Jackson, G. R. & Sang, T. K. (2011) Pathogenic VCP/TER94 alleles are dominant actives and contribute to neurodegeneration by altering cellular ATP level in a Drosophila IBMPFD model, *PLoS genetics.* **7**, e1001288.

56. Elliott, D. A. & Brand, A. H. (2008) The GAL4 system : a versatile system for the expression of genes, *Methods Mol Biol.* **420**, 79-95.

57. Burridge, K. & Nelson, A. (1995) An in-gel assay for protein tyrosine phosphatase activity: detection of widespread distribution in cells and tissues, *Analytical biochemistry.* **232**, 56-64.

58. Meng, T. C., Hsu, S. F. & Tonks, N. K. (2005) Development of a modified in-gel assay to identify protein tyrosine phosphatases that are oxidized and inactivated in vivo, *Methods.* **35**, 28-36.

59. Elsner, M. & Mak, H. C. (2011) A modENCODE snapshot, *Nature biotechnology.* **29**, 238-40.

60. Graveley, B. R., Brooks, A. N., Carlson, J. W., Duff, M. O., Landolin, J. M., Yang, L., Artieri, C. G., van Baren, M. J., Boley, N., Booth, B. W., Brown, J. B., Cherbas, L., Davis, C. A., Dobin, A., Li, R., Lin, W., Malone, J. H., Mattiuzzo, N. R., Miller, D., Sturgill, D., Tuch, B. B., Zaleski, C., Zhang, D., Blanchette, M., Dudoit, S., Eads, B., Green, R. E., Hammonds, A., Jiang, L., Kapranov, P., Langton, L., Perrimon, N., Sandler,

J. E., Wan, K. H., Willingham, A., Zhang, Y., Zou, Y., Andrews, J., Bickel, P. J., Brenner, S. E., Brent, M. R., Cherbas, P., Gingeras, T. R., Hoskins, R. A., Kaufman, T. C., Oliver, B. & Celniker, S. E. (2011) The developmental transcriptome of Drosophila melanogaster, *Nature.* **471**, 473-9.

61. Chintapalli, V. R., Wang, J. & Dow, J. A. (2007) Using FlyAtlas to identify better Drosophila melanogaster models of human disease, *Nature genetics.* **39**, 715-20.

62. Arbeitman, M. N., Furlong, E. E., Imam, F., Johnson, E., Null, B. H., Baker, B. S., Krasnow, M. A., Scott, M. P., Davis, R. W. & White, K. P. (2002) Gene expression during the life cycle of Drosophila melanogaster, *Science.* **297**, 2270-5.

63. Hsu, M. F. & Meng, T. C. (2010) Enhancement of insulin responsiveness by nitric oxide-mediated inactivation of protein-tyrosine phosphatases, *The Journal of biological chemistry.* **285**, 7919-28.

64. Yin, V. P. & Thummel, C. S. (2004) A balance between the diap1 death inhibitor and reaper and hid death inducers controls steroid-triggered cell death in Drosophila, *Proceedings of the National Academy of Sciences of the United States of America.* **101**, 8022-7.

65. Li, T. R. & White, K. P. (2003) Tissue-specific gene expression and ecdysone-regulated genomic networks in Drosophila, *Developmental cell.* **5**, 59-72.

66. Santhanam, A., Liang, S. Y., Chen, D. Y., Chen, G. C. & Meng, T. C. (2012) Midgut-enriched receptor protein tyrosine phosphatase PTP52F is required for Drosophila development during larva-pupa transition, *The FEBS journal*.

67. Lam, G. & Thummel, C. S. (2000) Inducible expression of double-stranded RNA directs specific genetic interference in Drosophila, *Current biology : CB.* **10**, 957-63.

68. Ku, H. Y., Wu, C. L., Rabinow, L., Chen, G. C. & Meng, T. C. (2009) Organization of F-actin via concerted regulation of Kette by PTP61F and dAbl, *Molecular and cellular biology.* **29**, 3623-32.

69. Chang, Y. C., Lin, S. Y., Liang, S. Y., Pan, K. T., Chou, C. C., Chen, C. H., Liao, C. L., Khoo, K. H. & Meng, T. C. (2008) Tyrosine phosphoproteomics and identification of substrates of protein tyrosine phosphatase dPTP61F in Drosophila S2 cells by mass spectrometry-based substrate trapping strategy, *Journal of proteome research.* **7**, 1055-66.

70. Amanchy, R., Zhong, J., Hong, R., Kim, J. H., Gucek, M., Cole, R. N., Molina, H. & Pandey, A. (2009) Identification of c-Src tyrosine kinase substrates in platelet-derived growth factor receptor signaling, *Molecular oncology.* **3**, 439-50.

71. Li, G., Zhao, G., Schindelin, H. & Lennarz, W. J. (2008) Tyrosine phosphorylation of ATPase p97 regulates its activity during ERAD, *Biochemical and biophysical research communications.* **375**, 247-51.

72. Pedraza, L. G., Stewart, R. A., Li, D. M. & Xu, T. (2004) Drosophila Src-family kinases function with Csk to regulate cell proliferation and apoptosis, *Oncogene.* **23**, 4754-62.

73. Takahashi, F., Endo, S., Kojima, T. & Saigo, K. (1996) Regulation of cell-cell contacts in developing Drosophila eyes by Dsrc41, a new, close relative of vertebrate c-src, *Genes & development.* **10**, 1645-56.

74. Kussick, S. J. & Cooper, J. A. (1992) Phosphorylation and regulatory effects of the carboxy terminus of a Drosophila src homolog, *Oncogene.* **7**, 1577-86.

75. Koike, M., Fukushi, J., Ichinohe, Y., Higashimae, N., Fujishiro, M., Sasaki, C., Yamaguchi, M., Uchihara, T., Yagishita, S., Ohizumi, H., Hori, S. & Kakizuka, A. (2010) Valosin-containing protein (VCP) in novel feedback machinery between abnormal protein accumulation and transcriptional suppression, *The Journal of biological chemistry.* **285**, 21736-49.

76. Zhao, G., Zhou, X., Wang, L., Li, G., Schindelin, H. & Lennarz, W. J. (2007) Studies on peptide:N-glycanase-p97 interaction suggest that p97 phosphorylation modulates endoplasmic reticulum-associated degradation, *Proceedings of the National Academy of Sciences of the United States of America.* **104**, 8785-90.

77. Yin, V. P., Thummel, C. S. & Bashirullah, A. (2007) Down-regulation of inhibitor of apoptosis levels provides competence for steroid-triggered cell death, *The Journal of cell biology.* **178**, 85-92.

78. Rumpf, S., Lee, S. B., Jan, L. Y. & Jan, Y. N. (2011) Neuronal remodeling and apoptosis require VCP-dependent degradation of the apoptosis inhibitor DIAP1, *Development.* **138**, 1153-60.

79. Yin, V. P. & Thummel, C. S. (2005) Mechanisms of steroid-triggered programmed cell death in Drosophila, *Seminars in cell & developmental biology.* **16**, 237-43.

80. Matozaki, T., Murata, Y., Mori, M., Kotani, T., Okazawa, H. & Ohnishi, H. (2010) Expression, localization, and biological function of the R3 subtype of receptor-type protein tyrosine phosphatases in mammals, *Cellular signalling.* **22**, 1811-7.

81. Noguchi, T., Tsuda, M., Takeda, H., Takada, T., Inagaki, K., Yamao, T., Fukunaga, K., Matozaki, T. & Kasuga, M. (2001) Inhibition of cell growth and spreading by stomach cancer-associated protein-tyrosine phosphatase-1 (SAP-1) through dephosphorylation of p130cas, *The Journal of biological chemistry.* **276**, 15216-24.

82. Takada, T., Noguchi, T., Inagaki, K., Hosooka, T., Fukunaga, K., Yamao, T., Ogawa, W., Matozaki, T. & Kasuga, M. (2002) Induction of apoptosis by stomach cancer-associated protein-tyrosine phosphatase-1, *The Journal of biological chemistry.* **277**, 34359-66.

83. Krause, C., Wolf, C., Hemphala, J., Samakovlis, C. & Schuh, R. (2006) Distinct functions of the leucine-rich repeat transmembrane proteins capricious and tartan in the Drosophila tracheal morphogenesis, *Developmental biology.* **296**, 253-64.

84. Broadus, J., McCabe, J. R., Endrizzi, B., Thummel, C. S. & Woodard, C. T. (1999) The Drosophila beta FTZ-F1 orphan nuclear receptor provides competence for stage-specific responses to the steroid hormone ecdysone, *Molecular cell.* **3**, 143-9.

85. Davis, M. B., Carney, G. E., Robertson, A. E. & Bender, M. (2005) Phenotypic analysis of EcR-A mutants suggests that EcR isoforms have unique functions during Drosophila development, *Developmental biology.* **282**, 385-96.

86. Lessard, L., Labbe, D. P., Deblois, G., Begin, L. R., Hardy, S., Mes-Masson, A. M., Saad, F., Trotman, L. C., Giguere, V. & Tremblay, M. L. (2012) PTP1B is an androgen receptor-regulated phosphatase that promotes the progression of prostate cancer, *Cancer research.* **72**, 1529-37.

APPENDIX-I

Mass Spectrometry results

Band number	Proteins identified
Band-1	argonaute-2, lingerer
Band-2	CytoplasmicFMR1-interacting protein, Dosage compensation regulator, Eukaryotic translation initiation factor 3 subunit
Band-3	Membrane-associated protein Hem, 5'-3'exoribonuclease 2 homolog, Caprin homolog
Band-4	Transitional endoplasmic reticulum ATPase TER94, AP-2 complex subunit alpha, ATP-dependent RNA helicase bel
Band-5	ATP-dependent RNA helicase bel, Fragile X mental retardation syndrome-related protein 1, Putative glycogen [starch] synthase, Protein no-on-transient A
Band-6	Putative glycogen [starch] synthase, ATP-dependent RNA helicase bel, Protein no-on-transient, Heat shock 70 kDa protein cognate 3
Band-7	ATP-dependent RNA helicase p62, Putative glycogen [starch] synthase, ATP-dependent RNA helicase bel, Heterogeneous nuclear ribonucleoprotein 27C, Actin-87E
Band-8	Heterogeneous nuclear ribonucleoprotein 27C, 60S ribosomal protein L4, Interleukin enhancer-binding factor 2 homolog, Polyadenylate-binding protein, Actin-5C
Band-9	RNA-binding protein squid, Heterogeneous nuclear

	ribonucleoprotein 87F, Heterogeneous nuclear ribonucleoprotein 27C, Heterogeneous nuclear ribonucleoprotein A1
Band-10	60S acidic ribosomal protein, RNA-binding protein squid, Heterogeneous nuclear ribonucleoprotein 87F, Heterogeneous nuclear ribonucleoprotein A1
Band-11	60S acidic ribosomal protein PO, 40S ribosomal protein S3a, 40S ribosomal protein S3a, 60S acidic ribosomal protein L5, Heterogeneous nuclear ribonucleoprotein 87F, Heterogeneous nuclear ribonucleoprotein A1, Heterogeneous nuclear ribonucleoprotein 27C

Peptides identified for each band

Band-1

1. AGO2_DROME **Mass:** 136765 **Score:** 54 **Queries matched:** 1 **emPAI:** 0.02

Protein argonaute-2 OS=Drosophila melanogaster GN=AGO2 PE=1 SV=3

Peptide
R.IANDFIVVSTR.V

2. LIG_DROME **Mass:** 139408 **Score:** 38 **Queries matched:** 3 **emPAI:** 0.02

Protein lingerer OS=Drosophila melanogaster GN=lig PE=1 SV=1

Peptide
R.GRETR.E
K.VLLLLTMTQR.S
R.MGGRTGGPRGDR.G

Band-2

1. CYFIP_DROME **Mass:** 149165 **Score:** 2942 **Queries matched:** 117 **emPAI:** 5.44

Cytoplasmic FMR1-interacting protein OS=Drosophila melanogaster GN=Sra-1 PE=1 SV=1

Peptide	K.GKKDPDGGFR.I	K.DPDGGFRIQVPR.L
K.GIQLKR.M	K.QRHVQLLGR.S	R.IETVLCEAIRR.N
K.SCKLPR.C	R.TMLESLIADK.S	K.GYEPTDDPVAKGK.K
K.DPDGGFR.I	R.NNRYETLLK.Q	R.VQRVDGKDEDVK.G
R.LDRIDR.I	R.YTNEVTTTVK.E	K.YLALDNFDGMVK.E
R.IDRIFK.N	K.IGTAKQAMIAR.E	K.ECPVEAEEYER.A
R.EGDLLTR.E	R.LDRIDRIFK.N	R.TKVNLSSSQAIQR.E
R.SIIMSVR.E	R.KAIEAFSGEVK.R	R.NNRYETLLKQR.H
R.HVQLLGR.S	K.GYEPTDDPVAK.G	K.FINMFAVLDELK.N
R.RAAQFLK.V	K.TVEVLAPEVNK.L	K.DFVSEAYLLTLGK.F
K.YISELAR.Y	K.VNLSSSQAIQR.E	R.EDHVKYISELAR.Y
R.ITADLALR.G	K.AIEAFSGEVKR.L	R.TMLESLIADKSGGK.R
K.GLQVLMAR.I	K.ANFDTNFEDR.N	K.SSVKNDYSTYRR.A
R.NGFVTGIAK.Y	K.LSEQIFAHYK.Q	K.KDPDGGFRIQVPR.L
K.NDYSTYR.R	K.LLNFMYFQR.K	K.QAMIAREGDLLTR.E
K.TLMIAMPK.S	K.QLAGSIFLDKR.F	R.VDGKDEDVKGIQLK.R
K.MYLTPEEK.H	R.SIDLNKLITQR.I	R.LNVGPSSTQLYMVR.T
K.TELFQSFR.E	R.EFYLEMTMGR.K	R.LNVGPSSTQLYMVR.T
K.ENPSDAENR.I	K.GGDGEGSNVEHVR.C	R.FEALDFCYHILR.V
R.DTVKDTLEK.I	K.IRDTVKDTLEK.I	K.SNEQPNRVEIYEK.T
K.AIEAFSGEVK.R	K.SSVKNDYSTYR.R	R.TMLESLIADKSGGKR.T
R.YETLLKQR.H	R.KAIEAFSGEVKR.L	K.MYLTPEEKHMLVK.V
K.IRLDRIDR.I	K.EANHNVLAPYGR.I	R.FQVLNSQIFSILNK.Y

2. MLE_DROME **Mass:** 143571 **Score:** 1170 **Queries matched:** 67 **emPAI:** 1.82

Dosage compensation regulator OS=Drosophila melanogaster GN=mle PE=1 SV=2

Peptide	R.QFSDGGGPPK.R	R.GRFETGRFTNSSFGR.R
R.LPIEPR.L	K.FDIRQTGPK.N	R.FQALEDNLTPEMFR.T
K.TNLEQR.K	K.IDLAANNIVR.V	R.SEILTAINDNPVVIIR.G
R.KLEAGLR.G	R.RISAISVAER.V	R.ERCEQLGDTVGYSVR.F
K.LPIAAMR.S	R.QRFLCEVR.V	K.QLSMVSPLQVILFGSR.K
R.GRFETGR.F	R.ESGILPHQSR.Q	R.QLFHLNVIEPFSGTLK.K
K.SCALSLVR.Q	K.YTPVGPEHAR.S	R.RQNDNEYRQFLEFR.E
R.FTNSSFGR.R	R.LGSIHHFLSK.A	K.ALEPPPVDAVIEAEVLLR.E
R.ISAISVAER.V	R.QFSDGGGPPKR.G	R.VGKLNTNDVPADAGASGGGPR.T
K.SAGDFGLQR.E	K.VCEDKYSQK.T	R.ARFQALEDNLTPEMFR.T
K.VVKDLCVK.S	K.SFLYQFCAK.S	R.QLFHLNVIEPFSGTLKK.K
K.VLTTESKAALLHK.T	R.GGFGDSFESNR.G	K.SAGDFGLQRESGILPHQSR.Q
K.VCEDKYSQKTR.N	R.LEEPYAQLVK.V	R.NIKIELDGPPIPLIVNLSR.I
R.TGLEGAGMAGGSGQQK.R	K.SQIEPKFDIR.Q	R.MKLFTSHNNLTSYATVWASK.T
R.CLDANDELTPLGR.L	K.QTNNIRDDYK.Y	K.ALEPPPVDAVIEAEVLLREMR.C
R.CEQLGDTVGYSVR.F	R.TPLHEMALTIK.L	K.QTNNIRDDYKYTPVGPEHAR.S
R.VRPGFCFTLCSR.A	R.KVFEPVPEGVTK.I	R.FLCEVRVEPNTYIGVGNSTNKK.D
R.GVSHIIVDEIHER.D	K.NACRDFVNYLVR.V	R.TPLHEMALTIKLLR.L
R.FETGRFTNSSFGR.R	K.LSPNLINKIDEVIK.G	K.LNTNDVPADAGASGGGPR.T
K.YFGICPVLEVPGR.A	R.TGLEGAGMAGGSGQQKR.V	-.MDIKSFLYQFCAK.S

3. EIF3A_DROER **Mass:** 133458 **Score:** 129 **Queries matched:** 9 **emPAI:** 0.10

Eukaryotic translation initiation factor 3 subunit A OS=Drosophila erecta GN=eIF3-S10 PE=3 SV=1

Peptide
R.QKIIEDR.K
K.KIDYFER.A
K.NLTKDDLQR.M
R.ALDTLQEVFR.N
K.KNLTKDDLQR.M
K.ELQSKLKSQEK.K
R.SQLVNMSTVLTR.A
R.ANEFIEVGKPLR.A

Band-3

1. HEM_DROME **Mass:** 129297 **Score:** 3234 **Queries matched:** 115 **emPAI:** 8.69 Membrane-associated protein Hem OS=Drosophila melanogaster GN=Hem PE=2 SV=1

Peptide	K.LSLVGNPAILLK.A	K.SKHFDDIRKPGDESYR.K
R.GLGILTR.I	K.LAEEFIPHQR.L	R.TDTMSCEYISLEAMDR.W
R.LQDVDR.V	M.ARPIFPNQQK.I	K.IAEKLIILNDRGLGILTR.I
K.SLVSTNK.E	R.LQDVDRVLQR.M	R.YYVQYLSGFDATDLNIR.M
K.SLESSIK.F	K.SLESSIKFIVK.R	R.TALKELALIMTDQPGLLGPK.A
R.LLTSALR.S	K.IAEKLIILNDR.G	K.TLNETLMWHIANQVQELK.S
K.HFDDIR.K	K.EFLALASSSLLR.L	R.LGQMILDYEVPLKK.L
R.FPNIDVK.G	R.MTIIGVIICFR.N	R.QLPELLFHMEELR.A
K.EVLITLR.T	R.EYLCQNLEHR.F	R.NRESIYLLLDEIVK.Q
K.LIILNDR.G	K.KLAEEFIPHQR.L	K.RIGEVKEAYNTAVQK.A
K.ILSVQSAR.K	R.VSAGNIVFSINQK.A	K.ELALIMTDQPGLLGPK.A
K.RLQDVDR.V	R.VASEMASAAGLLCK.V	R.TSFDKPEVMKEQFK.R
R.NENSFYR.A	R.ESIYLLLDEIVK.Q	K.HFDDIRKPGDESYR.K
K.GLNAIVNIK.A	R.NLVHEALVDVLDK.R	R.EMQKLSLVGNPAILLK.A
K.SNEDLVDR.Q	K.GLNAIVNIKAEIIK.S	K.QVEDNELFYFRPFR.L
K.QEQILGLAL.-	K.DFQEHLPGGDQIR.V	K.HFDDIRKPGDESYRK.T
K.RFPNIDVK.G	R.RVSAGNIVFSINQK.A	R.TSFDKPEVMKEQFKR.L
K.SKPGFLSEK.S	R.IGEVKEAYNTAVQK.A	R.TSFDKPEVMKEQFKR.L
K.AALMHRER.R	K.LIILNDRGLGILTR.I	K.TIAALYNTWYSEVLLR.R
R.NLPADKWR.E	K.SLVSTNKEVLITLR.T	R.NAYHGVYKQEQILGLAL.-
K.ILSVQSARK.K	R.MKEFLALASSSLLR.L	R.SLSVVNIFLEEMAKEAK.N
R.IPFLLSSVK.D	R.SLSVVNIFLEEMAK.E	R.IPFLLSSVKDFQEHLPGGDQIR.V

R.IAEHAELAR.L	R.NLVHEALVDVLDKR.I	K.AVLGLYNAAYELQNNQADTGFPR.L
K.SKHFDDIR.K	M.ARPIFPNQQKIAEK.L	K.SNEDLVDRQLPELLFHMEELR.A
K.EAYNTAVQK.A	R.LGQMILDYEVPLKK.L	R.KAVLGLYNAAYELQNNQADTGFPR.L
R.SLTSIYALR.N	K.GKSNEDLVDR.Q	R.DLVGMVMFNQETMEIAKPSELLASVR.A
K.TREDLTTMDK.L	K.RIPFLLSSVK.D	R.MQSLQMCPEDESIIFSSLYNTAAALTVK.Q
R.ALAELVGPYGIK.T	R.TSFDKPEVMK.E	K.MFDDQFHMCLEFPAQNR.Y
R.LGQESDKEATR.N	R.LLDSMVFHTR.V	R.AYMNVLQTVENYVHIDITR.V
R.LQTYMSVGK.A	M.ARPIFPNQQK.I	K.NIITTICDEQCTMADALLPK.H
R.LQTYMSVGK.A	R.KYSQVMQR.Y	R.VASEMASAAGLLCKVDPTLATTLK.S
R.HNDNPPLLK.N	R.DEILWLLR.H	K.VDPTLATTLK.S

2. XRN2_DROME **Mass:** 103895 **Score:** 236 **Queries matched:** 14 **emPAI:** 0.32

5'-3' exoribonuclease 2 homolog OS=Drosophila melanogaster GN=Rat1 PE=1 SV=2

Peptide	
R.MLNAGIR.N	K.KISEKDDESVCK.A
-.MGVPAFFR.W	R.KLLYMAIDGVAPR.A
R.AYVPDSGHR.M	R.GTLGKTELNTAISGVLK.S
R.IREELLSR.G	K.QTLEMPNLPFEYSFER.A
K.TELNTAISGVLK.S	R.TSDMANLDDEDEEENNDEVR.L
R.SVGNYKEEAAALR.N	R.NQDHGSLNQSAFGASAVGPNSQQR.S

3. CAPR1_DROME **Mass:** 103528 **Score:** 190 **Queries matched:** 5 **emPAI:** 0.13

Caprin homolog OS=Drosophila melanogaster GN=CG18811 PE=1 SV=1

Peptide
K.ELSGDQASAVAK.Y
R.SDFLNGENGAKK.L
K.YDAVLANLEFAR.E
K.SAELFYSTINARPK.S
R.RPETADDVSFIATAQK.S

Band-4

1. TERA_DROME **Mass:** 88803 **Score:** 1946 **Queries matched:** 92 **emPAI:** 9.54

Transitional endoplasmic reticulum ATPase TER94 OS=Drosophila melanogaster GN=TER94 PE=1 SV=1

R.QAIEAEIR.R	R.QAIEAEIRR.E	M.ADSKGEDLATAILK.R
R.GDTVILKGK.R	R.GDTVILKGKR.R	K.LAIRQAIEAEIRR.E
R.KAFEEAEK.N	R.GGNVGDAGGAADR.V	R.LDQLIYIPLPDDK.S
K.SPLAKEVDLTYIAK.V	R.GILMYGPPGTGKTLIAR.A	K.AIGVKPPRGILMYGPPGTGK.T
K.AIANECQANFISVK.G	R.RIVSQLLTLMDGMKK.S	R.FGRFDREIDIGIPDATGR.L

R.IVSQLLTLMDGMKK.S	R.VINQILTEMDGMGAKK.N	R.SAAPCVLFFDELDSIAKAR.G
R.IVSQLLTLMDGMKK.S	K.VTQGFSGADLTEICQR.A	R.LIVEEAQNDDNSVVSLSQAK.M
M.ADSKGEDLATAILKR.K	K.AFEEAEKNSPAIIFIDEIDAIAPKR.D	K.DRPNRLIVEEAQNDDNSVVSLSQAK.M
R.KYEMFAQTLQQSR.G	K.EVDLTYIAKVTQGFSGADLTEICQR.A	R.GGNVGDAGGAADRVINQILTEMDGMGAKK.N
R.VINQILTEMDGMGAKK.K	R.KDRPNRLIVEEAQNDDNSVVSLSQAK.M	R.LIVEEAQNDDNSVVSLSQAKMDELQLFR.G
R.KSPLAKEVDLTYIAK.V	K.EMVELPLRHPSLFK.A	K.SSHLIVMAATNRPNSIDPALRR.F
R.SVSDNDIRKYEMFAQTLQQSR.G	R.AENQNSAMDMDEDDPVPEITSAHFEEAMK.F	K.AFEEAEKNSPAIIFIDEIDAIAPK.R
R.SVSDNDIRKYEMFAQTLQQSR.G	R.EKMDLIDLEDDKIDAEVLASLAVTMENFR.Y	R.EKERAENQNSAMDMDEDDPVPEITSAHFEEAMK.F
K.KSSHLIVMAATNRPNSIDPALRR.F	R.AENQNSAMDMDEDDPVPEITSAHFEEAMKFAR.R	R.GGNVGDAGGAADRVINQILTEMDGMGAK.K

2. AP2A_DROME **Mass:** 105553 **Score:** 321 **Queries matched:** 12 **emPAI:** 0.32

AP-2 complex subunit alpha OS=Drosophila melanogaster GN=alpha-Adaptin PE=1 SV=1

Peptide	R.DMAESFSNEIPK.L
R.TNIQDVFR.Q	R.LLQNYNPVTEEAGVR.A
R.SADAELQQR.A	K.VGGYILGEFGNLIAGDSR.S
K.SEFRQNLGR.L	K.SPAPLTSAAQNNALVNNSHSK.L
K.AAQPLDLPGAR.N	R.LNETLETILNKAQEPPKSK.K
K.LLVSGDTMDVVK.Q	

3. DDX3_DROME **Mass:** 85029 **Score:** 308 **Queries matched:** 22 **emPAI:** 0.70

ATP-dependent RNA helicase bel OS=Drosophila melanogaster GN=bel PE=1 SV=1

Peptide	R.QTLMFSATFPK.Q	R.MGNLGVATSFFNEKNR.N
R.NNVALAR.Y	R.MLDMGFEPQIR.R	K.HVINFDLPSDVEEYVHR.I
K.VGLENIR.F	R.ELATQIFEEAKK.F	R.FLVLDEADRMLDMGFEPQIR.R
R.GLDIPHVK.H	R.IVEQLNMPPTGQR.Q	R.VGSTSENITQTILWVYEPDKR.S
K.EREEALR.C	R.SGDCPILVATAVAAR.G	R.GGGGNNNAADAESQGQGQGQGQGFDSR.S
R.GKVGLENIR.F	R.MGNLGVATSFFNEK.N	R.FLVLDEADRMLDMGFEPQIRR.I
K.HAIPIIINGR.D	R.RIVEQLNMPPTGQR.Q	R.SGNPRQETRDPQQSR.G
R.TQKEREEALR.C		

Band-5

DDX3_DROME **Mass:** 85029 **Score:** 2189 **Queries matched:** 94 **emPAI:** 8.68

ATP-dependent RNA helicase bel OS=Drosophila melanogaster GN=bel PE=1 SV=1

Peptide	K.TSTNSVTGGVYVPPHLR.G	R.WKEGGGSNVDYTK.L
R.NNVALAR.Y	R.MGNLGVATSFFNEKNR.N	R.KQYPLGLVLAPTR.E
R.YGGGFGSR.D	R.NNVALARYDKPTPVQK.H	R.QSGDYGYGSGGGGRR.G
K.VGLENIR.F	R.GGGGRFEDNYNGGEFDSR.R	R.IVEQLNMPPTGQR.Q
R.GLDIPHVK.H	R.ELATQIFEEAKKFAYR.S	R.IVEQLNMPPTGQR.Q
R.LEDMITR.G	R.MRPAVLYGGNNTSEQMR.E	R.SGDCPILVATAVAAR.G
K.EREEALR.C	R.GCHLIVATPGRLEDMITR.G	R.MLDMGFEPQIRR.I
R.GKVGLENIR.F	R.DGPEYTKDSLTLIFVETK.K	R.MGNLGVATSFFNEK.N
R.GFGRGPSYR.G	K.HVINFDLPSDVEEYVHR.I	R.RIVEQLNMPPTGQR.Q
R.YDKPTPVQK.H	R.SYLLDLLSSIRDGPEYTK.D	R.NICSDLLELLIETK.Q
R.FLVLDEADR.M	R.RGGGGRFEDNYNGGEFDSR.R	R.ELDRGCHLIVATPGR.L
R.SGGGGGGGRGFGR.G	R.DGPEYTKDSLTLIFVETKK.G	K.QEIPSFMEDMSSDR.G
K.HAIPIIINGR.D	K.QEIPSFMEDMSSDRGHGGAK.R	R.SGNPRQETRDPQQSR.G
K.EGGGSNVDYTK.L	K.QIQELASDFLSNYIFLAVGR.V	R.MGNLGVATSFFNEKNR.N
R.GCHLIVATPGR.L	K.HAIPIIINGRDLMACAQTGSGK.T	R.QSGDYGYGSGGGGR.R
R.QETRDPQQSR.G	R.FLVLDEADRMLDMGFEPQIR.R	K.QYPLGLVLAPTR.E
R.DLMACAQTGSGK.T	R.FLVLDEADRMLDMGFEPQIR.R	R.MLDMGFEPQIR.R
R.TQKEREEALR.C	R.VGSTSENITQTILWVYEPDKR.S	R.ELATQIFEEAKK.F
K.DSLTLIFVETK.K	R.MRPAVLYGGNNTSEQMRELDR.G	R.ELATQIFEEAK.K
R.QTLMFSATFPK.Q	R.GGGGNNNAADAESQGQGQGQGQGFDSR.S	R.SYLLDLLSSIR.D
R.QTLMFSATFPK.Q	R.ELDRGCHLIVATPGRLEDMITR.G	K.TAAFLVPILNQMYELGHVPPPQSTR.Q
R.FLVLDEADRMLDMGFEPQIRR.I	R.GGGGGSGSNLNEQTAEDGQAQQQQQPR.N	R.SYLLDLLSSIRDGPEYTKDSLTLIFVETK.K
K.GADSLEEFLYQCNHPVTSIHGDR.T	K.KGADSLEEFLYQCNHPVTSIHGDR.T	

2. FMR1_DROME **Mass:** 76030 **Score:** 892 **Queries matched:** 34 **emPAI:** 2.13

Fragile X mental retardation syndrome-related protein 1 OS=Drosophila melanogaster GN=Fmr1 PE=1 SV=1

K.VMLLKR.T	R.TVDGVTNIELEEK.S
K.AALNAGDASK.Q	R.IIQEIVDKSGVFR.I
K.NSNPPITAK.T	R.AMLEYAEEFFQVPR.E
R.ELVGKVIGK.N	R.AIQESSMGSTQSFPVTR.R
R.LDNGAYYK.G	R.DLDALIVISKFEHTQK.R
R.GNYVEEFR.V	R.IKVSAIAGDDEQDQNIPR.E
K.MEIDQQLR.A	R.DLDALIVISKFEHTQKR.A
R.GYSSDIESVR.S	R.TVDGVTNIELEEKSCTFK.I
K.DGIHKEFQR.T	R.SNNHTDQPSGQQQLAENVK.K
R.AKNSNPPITAK.T	R.ELAHVPFVFIGTVESIANAK.V
-.MEDLLVEVR.L	R.VRDDLMGLAIGSHGSNIQAAR.T
R.NLSQKVMLLK.R	R.SNNHTDQPSGQQQLAENVKK.E
R.QLETTKLMSR.G	K.AALNAGDASKQNSGNANAAGGASKPK.D
K.ISGETEESVQR.A	R.LPPEETVEVAAPIFEEGMEVEVFTR.T
R.TIDAGVCNYSR.D	R.NGDKQQAGTQQQQPSQVQQQQAAQQQQPKPR.R

3. GYS_DROME **Mass:** 81702 **Score:** 648 **Queries matched:** 29 **emPAI:** 1.20

Putative glycogen [starch] synthase OS=Drosophila melanogaster GN=CG6904 PE=1 SV=2

Peptide	
R.LNAMLK.H	K.RKPDIITPNGLNVK.K
R.QRIIQR.N	K.FSAIHEFQNLHAVAK.E
R.CMFAMQR.D	K.TNNFNVDSLRGHAVIK.Q
K.VGGIYTVIR.S	K.KFSAIHEFQNLHAVAK.E
K.FAVDEEAGKR.Q	K.QLRDTINNVQQAVGKR.M
K.GADIFIEALAR.L	R.LVEIATVFTTHATLLGR.Y
K.TNNFNVDSLR.G	K.HEKPDTTVVAFLIFPTK.T
R.GNPLLDAVNSLR.S	R.TRLVEIATVFTTHATLLGR.Y
R.DTINNVQQAVGK.R	R.VESGADLKDYFDRGDIASR.E
R.DTINNVQQAVGKR.M	R.YIGLENSVQQLSSFMMEFSR.L
R.MFDTCLQGNIPNADDLLQKDDLVK.I	R.TEMEEMEFPRGNPLLDAVNSLR.S
	R.LNAMLKHEKPDTTVVAFLIFPTK.T

4. NONA_DROME **Mass:** 76930 **Score:** 437 **Queries matched:** 25 **emPAI:** 0.65

Protein no-on-transient A OS=Drosophila melanogaster GN=nonA PE=1 SV=2

Peptide	
K.SSASACLR.M	R.VSNLTPFVSNELLYK.S
K.RALDGSMR.K	R.NAGNNQGGGFSGGPQNQQR.D
R.FAPNATILR.V	R.SISGPTFELEPVEVPTETK.F
K.MPDFNQER.S	-.MESAGKQDNNATQQLPQR.Q
R.ASITVDDRGK.H	R.SISGPTFELEPVEVPTETKFSGR.N
K.REEETMRR.H	R.SGPRPGGGAGGAMNSTNMGGGGGGGGGGGPR.G
R.GGEDFFITQR.L	K.NNEPATAAAGQNQANQNANKGQNQR.Q
K.SFEIFGPIER.A	K.AFNKKMPDFNQER.S
R.RQQETLFMK.A	R.FADPNSFEHEYGSR.W
R.VRFAPNATILR.V	R.YEQETELLRQELR.K

Band-6

1. GYS_DROME **Mass:** 81702 **Score:** 1532 **Queries matched:** 63 **emPAI:** 5.36

Putative glycogen [starch] synthase OS=Drosophila melanogaster GN=CG6904 PE=1 SV=2

Peptide		
R.LNAMLK.H	R.TEMEEMEFPR.G	R.TRLVEIATVFTTHATLLGR.Y
R.YCLER.G	R.CHLFNSRHDR.V	R.VESGADLKDYFDRGDIASR.E
R.YEFGNK.G	R.KPDIITPNGLNVK.K	K.ALQAVYPDYVDELSLYGSK.N
R.QRIIQR.N	R.DTINNVQQAVGKR.M	R.YIGLENSVQQLSSFMMEFSR.L
R.VESGADLK.D	R.WNFEVAWEVANK.V	R.TEMEEMEFPRGNPLLDAVNSLR.S
K.SEMWEK.C	R.KPDIITPNGLNVKK.F	R.LNAMLKHEKPDTTVVAFLIFPTK.T
	K.RKPDIITPNGLNVK.K	R.GATHLAHVFTTVSEITGYEAEHLLK.R

R.TLGIYYR.Q	K.QLRDTINNVQQAVGK.R	R.MFDTCLQGNIPNADDLLQKDDLVK.I
R.CHLFNSR.H	K.FSAIHEFQNLHAVAK.E	R.DSMPPVTTHNVADDWNDPVLSSIRR.C
K.FAVDEEAGK.R	K.TNNFNVDSLRGHAVIK.Q	R.GATHLAHVFTTVSEITGYEAEHLLKR.K
R.CMFAMQR.D	R.YLCAGNTDFYNNLDK.F	K.MVFHPEFLTSTNPLFGIDYEEFVR.G
K.VGGIYTVIR.S	R.NFAVTYSQNNELSAPR.I	R.YLCAGNTDFYNNLDKFAVDEEAGKR.Q
R.LSDLLDWR.T	K.KFSAIHEFQNLHAVAK.E	K.AYVSTEEMGEQLCMMGPYKEHCAR.T
K.SYGIYIVDR.R	K.QLRDTINNVQQAVGKR.M	R.VKMVFHPEFLTSTNPLFGIDYEEFVR.G
K.TLYFFIAGR.Y	R.LVEIATVFTTHATLLGR.Y	R.TRLVEIATVFTTHATLLGR.Y
R.RCHLFNSR.H	R.YEFGNKGADIFIEALAR.L	R.VESGADLKDYFDRGDIASR.E
K.FAVDEEAGKR.Q	K.HEKPDTTVVAFLIFPTK.T	K.ALQAVYPDYVDELSLYGSK.N
K.GADIFIEALAR.L	K.FSAIHEFQNLHAVAKEK.I	R.YIGLENSVQQLSSFMMEFSR.L
K.TNNFNVDSLR.G	R.TEMEEMEFPRGNPLLDAVNSLR.S	R.GATHLAHVFTTVSEITGYEAEHLLKR.K
K.SYGIYIVDRR.Y	R.LNAMLKHEKPDTTVVAFLIFPTK.T	K.MVFHPEFLTSTNPLFGIDYEEFVR.G
R.DSMPPVTTHNVADDWNDPVLSSIRR.C	R.GATHLAHVFTTVSEITGYEAEHLLK.R	R.YLCAGNTDFYNNLDKFAVDEEAGKR.Q
R.VKMVFHPEFLTSTNPLFGIDYEEFVR.G	R.MFDTCLQGNIPNADDLLQKDDLVK.I	K.AYVSTEEMGEQLCMMGPYKEHCAR.T

2. DDX3_DROME **Mass:** 85029 **Score:** 940 **Queries matched:** 39 **emPAI:** 2.35

ATP-dependent RNA helicase bel OS=Drosophila melanogaster GN=bel PE=1 SV=1

Peptide	
R.NNVALAR.Y	R.MLDMGFEPQIR.R
R.YGGGFGSR.D	R.ELATQIFEEAKK.F
K.VGLENIR.F	R.KQYPLGLVLAPTR.E
R.GLDIPHVK.H	R.IVEQLNMPPTGQR.Q
K.EREEALR.C	R.SGDCPILVATAVAAR.G
R.GKVGLENIR.F	R.MGNLGVATSFFNEK.N
R.YDKPTPVQK.H	R.RIVEQLNMPPTGQR.Q
R.FLVLDEADR.M	R.NICSDLLELLIETK.Q
K.HAIPIIINGR.D	K.QEIPSFMEDMSSDR.G
R.DLMACAQTGSGK.T	R.SGNPRQETRDPQQSR.G
R.TQKEREEALR.C	R.MGNLGVATSFFNEKNR.N
K.DSLTLIFVETK.K	K.HVINFDLPSDVEEYVHR.I
R.ELATQIFEEAK.K	R.SYLLDLLSSIRDGPEYTK.D
R.SYLLDLLSSIR.D	K.QIQELASDFLSNYIFLAVGR.V
R.QTLMFSATFPK.Q	R.FLVLDEADRMLDMGFEPQIR.R
K.QYPLGLVLAPTR.E	R.VGSTSENITQTILWVYEPDKR.S
R.GGGGGSGSNLNEQTAEDGQAQQQQQPR.N	R.GGGGNNNAADAESQGQGQGQGQGFDSR.S
K.TAAFLVPILNQMYELGHVPPPQSTR.Q	R.FLVLDEADRMLDMGFEPQIRR.I

3. NONA_DROME **Mass:** 76930 **Score:** 784 **Queries matched:** 32 **emPAI:** 1.40

Protein no-on-transient A OS=Drosophila melanogaster GN=nonA PE=1 SV=2

Peptide	
K.SSASACLR.M	R.VSNLTPFVSNELLYK.S
K.SSASACLR.M	R.LYVGNLTNDITDDELR.E
R.ASITVDDR.G	R.NAGNNQGGGFSGGPQNQQR.D
R.FAPNATILR.V	K.NNEPATAAAGQNQANQNANK.G
R.ASITVDDRGK.H	R.SISGPTFELEPVEVPTETK.F
R.QEEDMLRR.Q	-.MESAGKQDNNATQQLPQR.Q
R.GGEDFFITQR.L	R.ELKMEEDKLEAQMEYAR.Y
K.KMPDFNQER.S	R.SISGPTFELEPVEVPTETKFSGR.N
R.YEQETELLR.Q	R.SGPRPGGGAGGAMNSTNMGGGGGGGGGGPR.G
K.SFEIFGPIER.A	K.NNEPATAAAGQNQANQNANKGQNQR.Q
R.RQQETLFMK.A	K.AQQLNSLLDQQEGFGGGGGGNNSTFDNFAGNSNSPFEVFR.G
R.VRFAPNATILR.V	R.QGQNQNQNQVHGQGNQGGPGNQGGAGNQGGQGNQGGAGNQGNGQGFR.G
K.NFGNNKGGFVGNR.N	R.FADPNSFEHEYGSR.W
K.QDNNATQQLPQR.Q	R.YEQETELLRQELR.K

4. HSP7C_DROME **Mass:** 72216 **Score:** 540 **Queries matched:** 26 **emPAI:** 1.54

Heat shock 70 kDa protein cognate 3 OS=Drosophila melanogaster GN=Hsc70-3 PE=2 SV=2

Peptide	
R.NTVIPTK.K	R.AKFEELNLDLFR.S
R.STLKPVQK.V	K.VFAPEEISAMVLGK.M
R.ALSGSHQVR.I	R.ITPSYVAFTADGER.L
K.FADEDKKLK.E	K.NGRVEIIANDQGNR.I
K.DFFGGKEPSR.G	K.NSKPHISVDTSQGAK.V
K.VLEDADMNKK.D	R.QATKDAGVIAGLQVMR.I
R.VEIIANDQGNR.I	R.IINEPTAAAIAYGLDKK.E
K.DAGVIAGLQVMR.I	K.VQQLVKDFFGGKEPSR.G
K.NQIGDKDKLGAK.L	K.NQLTTNPENTVFDAKR.L
K.FEELNLDLFR.S	K.VTHAVVTVPAYFNDAQR.Q
K.DLEAIVQPVIAK.L	R.IEIESFFEGDDFSETLTR.A
K.DVHEIVLVGGSTR.I	K.VLEDADMNKKDVHEIVLVGGSTR.I
K.MKETAEAYLGKK.V	K.SQVFSTASDNQHTVTIQVYEGERPMTK.D

Band-7

1. DDX17_DROME **Mass:** 78500 **Score:** 1067 **Queries matched:** 36 **emPAI:** 2.42

ATP-dependent RNA helicase p62 OS=Drosophila melanogaster GN=Rm62 PE=1 SV=3

Peptide	K.SQSERDFVLR.E
R.VDNLVR.F	R.GDGPIALVLAPTR.E
K.ALVDVLR.E	R.FGGGGGGGDYHGIR.N
R.FGGGGFKK.G	R.YREEQEITVR.G
R.GLDVDGIK.Y	R.MLDMGFEPQIR.K
R.RVDNLVR.F	R.LIDFLSAGSTNLK.R
R.SPYEVQR.Y	K.NFYQEHPNVANR.S
K.IIIFVETK.R	R.LIDFLSAGSTNLKR.C
K.GTSFAFFTK.N	K.TLLSDIYDTSESPGK.I
R.GFGGGGGGGGEGR.H	R.EANQEINPALENLAR.N
K.RRVDNLVR.F	R.QVVDVCDEFSKEEK.L
R.FGGGGGFGDRR.G	R.CGAIHGDKSQSERDFVLR.E
K.IVSQIRPDR.Q	K.YVINFDYPQNSEDYIHR.I
K.SLFNDPDER.T	R.ELAQQIQQVATEFGSSSYVR.N
K.IIIFVETKR.R	K.TLGYILPAIVHINNQQPLQR.G
R.GCEIVIATPGR.L	R.GQVPNPIQDFSEVHLPDYVMK.E
R.KIVSQIRPDR.Q	R.GGGGGGSQDLPMRPVDFSNLAPFKK.N
K.SNILVATDVAAR.G	R.RGGGGGGSQDLPMRPVDFSNLAPFKK.N

2. GYS_DROME **Mass:** 81702 **Score:** 206 **Queries matched:** 9 **emPAI:** 0.27

Putative glycogen [starch] synthase OS=Drosophila melanogaster GN=CG6904 PE=1 SV=2

Peptide
K.VGGIYTVIR.S
-.MRRQQSYR.F
K.GADIFIEALAR.L
K.TNNFNVDSLR.G
R.GNPLLDAVNSLR.S
R.LVEIATVFTTHATLLGR.Y
R.TRLVEIATVFTTHATLLGR.Y

3. DDX3_DROME **Mass:** 85029 **Score:** 166 **Queries matched:** 11 **emPAI:** 0.41

ATP-dependent RNA helicase bel OS=Drosophila melanogaster GN=bel PE=1 SV=1

Peptide	R.QTLMFSATFPK.Q
R.NNVALAR.Y	R.MLDMGFEPQIR.R
R.GLDIPHVK.H	R.ELATQIFEEAKK.F
R.GKVGLENIR.F	R.IVEQLNMPPTGQR.Q
K.HAIPIIINGR.D	R.SGDCPILVATAVAAR.G
R.TQKEREEALR.C	K.HVINFDLPSDVEEYVHR.I

4. RB27C_DROME **Mass:** 44742 **Score:** 119 **Queries matched:** 4 **emPAI:** 0.24

Heterogeneous nuclear ribonucleoprotein 27C OS=Drosophila melanogaster GN=Hrb27C PE=1 SV=2

Peptide
K.KAEPR.D
K.VTEVVIMYDQEK.K
K.VFLGGLPSNVTETDLR.T

R.DGSGGQNSNNSTVGGAYGK.L

5. ACT5_DROME **Mass:** 41775 **Score:** 116 **Queries matched:** 6 **emPAI:** 0.46

Actin-87E OS=Drosophila melanogaster GN=Act87E PE=1 SV=1

Peptide
K.AGFAGDDAPR.A
R.GYSFTTTAER.E
R.HQGVMVGMGQK.D
R.AVFPSIVGRPR.H
K.DSYVGDEAQSKR.G
K.QEYDESGPGIVHR.K

Band-8

1. RB27C_DROME **Mass:** 44742 **Score:** 2367 **Queries matched:** 82 **emPAI:** 20.38 Heterogeneous nuclear ribonucleoprotein 27C OS=Drosophila melanogaster GN=Hrb27C PE=1 SV=2

Peptide	
R.TLQKPK.K	R.YGKVTEVVIMYDQEK.K
R.YINLNGK.Q	R.AQAWATGGPSTTGPVGGMPR.T
R.TFFNRYGK.V	R.FGDIIDCVVMKNNESGR.S
-.MEEDERGK.L	R.AQAWATGGPSTTGPVGGMPR.T
-.MEEDERGK.L	K.LFVGGLSWETTQENLSR.Y
R.TIDPKPCNPR.T	R.SAYGNDSSTQPPYATSQAV.-
K.QVEIKKAEPR.D	R.YGKVTEVVIMYDQEKK.K
K.QEGASNYGAGPR.S	R.FGDIIDCVVMKNNESGR.S
R.FGDIIDCVVMK.N	R.FGDIIDCVVMKNNESGR.S
R.YINLNGKQVEIK.K	R.GKLFVGGLSWETTQENLSR.Y
K.VTEVVIMYDQEK.K	K.GGGYKVFLGGLPSNVTETDLR.T
K.VTEVVIMYDQEK.K	R.GFGFLSFEEESSVEHVTNER.Y
R.YINLNGKQVEIKK.A	K.VFLGGLPSNVTETDLRTFFNR.Y
K.VTEVVIMYDQEKK.K	R.TFFNRYGKVTEVVIMYDQEK.K
K.VTEVVIMYDQEKK.K	K.SRGFGFLSFEEESSVEHVTNER.Y
K.VTEVVIMYDQEKKK.S	K.SGSEYDYGGYGSGYDYDYSNYVK.Q
K.VFLGGLPSNVTETDLR.T	K.VFLGGLPSNVTETDLRTFFNRYGK.V
K.VTEVVIMYDQEKKK.S	R.GFGFVTFADPTNVNHVLQNGPHTLDGR.T
R.DGSGGQNSNNSTVGGAYGK.L	-.MEEDERGKLFVGGLSWETTQENLSR.Y
R.YGKVTEVVIMYDQEK.K	R.SRGFGFVTFADPTNVNHVLQNGPHTLDGR.T
	K.SGSEYDYGGYGSGYDYDYSNYVKQEGASNYGAGPR.S

2. RL4_DROME **Mass:** 44998 **Score:** 520 **Queries matched:** 23 **emPAI:** 2.58 60S ribosomal protein L4 OS=Drosophila melanogaster GN=RpL4 PE=2 SV=2

Peptide	
R.MFAPTK.T	K.LNPYAEVLKR.R
	R.FVIWTESAFAR.L

K.QAVIFLR.R	R.GPLVVYDKDEGLRK.A
R.LNPLTNVR.Q	R.RGPLVVYDKDEGLR.K
K.SHFANVATK.A	M.SLGNARPLVSVYTEK.N
R.RAALAAEKR.T	R.YALVSAIAASGVPALVQSK.G
R.LLKSEEIR.K	K.APIRPDVVNEVHQLLR.R
K.LNPYAEVLK.R	R.NIPGIETINVDKLNLLK.L
K.NICLPAVFK.A	R.RYALVSAIAASGVPALVQSK.G
R.RLNPLTNVR.Q	K.APIRPDVVNEVHQLLRR.N
R.LKIWADIQK.V	K.GHVIDGVSEFPLVVSDEVQK.V
R.LLKSEEIRK.V	K.GHVIDGVSEFPLVVSDEVQKVQK.T

3. ILF2_DROME **Mass:** 43630 **Score:** 339 **Queries matched:** 11 **emPAI:** 0.93

Interleukin enhancer-binding factor 2 homolog OS=Drosophila melanogaster GN=CG5641 PE=1 SV=1

Peptide	K.GTILTGNNVADVVVILK.T
K.LMQSHLAAIR.H	K.VPSAGAVDDSALTAALLKR.N
R.ILIATLPQNLR.K	R.NQDLSPTPSEQTAIGNLVTK.V
R.QALPINLAFRR.V	R.VLAHGGYKHILGLEGNTSVVR.E
K.TLPTKEAVDALAK.K	R.VFQLLSAGLFLPGSAGITDPTEPGHIR.V

4. PABP_DROME **Mass:** 69882 **Score:** 306 **Queries matched:** 15 **emPAI:** 0.58

Polyadenylate-binding protein OS=Drosophila melanogaster GN=pAbp PE=1 SV=3

Peptide	R.IAFSPYGNITSAK.V
R.DPSLR.R	R.HESVFGVNLYVK.N
K.ELGEKAK.L	K.NLDDTIDDDRLR.I
R.KFEELK.Q	R.VVGSKPLYVALAQR.K
K.LFTNVYVK.N	K.RHESVFGVNLYVK.N
R.KFEELKQK.R	K.AIYDTFSAFGNILSCK.V
K.AKLFTNVYVK.N	R.SLGYAYVNFQQPADAER.A
R.FFGSQVATQMR.N	R.ALDTMNFDLVR.N

5. ACT1_DROME **Mass:** 41795 **Score:** 271 **Queries matched:** 19 **emPAI:** 1.49

Actin-5C OS=Drosophila melanogaster GN=Act5C PE=1 SV=4

Peptide	R.AVFPSIVGRPR.H
K.IIAPPER.K	K.DSYVGDEAQSKR.G
K.CDVDIRK.D	K.EITALAPSTMKIK.I
K.AGFAGDDAPR.A	K.QEYDESGPSIVHR.K
R.DLTDYLMK.I	R.MQKEITALAPSTMK.I
R.EIVRDIKEK.L	R.GYSFTTTAEREIVR.D
R.GYSFTTTAER.E	R.LDLAGRDLTDYLMK.I
K.IKIIAPPERK.Y	R.VAPEEHPVLLTEAPLNPK.A
K.EITALAPSTMK.I	R.HQGVMVGMGQKDSYVGDEAQSKR.G

Band-9

1. SQD_DROME **Mass:** 36162 **Score:** 1805 **Queries matched:** 66 **emPAI:** 24.59

RNA-binding protein squid OS=Drosophila melanogaster GN=sqd PE=1 SV=3

Peptide	R.KLFVGGLSWETTEK.E	K.TYFGQFGNIVEVEMPFDK.Q
K.EVDVKR.A	R.ATPKPENQMMGGMR.G	R.KGFCFITFDSEQVVTDLLK.T
K.IAGKEVDVK.R	R.GFAFIVFTNTEAIDK.V	K.TYFGQFGNIVEVEMPFDKQK.S
K.ELRDHFGK.Y	R.DHFGKYGEIESINVK.T	K.GFCFITFDSEQVVTDLLKTPK.Q
K.IAGKEVDVKR.A	K.IFVGGLTTEISDEEIK.T	K.LFVGGLSWETTEKELRDHFGK.Y
K.YGEIESINVK.T	K.RATPKPENQMMGGMR.G	R.DHFGKYGEIESINVKTDPQTGR.S
K.QKIAGKEVDVK.R	K.LFVGGLSWETTEKELR.D	R.KGFCFITFDSEQVVTDLLKTPK.Q
K.VSAADEHIINSK.K	K.YGEIESINVKTDPQTGR.S	R.GFAFIVFTNTEAIDKVSAADEHIINSK.K
K.VSAADEHIINSKK.V	R.SRGFAFIVFTNTEAIDK.V	R.GFAFIVFTNTEAIDKVSAADEHIINSKK.V
K.LFVGGLSWETTEK.E	M.AENKQVDTEINGEDFTK.D	K.DVTADGPGSENGDAGAAGSTNGSSDNQSAASGQR.D
K.QVDTEINGEDFTK.D	R.KLFVGGLSWETTEKELR.D	R.SRGFAFIVFTNTEAIDKVSAADEHIINSK.K
R.ATPKPENQMMGGMR.G	R.DDDRKLFVGGLSWETTEK.E	K.IFVGGLTTEISDEEIKTYFGQFGNIVEVEMPFDK.Q
R.ATPKPENQMMGGMR.G	K.GFCFITFDSEQVVTDLLK.T	K.IFVGGLTTEISDEEIKTYFGQFGNIVEVEMPFDKQK.S
K.ELRDHFGKYGEIESINVK.T		

2. RB87F_DROME **Mass:** 39476 **Score:** 571 **Queries matched:** 20 **emPAI:** 2.34

Heterogeneous nuclear ribonucleoprotein 87F OS=Drosophila melanogaster GN=Hrb87F PE=1 SV=2

Peptide	R.GFAFIEFDDYDPVDK.I
K.LFVGGLR.D	R.AVPRQEIDSPNAGATVKK.L
K.LFIGGLDYR.T	K.RAVPRQEIDSPNAGATVK.K
R.KLFIGGLDYR.T	K.DFGQIVSVNIVSDKDTGK.K
R.QEIDSPNAGATVK.K	R.NSNFGNNRPAPYSQGGGGGGFNK.G
R.TTDDGLKAHFEK.W	R.GFAFIEFDDYDPVDKIILQK.T
R.QEIDSPNAGATVKK.L	K.RGFAFIEFDDYDPVDKIILQK.T
K.WGNIVDVVVMKDPK.T	R.GFGFITYSQSYMIDNAQNARPHK.I
K.AIAKQDMDRQGGGGGR.G	R.SRGFGFITYSQSYMIDNAQNARPHK.I
R.AVPRQEIDSPNAGATVK.K	

3. RB27C_DROME **Mass:** 44742 **Score:** 413 **Queries**

matched: 18 **emPAI:** 1.04

Heterogeneous nuclear ribonucleoprotein 27C OS=Drosophila melanogaster GN=Hrb27C PE=1 SV=2

Peptide	
R.YINLNGK.Q	K.VTEVVIMYDQEKKK.S
R.TFFNRYGK.V	R.DGSGGQNSNNSTVGGAYGK.L
R.TIDPKPCNPR.T	R.YGKVTEVVIMYDQEK.K
K.VTEVVIMYDQEK.K	R.FGDIIDCVVMKNNESGR.S
K.VTEVVIMYDQEK.K	R.GFGFLSFEEESSVEHVTNER.Y
K.VTEVVIMYDQEKK.K	K.SRGFGFLSFEEESSVEHVTNER.Y
K.VFLGGLPSNVTETDLR.T	R.GFGFVTFADPTNVNHVLQNGPHTLDGR.T

4. ROA1_DROME **Mass:** 39014 **Score:** 407 **Queries matched:** 15 **emPAI:** 1.66

Heterogeneous nuclear ribonucleoprotein A1 OS=Drosophila melanogaster GN=Hrb98DE PE=1 SV=1

Peptide	
K.IDGRVVEPK.R	R.AVPRQDIDSPNAGATVKK.L
R.QDIDSPNAGATVK.K	R.GFGFITYSHSSMIDEAQK.S
R.QDIDSPNAGATVKK.L	R.SRGFGFITYSHSSMIDEAQK.S
K.ALPKQNDQQGGGGGR.G	R.GFAFVEFDDYDPVDKVVLQK.Q
R.AVPRQDIDSPNAGATVK.K	K.RGFAFVEFDDYDPVDKVVLQK.Q

Band-10

1. RB87F_DROME **Mass:** 39476 **Score:** 2075 **Queries matched:** 87 **emPAI:** 36.27

Heterogeneous nuclear ribonucleoprotein 87F OS=Drosophila melanogaster GN=Hrb87F PE=1 SV=2

Peptide	
K.TLDVKK.A	R.DDHDEECLREYFK.D
R.TVEPKR.A	R.GFAFIEFDDYDPVDK.I
K.LFVGGLR.D	R.AVPRQEIDSPNAGATVKK.L
K.NKTLDVK.K	K.RAVPRQEIDSPNAGATVK.K
K.KLFVGGLR.D	K.DFGQIVSVNIVSDKDTGK.K
K.NKTLDVKK.A	K.LFVGGLRDDHDEECLR.E
K.AIAKQDMDR.Q	K.RGFAFIEFDDYDPVDK.I
K.LFIGGLDYR.T	K.DFGQIVSVNIVSDKDTGKK.R
K.AIAKQDMDR.Q	K.KRGFAFIEFDDYDPVDK.I
K.TLDVKKAIAK.Q	R.EYFKDFGQIVSVNIVSDK.D
R.KLFIGGLDYR.T	R.NSNFGNNRPAPYSQGGGGGGFNK.G
K.WGNIVDVVVMK.D	R.GFAFIEFDDYDPVDKIILQK.T
R.QEIDSPNAGATVK.K	R.EYFKDFGQIVSVNIVSDKDTGK.K
R.TTDDGLKAHFEK.W	K.RGFAFIEFDDYDPVDKIILQK.T
K.THSIKNKTLDVK.K	R.GFGFITYSQSYMIDNAQNARPHK.I
R.QEIDSPNAGATVKK.L	R.GFGFITYSQSYMIDNAQNARPHK.I
K.DFGQIVSVNIVSDK.D	M.AEQNDSNGNYDDGEEITEPEQLR.K
K.WGNIVDVVVMKDPK.T	K.GNQGGGQGFAGNNYNTGGGGQGGNMGGGNR.R
	M.AEQNDSNGNYDDGEEITEPEQLRK.L

K.AIAKQDMDRQGGGGGR.G	K.GNQGGGQGFAGNNYNTGGGGQGGNMGGGNRR.Y
K.AIAKQDMDRQGGGGGR.G	R.SRGFGFITYSQSYMIDNAQNARPHK.I
R.AVPRQEIDSPNAGATVK.K	R.SRGFGFITYSQSYMIDNAQNARPHK.I
R.DDHDEECLREYFK.D	R.DDHDEECLREYFKDFGQIVSVNIVSDK.D

2. ROA1_DROME **Mass:** 39014 **Score:** 1566 **Queries matched:** 87 **emPAI:** 29.69

Heterogeneous nuclear ribonucleoprotein A1 OS=Drosophila melanogaster GN=Hrb98DE PE=1 SV=1

Peptide	
R.GGPGGR.A	K.WGNIVDVVVMKDPR.T
K.MVDVKK.A	K.WGNIVDVVVMKDPR.T
R.VVEPKR.A	R.AVPRQDIDSPNAGATVK.K
K.MVDVKK.A	R.GFAFVEFDDYDPVDK.V
K.LFVGALK.D	K.LFVGALKDDHDEQSIR.D
R.TTDENLK.A	R.AVPRQDIDSPNAGATVKK.L
K.KLFVGALK.D	R.RGFAFVEFDDYDPVDK.V
R.GGGNFNNNR.M	K.ALPKQNDQQGGGGGRGGPGGR.A
K.IDGRVVEPK.R	R.GFGFITYSHSSMIDEAQK.S
K.SRPHKIDGR.V	R.GFGFITYSHSSMIDEAQK.S
K.DDHDEQSIR.D	K.AGGGNQGNYGGNNQGFNNGGNNR.R
K.IDGRVVEPKR.A	R.SRGFGFITYSHSSMIDEAQK.S
R.KLFIGGLDYR.T	R.SRGFGFITYSHSSMIDEAQK.S
R.MQPYQGGGGFK.A	R.GFAFVEFDDYDPVDKVVLQK.Q
K.WGNIVDVVVMK.D	K.RGFAFVEFDDYDPVDKVVLQK.Q
R.QDIDSPNAGATVK.K	R.DYFQHFGNIVDINIVIDKETGK.K
K.QHQLNGKMVDVK.K	R.DYFQHFGNIVDINIVIDKETGKK.R
R.TTDENLKAHFEK.W	K.DDHDEQSIRDYFQHFGNIVDINIVIDK.E
R.QDIDSPNAGATVKK.L	M.VNSNQNQNGNSNGHDDDFPQDSITEPEHMR.K
K.ALPKQNDQQGGGGGR.G	M.VNSNQNQNGNSNGHDDDFPQDSITEPEHMRK.L
K.QNDQQGGGGGRGGPGGR.A	K.DDHDEQSIRDYFQHFGNIVDINIVIDKETGK.K

3. RLA0_DROME **Mass:** 34181 **Score:** 203 **Queries matched:** 10 **emPAI:** 1.52

60S acidic ribosomal protein P0 OS=Drosophila melanogaster GN=RpLP0 PE=1 SV=1

Peptide
K.GDLAEVR.D
R.DKLLESK.V
R.GLAVVLMGK.N
K.VVELFDEFPK.C
K.CFIVGADNVGSK.Q
R.GHLENNPQLEK.L
K.TSFFQALSIPTK.I
K.GTIEIINDVPILKPGDK.V
R.APARPGAIAPLHVIIPAQNTGLGPEK.T

4. SQD_DROME **Mass:** 36162 **Score:** 1130 **Queries matched:** 28 **emPAI:** 5.30

RNA-binding protein squid OS=Drosophila melanogaster GN=sqd PE=1

SV=3

Peptide	K.GFCFITFDSEQVVTDLLK.T
K.EVDVKR.A	K.ELRDHFGKYGEIESINVK.T
K.ELRDHFGK.Y	K.TYFGQFGNIVEVEMPFDK.Q
K.IAGKEVDVKR.A	R.KGFCFITFDSEQVVTDLLK.T
K.YGEIESINVK.T	K.TYFGQFGNIVEVEMPFDKQK.S
K.VSAADEHIINSK.K	K.LFVGGLSWETTEKELRDHFGK.Y
R.ATPKPENQMMGGMR.G	R.KGFCFITFDSEQVVTDLLKTPK.Q
R.GFAFIVFTNTEAIDK.V	R.GFAFIVFTNTEAIDKVSAADEHIINSK.K
K.IFVGGLTTEISDEEIK.T	R.SRGFAFIVFTNTEAIDKVSAADEHIINSK.K
K.LFVGGLSWETTEKELR.D	K.IFVGGLTTEISDEEIKTYFGQFGNIVEVEMPFDK.Q
K.YGEIESINVKTDPQTGR.S	K.IFVGGLTTEISDEEIKTYFGQFGNIVEVEMPFDKQK.S
R.SRGFAFIVFTNTEAIDK.V	K.QVDTEINGEDFTKDVTADGPGSENGDAGAAGSTNGSSDNQSAASGQR.D
M.AENKQVDTEINGEDFTK.D	

Band-11

1. RLA0_DROME **Mass:** 34181 **Score:** 1048 **Queries matched:** 38 **emPAI:** 15.09

60S acidic ribosomal protein P0 OS=Drosophila melanogaster GN=RpLP0 PE=1 SV=1

Peptide	K.EATTIKEYIKDPSK.F
K.LLPHIK.G	K.TSFFQALSIPTKISK.G
K.GDLAEVR.D	K.GNVGFVFTKGDLAEVR.D
K.AQYFIK.V	K.FAAAASASAAPAAGGATEKK.E
K.QMQNIR.T	K.GTIEIINDVPILKPGDK.V
R.DKLLESK.V	K.GNVGFVFTKGDLAEVRDK.L
R.GLAVVLMGK.N	K.CFIVGADNVGSKQMQNIR.T
K.GNVGFVFTK.G	K.ISKGTIEIINDVPILKPGDK.V
K.EYIKDPSK.F	K.FAAAASASAAPAAGGATEKKEEAK.K
K.GDLAEVRDK.L	K.VVELFDEFPKCFIVGADNVGSK.Q
K.VVELFDEFPK.C	K.EYIKDPSKFAAAASASAAPAAGGATEK.K
K.CFIVGADNVGSK.Q	R.APARPGAIAPLHVIIPAQNTGLGPEK.T
R.GHLENNPQLEK.L	K.VRAPARPGAIAPLHVIIPAQNTGLGPEK.T
K.TSFFQALSIPTK.I	K.GDLAEVRDKLLESK.V
R.TSLRGLAVVLMGK.N	K.FAAAASASAAPAAGGATEK.K
K.NLLAIAATTEVEFK.E	

2. ROA1_DROME **Mass:** 39014 **Score:** 701 **Queries matched:** 35 **emPAI:** 4.11

Heterogeneous nuclear ribonucleoprotein A1 OS=Drosophila melanogaster GN=Hrb98DE PE=1 SV=1

Peptide	K.WGNIVDVVVMKDPR.T
K.KLFVGALK.D	R.AVPRQDIDSPNAGATVK.K
K.IDGRVVEPK.R	R.GFAFVEFDDYDPVDK.V

K.LFIGGLDYR.T	K.LFVGALKDDHDEQSIR.D
R.KLFIGGLDYR.T	R.AVPRQDIDSPNAGATVKK.L
R.MQPYQGGGGFK.A	R.GFGFITYSHSSMIDEAQK.S
R.QDIDSPNAGATVK.K	R.SRGFGFITYSHSSMIDEAQK.S
R.TTDENLKAHFEK.W	R.GFAFVEFDDYDPVDKVVLQK.Q
R.QDIDSPNAGATVKK.L	K.RGFAFVEFDDYDPVDKVVLQK.Q
K.ALPKQNDQQGGGGGR.G	

3. RL5_DROME **Mass:** 34016 **Score:** 672 **Queries matched:** 30 **emPAI:** 7.53

60S ribosomal protein L5 OS=Drosophila melanogaster GN=RpL5 PE=1 SV=2

Peptide	R.REGKTDYYAR.K
R.LTFQDK.N	K.GAVDGGLNIPHSVK.R
K.TDYYAR.K	R.VVCAAYSHELPK.Y
K.RLTFQDK.N	R.SLEEEDEESFKR.Q
K.SFNADVHR.A	K.GAVDGGLNIPHSVKR.F
K.NKQYFKR.Y	K.LGIRADDLEDIYK.K
R.FPGYSAETK.S	R.AHIFGQHVADYMR.S
R.CFLDVGLAR.T	R.LSNKDITVQIAYAR.I
R.ADDLEDIYK.K	R.LTFQDKNKYNTPK.Y
R.EGKTDYYAR.K	K.LGIRADDLEDIYKK.A
K.RFPGYSAETK.S	K.AHQAIRNDPTHKVTAK.K
R.ADDLEDIYKK.A	R.IEGDRVVCAAYSHELPK.Y
R.EGKTDYYARK.R	R.VFGAMKGAVDGGLNIPHSVK.R
	R.VFGAMKGAVDGGLNIPHSVKR.F

4. RB87F_DROME **Mass:** 39476 **Score:** 629 **Queries matched:** 30 **emPAI:** 2.08

Heterogeneous nuclear ribonucleoprotein 87F OS=Drosophila melanogaster GN=Hrb87F PE=1 SV=2

Peptide	R.AVPRQEIDSPNAGATVK.K
K.TLDVKK.A	R.GFAFIEFDDYDPVDK.I
K.LFVGGLR.D	R.AVPRQEIDSPNAGATVKK.L
R.QEIDSPNAGATVK.K	K.DFGQIVSVNIVSDKDTGK.K
R.TTDDGLKAHFEK.W	R.GFAFIEFDDYDPVDKIILQK.T
R.QEIDSPNAGATVKK.L	K.RGFAFIEFDDYDPVDKIILQK.T
K.WGNIVDVVVMKDPK.T	R.GFGFITYSQSYMIDNAQNARPHK.I
K.AIAKQDMDRQGGGGGR.G	R.SRGFGFITYSQSYMIDNAQNARPHK.I

5. RS3A_DROER **Mass:** 30321 **Score:** 528 **Queries matched:** 19 **emPAI:** 4.29

40S ribosomal protein S3a OS=Drosophila erecta GN=RpS3A PE=3 SV=1

Peptide	R.IYPLHDVYIR.K
R.IASDYLK.G	K.LALDSIAKDIEK.S
K.VVDPFSR.K	R.KTCYAQQSQVR.K

K.TVDGYLLR.V	K.GRVFEVSLADLQK.D
K.APNMFQTR.Q	R.MTDIITNEVSGADLK.Q
R.VFCIGFTAK.D	R.VFCIGFTAKDQQSQR.K
R.LIAEDVQDR.N	R.ARMTDIITNEVSGADLK.Q
K.LLELHGDGGGK.S	R.VFEVSLADLQKDIDPER.S
K.TCYAQQSQVR.K	K.GRVFEVSLADLQKDIDPER.S

6. RS3_DROME **Mass:** 27454 **Score:** 311 **Queries matched:** 13 **emPAI:** 2.53

40S ribosomal protein S3 OS=Drosophila melanogaster GN=RpS3 PE=1 SV=1

Peptide	K.VKVMLPYDPK.N
K.VMLPYDPK.N	R.GLCAIAQAESLR.Y
-.MNANLPISK.K	K.KPLPDNVSVVEPK.E
R.YKLTGGLAVR.R	R.ELAEDGYSGVEVR.V
R.ELTAMVQKR.F	R.VTPSRTEIIIMATK.T
K.TQQVLGEKGR.R	R.FNFETGRIELYAEK.V
-.MNANLPISKK.R	

7. RB27C_DROME **Mass:** 44742 **Score:** 231 **Queries matched:** 9 **emPAI:** 0.53

Heterogeneous nuclear ribonucleoprotein 27C OS=Drosophila melanogaster GN=Hrb27C PE=1 SV=2

Peptide
R.TFFNRYGK.V
R.TIDPKPCNPR.T
K.VTEVVIMYDQEK.K
K.VFLGGLPSNVTETDLR.T
K.VTEVVIMYDQEKKK.S
R.DGSGGQNSNNSTVGGAYGK.L
R.GFGFLSFEEESSVEHVTNER.Y
R.GFGFVTFADPTNVNHVLQNGPHTLDGR.T

APPENDIX-II

the FEBS Journal

Midgut-enriched receptor protein tyrosine phosphatase PTP52F is required for *Drosophila* development during larva–pupa transition

Abirami Santhanam[1,2,3], Suh-Yuen Liang[4], Dong-Yuan Chen[2,3], Guang-Chao Chen[1,2,3] and Tzu-Ching Meng[1,2,3]

1 Taiwan International Graduate Program, Academia Sinica, Taipei, Taiwan
2 Institute of Biochemical Sciences, National Taiwan University, Taipei, Taiwan
3 Institute of Biological Chemistry, Academia Sinica, Taipei, Taiwan
4 Core Facility for Protein Structural Analysis, Academia Sinica, Taipei, Taiwan

Keywords
Drosophila development; metamorphosis; midgut; PTP52F; receptor protein tyrosine phosphatase

Correspondence
G.-C. Chen and T.-C. Meng, Institute of Biological Chemistry, Academia Sinica, 128 Academia Rd, Section 2, Taipei 11529, Taiwan
E-mails: gcchen@gate.sinica.edu.tw; tcmeng@gate.sinica.edu.tw

(Received 20 March 2012, revised 22 June 2012, accepted 3 July 2012)

doi:10.1111/j.1742-4658.2012.08696.x

To date our understanding of *Drosophila* receptor protein tyrosine phosphatases (R-PTPs) in the regulation of signal transduction is limited. Of the seven R-PTPs identified in flies, six are involved in the axon guidance that occurs during embryogenesis. However, whether and how R-PTPs may control key steps of *Drosophila* development is not clear. In this study we investigated the potential role of *Drosophila* R-PTPs in developmental processes outside the neuronal system and beyond the embryogenesis stage. Through systematic data mining of available microarray databases, we found the mRNA level of PTP52F to be highly enriched in the midgut of flies at the larva–pupa transition. This finding was confirmed by gut tissue staining with a specific antibody. The unique spatiotemporal expression of PTP52F suggests that it is possibly involved in regulating metamorphosis during the transformation from larva to pupa. To test this hypothesis, we employed RNA interference to examine the defects of transgenic flies. We found that ablation of endogenous PTP52F led to high lethality characterized by the pharate adult phenotype, occurring due to post pupal eclosion failure. These results show that PTP52F plays an indispensable role during the larva–pupa transition. We also found that PTP52F could be reclassified as a member of the subtype R3 PTPs instead of as an unclassified R-PTP without a human ortholog, as suggested previously. Together, these findings suggest that *Drosophila* R-PTPs may control metamorphosis and other biological processes beyond our current knowledge.

Introduction

Reversible tyrosine phosphorylation is a very important post-translational modification. A diverse array of biological processes controlled by protein tyrosine phosphorylation and dephosphorylation in various metazoans are mediated by the coordinated action between protein tyrosine kinases (PTKs) and protein tyrosine phosphatases (PTPs) [1,2]. The characterization of PTKs, PTPs and their numerous substrates is of critical importance to our understanding of how the homeostasis of signal transduction is achieved. Over the last two decades, because of advances in biochemical, molecular and genetic approaches, the

Abbreviations
ConA, concanavalin A; CS, C1290S mutant; EcR, ecdysone receptor; HA, hemagglutinin; PTK, protein tyrosine kinase; PTP, protein tyrosine phosphatase; PTP-d, PTP-δelta; PTP-σ, PTP-sigma; RNAi, RNA interference; R-PTP, receptor protein tyrosine phosphatase; WT, wild-type.

functions of many of the key players involved in this context, in particular PTKs, have been clarified [3,4]. In contrast, our understanding of PTPs in the regulation of protein tyrosine phosphorylation dependent signal transduction has lagged behind. Issues including substrate specificity as well as spatial and temporal control of cell signaling determined by PTPs remain elusive.

Since its development more than 15 years ago, the substrate trapping technique [5] has been used to identify numerous bona fide and potential substrates of PTPs, significantly accelerating the biochemical characterization of these enzymes. Recently, studies have used specific PTP knockout mice to delineate their roles in developmental control and disease conditions. A few studies have clearly defined the critical role of some non-receptor PTPs, such as PTP1B in regulating insulin responsiveness [6,7], leptin signaling [8–10] and breast tumorigenesis [11], T-cell PTP in regulating T-cell signaling [12], as well as SHP-2, which participates in *Helicobacter pylori* induced gastric ulcer [13], Noonan syndrome [14] and LEOPARD syndrome [15,16]. Genetic studies of other PTPs in mice, however, have encountered some difficulties, mostly due to the redundancy of multiple regulatory components in a given signaling pathway. This problem was particularly present in the investigation of receptor PTPs (R-PTPs). One such problem has been encountered in the genetic characterization for the functional role of R-PTPs belonging to the subtype R2A phosphatases [17]. Since the first knockout mouse model was generated, it has been suggested that PTP-sigma (PTP-σ) might participate in determining axon regeneration and extension [18]. However, detailed investigations found that the deletion of PTP-σ *per se* failed to produce an obvious phenotype during neuronal development [19], largely due to the functional compensation contributed by other R-PTPs in the same subtype. To date, it is clear that PTP-σ and PTP-delta (PTP-δ), both subtype R2A PTPs, compensate for each other in the control of neuronal development. Quantitative analyses have demonstrated that PTP-$\sigma^{+/-}$/PTP-$\delta^{-/-}$ and PTP-$\sigma^{-/-}$/PTP-$\delta^{+/-}$ mutants exhibit intermediate phenotypes in motoneuron survival and phrenic nerve branching, whereas no significant defect has been detected in either PTP-σ or PTP-δ single mutants [17]. These data suggest that more studies involving multiple knockouts in mice are needed to clarify the functional role of individual PTPs. Considering the complexity of functional compensation among mammalian PTPs, we proposed that other simpler model organisms might provide alternatives for genetically characterizing the PTPome.

Drosophila is an excellent model organism for investigating diverse tyrosine phosphorylation dependent signaling pathways, which are regulated by many modulators exhibiting similar functions across species throughout evolution [20–22]. Its relatively simple genome allows the precise dissection of signaling networks without the genetic redundancy related complications often seen in mammalian genetic screenings [23–25]. Moreover, while there are a large number of classical PTPs in mammals (38 in humans), there are only 15 putative *ptp* genes in the Drosophila genome (eight non-receptor PTPs and seven R-PTPs). Several of the *Drosophila* PTPs have been classified as orthologs of human PTPs based on the similar sequence alignment between the two, suggesting evolutionarily conserved functions [26]. In fact, a number of early breakthroughs in functional characterizations of R-PTPs have been made in genetic studies of *Drosophila*, and all R-PTPs have been found to be involved in axon guidance during embryogenesis [27–30].

To date, the findings used to define the functional role of R-PTPs in axon guidance have been limited to embryogenesis, however. Other than this stage, it is not clear whether and how R-PTPs participate in the regulation of *Drosophila* development. Therefore, in this study we investigated potential R-PTP involvement in development beyond the embryonic stage. Systematic data mining of available microarray databases found PTP52F to be highly enriched in the midgut tissue of prepupal flies. Our genetic studies demonstrated that PTP52F plays a critical role in the control of *Drosophila* development during the larva–pupa transition.

Results

Profiling of PTPs during *Drosophila* development by in-gel phosphatase activity assay

While individual PTPs have been implicated in the regulation of *Drosophila* development during embryogenesis, the expression and activity profile of PTPs at other developmental stages remain uncharacterized. Such data might provide more insight into the role of PTPs in the control of the developmental process. We used an in-gel phosphatase activity assay to visualize the possible participation of PTPs at each developmental stage. This assay displays a diverse array of active PTPs in total extracts of cells and tissues according to the molecular weights of these phosphatases resolved by SDS/PAGE. As shown in Fig. 1, the overall PTP activity in the embryonic stage was significantly higher than in other developmental stages, suggesting that

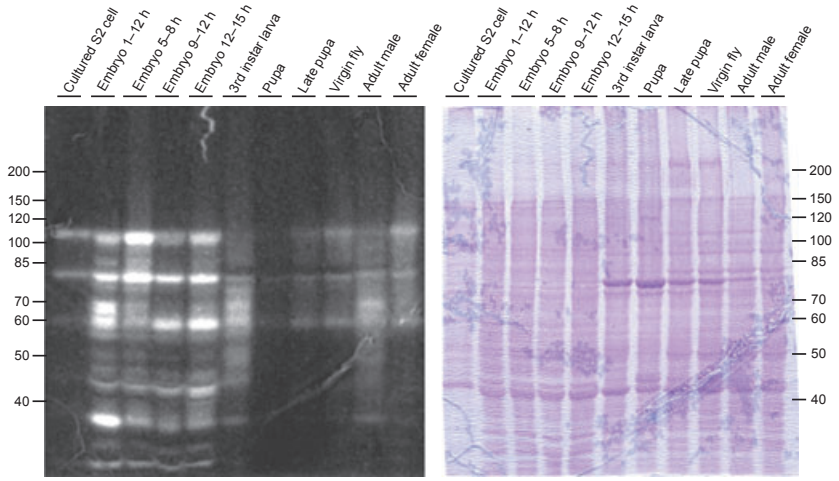

Fig. 1. In-gel assay reveals the dynamic change of PTP activity in multiple stages during *Drosophila* development. The total protein extracts (35 μg each) were collected from the whole fly at various developmental stages as indicated, and then applied to an SDS gel cast in the presence of radioisotope-labeled PTP substrate. Left panel: After the complete process with the denaturation and renaturation buffers, the gel was exposed to an X-ray film for visualization of the PTPs. The clear zones shown in each lane represent the activity of phosphatases according to their molecular weights resolved by SDS/PAGE. Right panel: The Coomassie blue staining of the same gel indicates an equal amount of protein extract loaded in each lane.

rapid protein tyrosine dephosphorylation plays a critical role in signal transduction during this stage. We found the activity of many PTPs to be diminished during the larva–pupa transition, and increased slightly in adult flies (Fig. 1). Although some PTPs were visible in adult flies, their activity was far weaker than the activity of those in embryos (Fig. 1). The biological implication of such interesting observations requires further investigation. Nonetheless, it should be addressed that all phosphatases detected by this assay format are likely to be non-R-PTPs due to the inherent limitation of the technique [31,32]. Indeed none of the *Drosophila* R-PTPs, which run greater than 100 kDa in SDS gels according to theoretical calculation (http://www.uniprot.org), was unraveled by the in-gel phosphatase activity assay (Fig. 1). Obviously, other methods are needed to collect information for profiling R-PTPs at different stages of *Drosophila* development.

Data mining of microarray databases to depict the mRNA expression profiles of R-PTPs during *Drosophila* development

Since the protein expression profiles of R-PTPs were not available, we switched our focus to other information such as the mRNA level of these phosphatases over various developmental stages. Flybase provides modENCODE temporal expression data for each gene [33,34] (http://www.modencode.org). Since this database shows the expression pattern of every gene throughout the development of flies and is easily accessed, we decided to perform data mining to profile R-PTPs using already existing information embedded in Flybase. We analyzed all R-PTPs in the *Drosophila* genome, including dLAR, PTP4E, PTP10D, PTP52F, PTP99A and PTP69D but excepting dIA2 which is a naturally inactive phosphatase. We examined the mRNA levels of these R-PTPs at various developmental stages (the embryo, early and late third instar larva, white prepupa, pupa and adult). As seen in Fig. 2, all R-PTPs except PTP52F were highly expressed during embryogenesis. PTP4E, PTP10D and PTP69D levels were particularly pronounced in embryos (Fig. 2A,B), suggesting that they may play essential roles in the control of developmental events at this time. These findings are in agreement with those of two recent studies reporting that PTP4E, PTP10D and PTP69D act in coordination of axon guidance during embryogenesis and that they have redundant and compensating functions [35]. Perhaps the most interesting observation in the profiling was the gradually increased expression of PTP52F from the embryonic stage to the larva–pupa transition (Fig. 2A,B), at which time metamorphosis begins and most larval tissues are readily remodeled for the development to adult flies [36]. The discovery that PTP52F is specifically expressed at this particular stage of development suggested that R-PTPs may be involved in the control of metamorphosis, despite a very low activity of non-R-PTPs being observed at this time of pupal formation (Fig. 1).

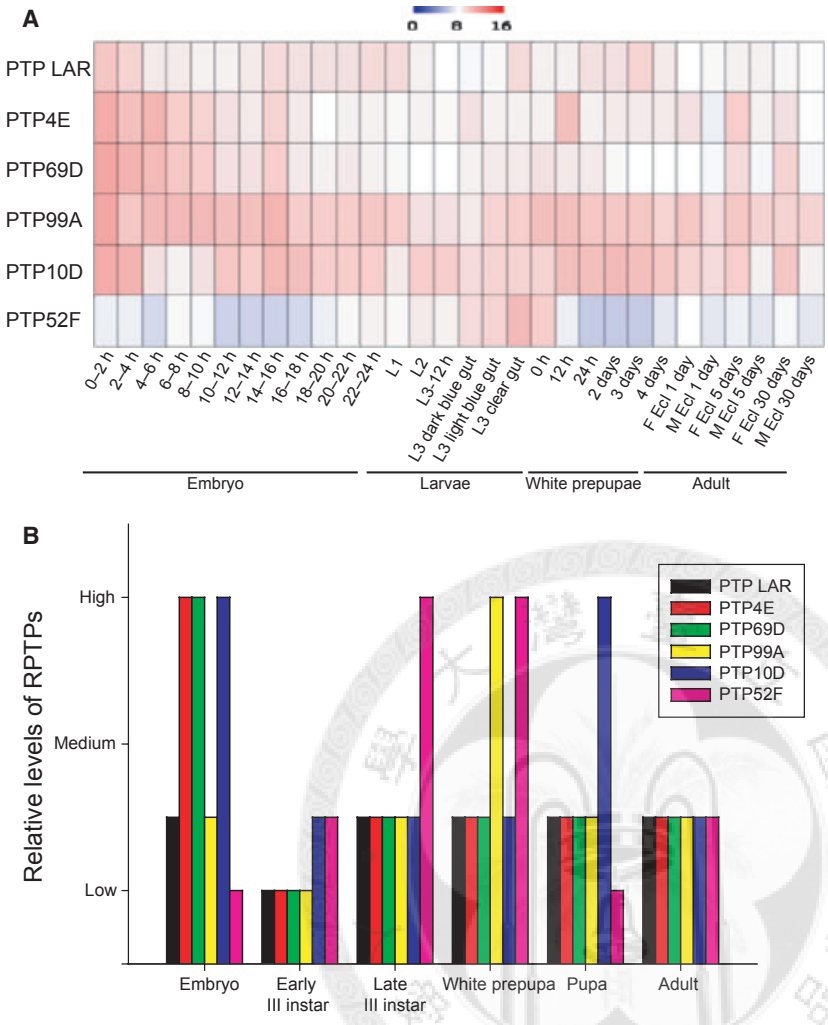

Fig. 2. Data mining reveals the mRNA expression profile of R-PTPs in multiple stages during *Drosophila* development. The mRNA levels of six *Drosophila* R-PTPs at various developmental stages were obtained from the modENCODE Temporal Expression Data of the Flybase. (A) Heat map showing relative changes in R-PTP expressions following the onset of embryogenesis until adult. The heat map scale indicates the relative fold expression of genes within this group as $\log_2$ of the actual value. (B) A simple graphical representation of the heat map for easy visualization. Note that PTP52F and PTP99A were expressed in relatively high levels during the larva–pupa transition.

PTP52F is highly enriched in midgut during the larva–pupa transition

We wanted to examine the expression of R-PTPs in various tissues of *Drosophila*, particularly focusing on the tissue distribution of PTP52F, which is highly expressed during the larva–pupa transition (Fig. 2). We used data mining to profile the expression of R-PTPs in the third instar larval tissues including salivary gland, central nervous system, trachea, tubule, hindgut and midgut using the FlyAtlas database, which provides the most comprehensive collection of the mRNA level data on each gene in each tissue during the third instar larva and adult stages of development [37] (http://www.flyatlas.org). Data were mined using three criteria: (a) mRNA SIGNAL, the abundance of mRNA; (b) mRNA ENRICHMENT, mRNA of the specific gene compared with the total mRNA of the whole flies; and (c) the Affymetrix PRESENT CALL, the number of times a specific gene was detectably expressed out of four arrays being analyzed. To summarize our findings, we present a simplified anatomy of the third instar larvae showing major tissues with relative expression levels of R-PTPs (Fig. 3). Four out of six R-PTPs (dLAR, PTP4E, PTP99A and PTP69D) were detected in the central nervous system, suggesting that they play important roles in the neuronal formation not only during embryogenesis but also at the beginning of metamorphosis. To our surprise, we found PTP52F to be exclusively expressed in gut tissues, and to be particularly enriched in the midgut (Fig. 3). Since this kind of tissue distribution of R-PTPs had never been recorded in flies, we hypothesized that PTP52F may have a specific role in the regulation of gut tissue during the larva–pupa transition. Thus, the remainder of the study was devoted to the characterization of PTP52F and the study of its potential involvement in *Drosophila* development.

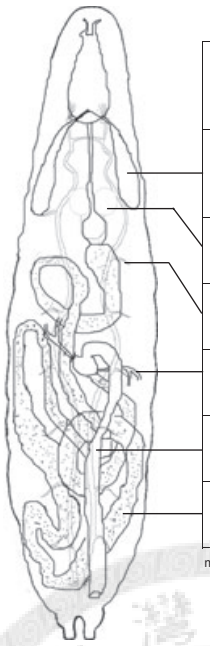

Tissue	mRNA level					
	PTP LAR	PTP4E	PTP69D	PTP99A	PTP10D	PTP52F
Salivary gland	--	+	+	--	--	--
CNS	++	+	+++	++++	--	--
Trachea	--	+++	--	+	+	--
Tubule	--	--	+	--	--	--
Hindgut	--	++++	--	--	+	+
Midgut	--	--	--	--	--	+++

mRNA level scale : <50 = --;100-199 = +; 200-299 = ++; 300-399 = +++; 400-499 = ++++; >500 = +++++

Fig. 3. Tissue distribution of R-PTPs at the third instar larval stage. The diagram on the left shows the major tissues that are undergoing metamorphosis during the transformation from larva to pupa. The relative mRNA level of each R-PTP in these tissues obtained from the FlyAtlas is shown in the right panel. For easy visualization, the numerical value of mRNA expression has been converted into a scale of enrichment indicated by the plus sign. Note that PTP52F was specifically enriched in the midgut.

Identification of PTP52F as an active plasma-membrane-localized phosphatase

We performed sequence analysis on the full-length cDNA of *Ptp52F* gene that we cloned from flies and found it to be identical to the one published previously [38]. As shown in Fig. 4(A), the PTP52F protein contains a putative signal sequence, six fibronectin type III repeats, a single transmembrane segment and a single phosphatase domain in the intracellular region. We generated an antibody specifically targeting the C-terminal tail outside the phosphatase domain (Fig. 4A). This antibody recognized the wild-type (WT) phosphatase ectopically expressed in *Drosophila* S2 cells (Fig. 4B). We noticed that the full-length PTP52F ran as a single band at a higher position ($\sim$ 200 kDa) than the predicted size ($\sim$ 160 kDa) in SDS gels (Fig. 4B), suggesting the occurrence of post-translational modifications. The phosphatase activity of the WT form of PTP52F, but not the C1290S mutant (CS) form, was confirmed by the typical pNPP assay (Fig. 4C). Furthermore, an *in vitro* assay demonstrated that partially purified PTP52F could dephosphorylate pTyr proteins in S2 cell lysates (Fig. S1), suggesting the tyrosine phosphatase activity of this R-PTP. To examine the subcellular localization of PTP52F, we performed immunofluorescence staining with PTP52F antibody together with F-actin co-staining in S2 cells attached to the lectin concanavalin A (ConA) substrate. When spreading on the ConA-coated surface, cortical actin structure in S2 cells would be concentrated at the cell periphery, thus allowing us to determine the leading edge of the plasma membrane as demonstrated in our previous study [39]. Using F-actin staining as the guidance, we have observed that the ectopically expressed WT form of PTP52F is highly enriched near the plasma membrane (Fig. 4D). Considered together, these findings suggest that PTP52F acts as an active form of receptor tyrosine phosphatase.

Endogenous PTP52F protein is localized specifically in the larval midgut

We used the antibody that we generated to examine the expression of endogenous PTP52F in total protein extracts isolated from both WT and PTP52F knockdown (RNA interference, RNAi) flies at the third instar larval stage, when mRNA of PTP52F was robustly enriched (Figs 2 and 3). As shown in Fig. 5A, the specific band at $\sim$ 200 kDa appeared only in the WT flies but not in the RNAi line, suggesting that endogenous PTP52F protein was indeed expressed during the larva–pupa transition. The excellent performance of this antibody indicated that we could use it to further characterize PTP52F in developing flies with various genetic backgrounds. The results of our data mining of the FlyAtlas (Fig. 3) suggested that there would be a robust level of PTP52F protein in the prepupal midgut tissue. To find out, we performed immunofluorescence staining with anti-PTP52F antibody. As shown in Fig. 5B, there was a strong signal of PTP52F in the midgut of WT flies, suggesting that a high level of mRNA at this developmental stage (Figs 2 and 3) might lead to enhanced expression of its protein in

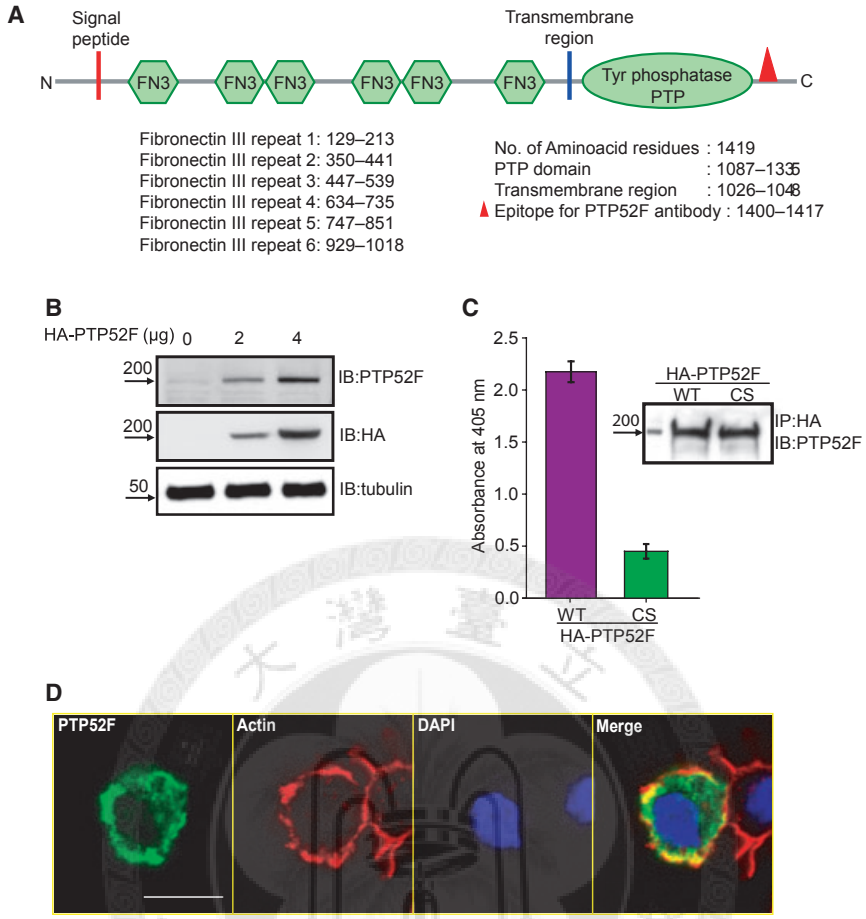

Fig. 4. Characterization of PTP52F as an active phosphatase located in the cell periphery. (A) The layout of fibronectin III repeats (FN3) and a phosphatase domain in the basic architecture of full-length PTP52F. The motif used as the epitope for antibody generation on the C-terminal region is marked. (B) Various amounts of plasmid were used for expressing the WT form of HA-tagged PTP52F in S2 cells. Aliquots of total lysates were subjected to immunoblotting with anti-PTP52F antibody and anti-HA antibody. (C) The HA-tagged WT form and CS form of full-length PTP52F were expressed in S2 cells and then purified by immunoprecipitation with anti-HA antibody. Equal amounts of both WT and CS forms of immunoprecipitated PTP52F were subjected to the phosphatase activity assay using pNPP as a substrate. The inset summarizes the results of immunoblotting with anti-PTP52F antibody. Similar levels of immunoprecipitated PTP52F were used for the activity assay. (D) The WT form of PTP52F was expressed in S2 cells. The subcellular localization of PTP52F was then examined in ConA-coated coverslips by immunofluorescence staining with anti-PTP52F antibody. Co-staining with cortical F-actin showed the clear localization of PTP52F in the cell periphery. Bar, 10 μm.

larval epidermal cells or adult epidermal progenitor cells, both of which are major types of cells in the larval midgut [40]. In contrast, immunofluorescence staining of the salivary gland with anti-PTP52F antibody resulted in negative signal (Fig. S2), consistent with an undetectable level of PTP52F mRNA in this part of the prepupal flies (Fig. 3). We further performed immunofluorescence staining using PTP52F knockdown flies driven by *Tubulin-Gal4* to ensure the specificity of the antibody *in vivo*. Focusing on the midgut tissues, we observed that the PTP52F signal was completely ablated in the RNAi transgenic flies, whereas the staining of PTP52F in the WT flies was robust (Fig. 5C). Using this antibody, we further tested the distribution of endogenous PTP52F in the whole gut tissue of the WT flies at the pupal stage. Interestingly, the staining of PTP52F protein was highly enriched in the midgut but much weaker in the hindgut region (Fig. 5D), consistent with the information of its mRNA distribution provided by the FlyAtlas (Fig. 3).

The essential role of PTP52F in *Drosophila* development

To test whether enriched expression of PTP52F in the midgut of prepupal flies plays a key role in development,

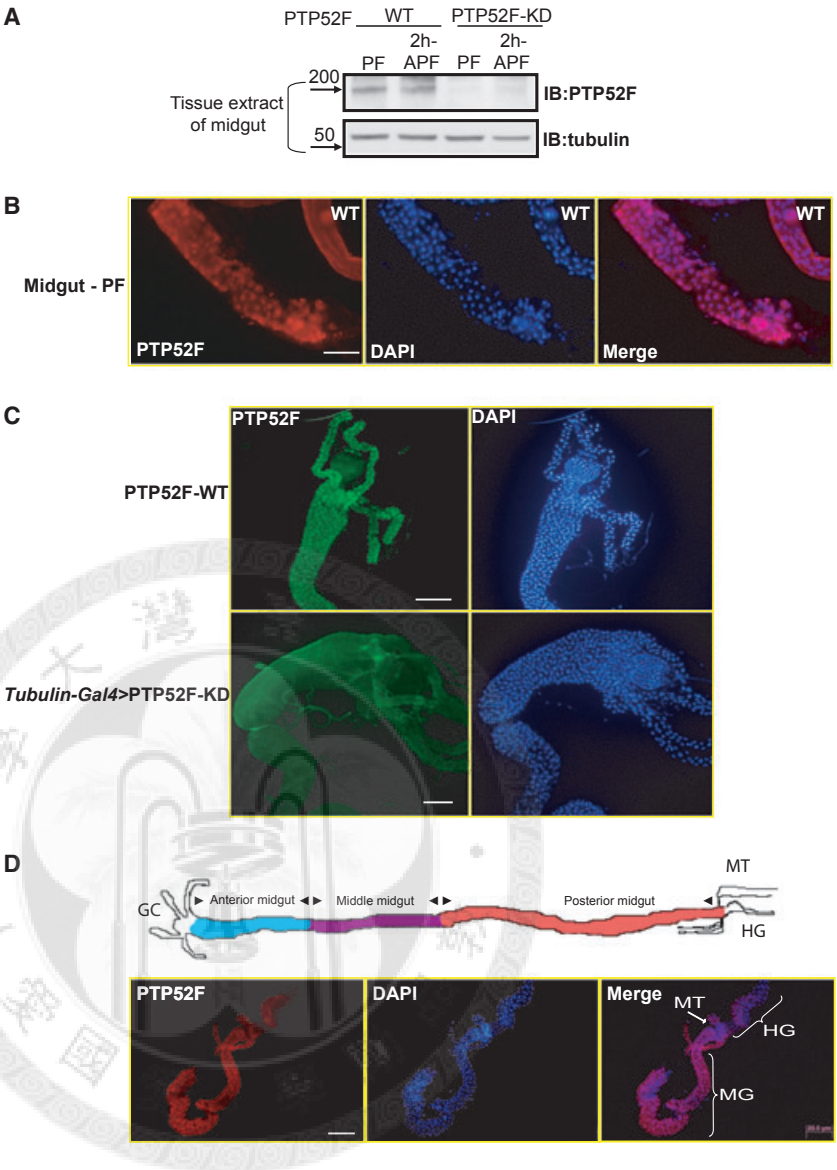

Fig. 5. Expression of endogenous PTP52F in the larval midgut. (A) Aliquots of total protein extracts isolated from the WT and PTP52F knockdown (RNAi) flies at pupal formation (PF) and 2 h after pupal formation (2 h-APF) were subjected to immunoblotting with anti-PTP52F antibody. (B) The midgut tissues isolated from the PF stage of WT flies were subjected to immunofluorescence staining with anti-PTP52F antibody. Bar, 20 μm. (C) The midgut tissues isolated from both WT and PTP52F knockdown (KD) flies were stained with anti-PTP52F antibody. Note that the fuzzy green color shown in the PTP52F KD tissue was contributed by the background auto-fluorescence. Bar, 200 μm. (D) The diagram shown at the top indicates the layout of gut tissue at the prepupal stage. Abbreviations: GC, gastric ceaca; MT, malphigian tubule; HG, hindgut. Images in the lower panel show that the expression of PTP52F was specifically restricted to cells located in the midgut but not in the hindgut, as revealed by immunofluorescence staining with anti-PTP52F antibody. Bar, 20 μm.

we ablated endogenous PTP52F from the whole body of flies using the Tub-Gal4 driver and then examined the phenotype. The RNAi transgenic flies developed throughout embryogenesis up to the larval stage, although the speed was significantly slower than WT flies (data not shown). Interestingly, knockdown of PTP52F led to death of organisms during the post pupal stage (Fig. 6A). We observed a high percentage of pupal death, which was shown as the typical pharate adult phenotype (53%) due to eclosion failure at the pupal cage (Fig. 6A). A small fraction of flies died as early pupa (17%), presumably also caused by eclosion failure (Fig. 6B). Some flies (30%) survived for a little longer beyond the pupal stage, although they eventually died either during eclosion or soon after eclosion (Fig. 6B). Since PTP52F is highly enriched in the midgut during the larva–pupa transition (Fig. 5) and the midgut undergoes extensive metamorphic changes during this stage, we also checked whether PTP52F knockdown affects the developmental process of the midgut. As shown in Fig. 6C we noticed a significant delay of midgut degradation in PTP52F RNAi transgenic flies, whereas the midgut of WT flies became much shorter at 4 h after the pupal formation stage. Taken together, these results demonstrate that PTP52F plays an essential role in the control of key steps that guide metamorphosis and eclosion and it must be expressed properly during the larva–pupa transition.

A ***Tubulin-Gal4*>PTP52F-KD**

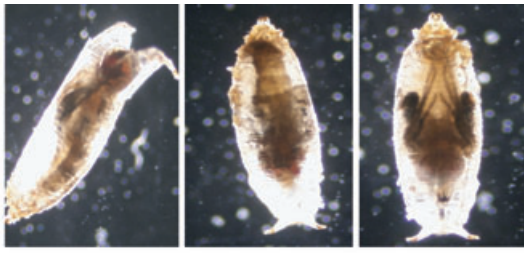

B Analysis of lethality in *Tubulin-Gal4*>PTP52F-KD (n = 200)

Stage	Percentage
Early Pupa	17
Pharate adult	53
Die during eclosion	17
Eclose and die	13
Total	100

C **WT** ***Tubulin-Gal4*>PTP52F-KD**

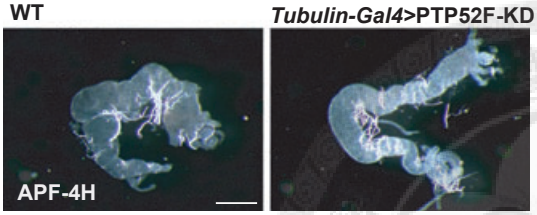

Fig. 6. Ablation of endogenous PTP52F via RNAi led to pupal lethality. (A) The pharate adult phenotype was observed when endogenous PTP52F expression was knocked down by the *Tubulin-Gal4* driver. (B) The table summarizes the lethal phase analysis of PTP52F knockdown flies. Note that over 50% of flies died as pharate adults. Most flies developed until the pupal stage but then died due to eclosion failure. Only a small fraction of flies (13%) died upon completion of eclosion. (C) The images of midgut tissues isolated from both WT and PTP52F knockdown (KD) flies at 4 h after pupal formation (4 h-APF) were captured for a morphological comparison. Note that the metamorphosis of PTP52F-KD flies was significantly delayed as demonstrated by the much longer gut tissue compared with the WT flies. Bar, 1 mm.

Discussion

Data accumulated so far have suggested that the involvement of *Drosophila* R-PTPs is mostly in neural-specific functions [27,38,41]. Essentially nothing was known about the functions for *Drosophila* R-PTPs outside the nervous system until a very recent finding that demonstrated the role of PTP4E and PTP10D in the determination of tracheal tube geometries in embryos [42]. However, it must be noticed that, no matter what the origin of the cell type or what signaling pathway has been discussed so far, the functional role of R-PTP was only shown in *Drosophila* embryos due to the lethality of R-PTP mutant flies during embryonic development. In the current study, PTP52F was found by data mining to be specifically enriched in the midgut during the larva–pupa transition, a finding we confirmed through genetic manipulation combined with immunoblotting and immunofluorescence approaches. Thus, we were able to show for the first time that an endogenous R-PTP protein is highly expressed outside the nervous and tracheal systems at a developmental stage other than embryos.

To date, our understanding of PTP52F in the regulation of signal transduction is limited, largely due to the lack of knowledge about substrates and signaling pathways regulated by this phosphatase. A recent study showed that Tartan, a transmembrane protein, is a candidate substrate of PTP52F [41]. Genetic experiments further illustrate that PTP52F and Tartan act synergistically in pathways of motor axon guidance in embryos [41]. Tartan was also detected in tracheal tissue [43]. However, nothing is known about the distribution or potential functions of Tartan in the midgut of larva and pupa. Therefore, it is difficult to predict whether the phenotype of pharate adult lethality shown in the PTP52F knockdown flies (Fig. 6) was influenced by the deregulation of Tartan or other yet-to-be-identified substrates of PTP52F. Further investigations are required to delineate the molecular basis for PTP52F-mediated regulation of signaling pathways in the midgut during the larva–pupa transition. Nonetheless, it is interesting to point out that the pharate adult phenotype revealed by the ablation of PTP52F has also been reported in some mutants of ecdysone response genes [40,44], including ecdysone receptor (EcR) [45], a key mediator of metamorphosis during the transformation from larva to pupa. The similarity of the phenotype suggests a possibility that PTP52F may participate in ecdysone-mediated signal transduction. Indeed our preliminary data support a genetic interaction between EcR and PTP52F. Using the eye phenotype as a readout, we found that overexpression of EcR B1 form driven by *GMR-Gal4* led to the severe loss of hexagonal ommatidia (Fig. S3), whereas only mild disruption of the ommatidia arrangement was observed in PTP52F RNAi lines (Fig. S3). Interestingly, the eye phenotype revealed in EcR overexpressed flies could be rescued through the knockdown of PTP52F (Fig. S3), suggesting a possible synergistic interaction between these gene products in a signaling pathway. Based on these observations, we hypothesized that *Ptp52F* might be a downstream gene transcriptionally regulated by EcR. As a typical steroid hormone receptor, EcR recognizes specific consensus motifs on the promoter region of effector genes [46,47]. We therefore analyzed the 2 kb region upstream of the first exon of the *Ptp52F* gene to search for potential ecdysone response elements using the

software NUBISCAN-2.0 (http://www.nubiscan.unibas.ch/), which is an *in silico* tool that helps predict nuclear receptor binding sites. Based on the analysis, two possible ecdysone response elements with high scores were identified (Fig. S4A). Importantly, the sequences of these elements are similar to the consensus motif shown in the known EcR-regulated genes (Fig. S4B). Together these results suggest that *Ptp52F* may be a downstream gene of ecdysone action.

The latest version of computational and bioinformatics analysis defined PTP52F as an unclassified member in the PTP super family without a clear ortholog in humans [26]. However, based on the sequence of full-length PTP52F clones obtained by us (Fig. 4A) and in an earlier report by Zinn's group [26,38], we propose that the classification of *Drosophila* R-PTPs be revised. Apparently PTP52F contains only one catalytic domain in the intracellular region instead of two tandem putative phosphatase domains, as suggested previously [38]. The overall layout of PTP52F architecture composed of multiple fibronectin repeats, a single transmembrane segment plus a single phosphatase domain (Fig. 4A) reclassifies this phosphatase as a member belonging to the subtype R3, together with PTP4E and PTP10D in the *Drosophila* PTP family (Fig. 7A). Thus, the earlier study, which defined PTP52F as an unclassified phosphatase, should be modified. As shown in Fig. 7A, there are three *Drosophila* R-PTPs and six human R-PTPs in the subtype R3. Obviously, it is difficult to classify the ortholog pair merely based on the sequence alignment. Other important criteria such as the regulatory role in evolutionarily conserved signaling pathways or the tissue-specific expression profile of R-PTPs across species must be taken into consideration. Recently, PTP10D and PTP4E were regarded as the functional orthologs of human density-enriched PTP-1 due to their similar expression in epithelial cells and their shared ability to downregulate receptor tyrosine kinase mediated signaling [42]. Following the same principle of consideration, we propose that PTP52F might be the functional ortholog of human and mouse stomach-associated PTP-1 (SAP-1) (Fig. 7B). Accumulated data clearly show that mammalian SAP-1 is exclusively expressed in gastrointestinal epithelial cells [48], similar to the midgut-enriched expression of PTP52F in flies. Such a specific expression profile of both PTP52F and SAP-1 suggests that they may regulate evolutionarily conserved signaling pathways in the gut tissue.

In conclusion, data shown in the present study suggest that endogenous *Drosophila* R-PTPs act in developmental control outside the nervous and tracheal systems and also beyond the early embryonic stage

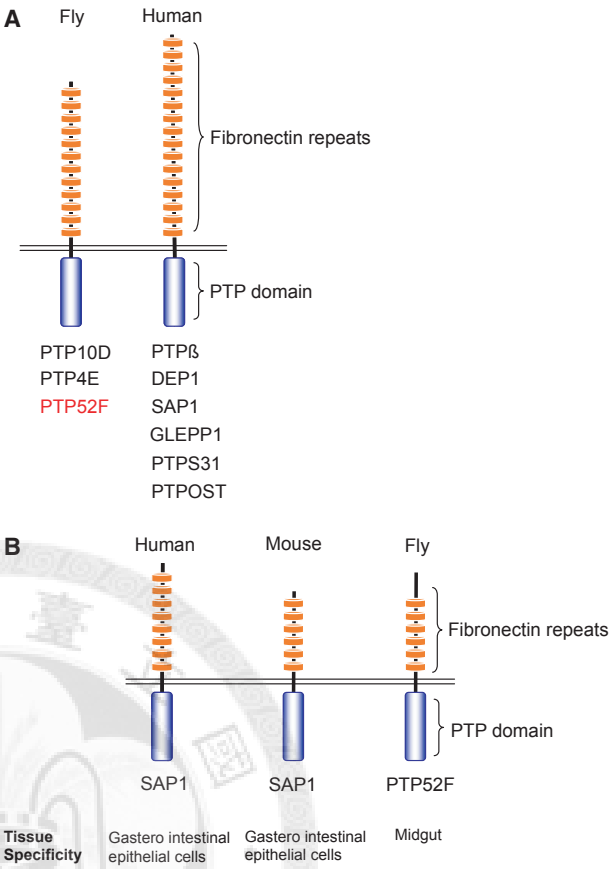

Fig. 7. Reclassification of PTP52F as a member of subtype R3 PTPs. (A) Sequence analysis suggests that PTP52F, together with PTP10D and PTP4E, belongs to the subtype R3 in the PTP superfamily. There are six members of human R-PTPs in this subtype. (B) A proposed model showing that PTP52F might be the functional ortholog of human and mouse SAP-1.

and thus potentially play an indispensable role in the regulation of metamorphosis. Although additional experiments are needed to support this hypothesis, our study has opened a new avenue for understanding the role of *Drosophila* R-PTPs that may mediate signal transduction during development and other biological processes in areas beyond our current knowledge.

Materials and methods

In-gel phosphatase activity assay

An in-gel phosphatase activity assay was performed as described in previous studies [31,32]. The SDS gel was prepared with the ^{32}P-labeled substrate to obtain a gel solution of 1.5×10^6 cpm $(20\ \text{mL})^{-1}$, equivalent to approximately 2 μM pTyr. The fly lysates of specific stages were collected with lysis buffer containing 1% NP-40 and stored at

−80 °C. For each lane, 35 μg of total protein was loaded. After electrophoresis, the gel was processed with various buffers sequentially for fixation, protein denaturation and renaturation. In the final step of renaturation, dithiothreitol (3 mM) was included in the buffer for activation of PTPs in the gel. The dephosphorylation reaction was terminated by staining the gel with Coomassie blue. After destaining, the gel was dried and exposed to X-ray film.

Microarray data mining

For the expression profile of R-PTPome, we utilized the modENCODE Temporal Expression Data from Flybase. The National Human Genome Research Institute's model organism encyclopedia of DNA elements (modENCODE) project provides the biological research community with a comprehensive encyclopedia of genomic functional elements in the model organisms *Caenorhabditis elegans* and *D. melanogaster* [33,34]. The expression levels were analyzed and different levels of expression were recorded. The tissue-specific expressions of R-PTPs were found in FlyAtlas, which is the *Drosophila* gene expression atlas available online [37] (http:http://www.flyatlas.org).

Generation of PTP52F antibody

A fragment of synthetic peptide from the intracellular domain of PTP52F (amino acids 1400–1417) was used as the peptide for antibody production. The epitope was selected based on the scores from an antigenicity prediction program. The rabbit antisera showing the specificity was further purified by affinity chromatography. The purified antiserum was used at a final dilution of 1 : 10 000 for immunoblots and 1 : 1000 for immunofluorescence staining.

Cloning and expression of PTP52F

The cDNA sequence corresponding to full-length PTP52F was obtained by reverse transcription of total mRNA from the pupa formation stage of the fly. The full-length WT and CS mutant were constructed with a hemagglutinin (HA) tag at the C terminus and cloned into pAc5.1A (for protein expression in S2 cells) vector. All cDNAs were examined by sequencing.

Cell culture, transfection, and immunoprecipitation and immunoblotting of PTP52F

Drosophila S2 cells were routinely maintained in Schneider's medium supplemented with 10% fetal bovine serum. For transient transfection with the PTP52F expression vector, S2 cells (5×10^5 cells per 6 cm plate) were incubated with a mixture of plasmid DNA (5 μg per 6 cm plate) and Lipofectamine 2000 (Invitrogen, Carlsbad, CA, USA), according to the manufacturer's instructions. For immunoprecipitation, the cells were lysed in buffer containing 50 mM Tris/HCl (pH 8.0), 1% NP-40, 150 mM NaCl, 2 mM Na_3VO_4 and protease inhibitors. An aliquot of total lysate (1 mg) was precleaned with protein G-Sepharose (GE Healthcare, Uppsala, Sweden) for 30 min at room temperature followed by immunoprecipitation with anti-HA antibody (clone HA-7, Sigma) at 4 °C for 3 h and then by the elution of the beads with 2× sample buffer. For immunoblotting, 35 μg of total protein was loaded with 2× sample buffer for each sample followed by gel running and blocking with primary antibody and secondary antibody. Rabbit anti-PTP52F antiserum and mouse anti-HA IgG (Sigma, St. Louis, MO, USA) was used in this study.

Phosphatase activity assay

Assays were performed as previously described [49] with a few modifications. Briefly, S2 cells overexpressing HA-tagged PTP52F-WT or PTP52F-CS were harvested in lysis buffer. HA-PTP52F was immunoprecipitated from an aliquot of total lysate (1.5 mg) by HA antibody. The immunocomplex was incubated in phosphatase activity assay buffer (50 mM Hepes, pH 7.5, 1% NP-40, 10 mM dithiothreitol and 20 mM *p*-nitrophenyl phosphate). The reaction was carried out at 37 °C for 1 h. After the reaction was terminated by 2 M NaOH, the phosphatase activity in the immunocomplex was measured by spectrometric analysis at 405 nm.

Fly stocks

All flies were maintained at 25 °C unless otherwise indicated. The following strains were obtained from various sources: OreR flies (Bloomington), PTP52F knockdown line (3116, VDRC), *Tubulin-gal4*, *GMR-gal4* (Bloomington). The GAL4-UAS system was used to generate progeny expressing the target gene in a tissue-specific pattern [50].

Immunofluorescence staining

S2 cells were plated and transfected as described above. After 48 h of incubation, the cells were suspended and replated on ConA (0.5 $mg \cdot mL^{-1}$; C2010; Sigma) coated glass coverslips and stained with anti-PTP52F antibody followed by Cy2-conjugated goat anti-rabbit IgG (Jackson ImmunoResearch, West Grove, PA, USA). For F-actin staining, cells were stained with tetramethyl rhodamine isocyanate conjugated phallodin (Jackson ImmunoResearch, West Grove, PA, USA). The samples were visualized using a Zeiss LSM 510 confocal microscope. Late third instar larval midguts were dissected in NaCl/P_i, and were fixed, permeabilized and stained with PTP52F antibody followed by Cy3-conjugated goat anti-mouse IgG (Jackson ImmunoResearch, West Grove, PA, USA) according to the protocol

described in a previous study [51]. The samples were visualized using a Zeiss LSM 510 confocal microscope.

References

1 Lemmon MA & Schlessinger J (2010) Cell signaling by receptor tyrosine kinases. *Cell* **141**, 1117–1134.

2 Tonks NK (2005) Redox redux: revisiting PTPs and the control of cell signaling. *Cell* **121**, 667–670.

3 Lahiry P, Torkamani A, Schork NJ & Hegele RA (2010) Kinase mutations in human disease: interpreting genotype–phenotype relationships. *Nat Rev Genet* **11**, 60–74.

4 Rikova K, Guo A, Zeng Q, Possemato A, Yu J, Haack H, Nardone J, Lee K, Reeves C, Li Y *et al.* (2007) Global survey of phosphotyrosine signaling identifies oncogenic kinases in lung cancer. *Cell* **131**, 1190–1203.

5 Flint AJ, Tiganis T, Barford D & Tonks NK (1997) Development of 'substrate-trapping' mutants to identify physiological substrates of protein tyrosine phosphatases. *Proc Natl Acad Sci USA* **94**, 1680–1685.

6 Elchebly M, Payette P, Michaliszyn E, Cromlish W, Collins S, Loy AL, Normandin D, Cheng A, Himms-Hagen J, Chan CC *et al.* (1999) Increased insulin sensitivity and obesity resistance in mice lacking the protein tyrosine phosphatase-1B gene. *Science* **283**, 1544–1548.

7 Klaman LD, Boss O, Peroni OD, Kim JK, Martino JL, Zabolotny JM, Moghal N, Lubkin M, Kim YB, Sharpe AH *et al.* (2000) Increased energy expenditure, decreased adiposity, and tissue-specific insulin sensitivity in protein-tyrosine phosphatase 1B-deficient mice. *Mol Cell Biol* **20**, 5479–5489.

8 Cheng A, Uetani N, Simoncic PD, Chaubey VP, Lee-Loy A, McGlade CJ, Kennedy BP & Tremblay ML (2002) Attenuation of leptin action and regulation of obesity by protein tyrosine phosphatase 1B. *Dev Cell* **2**, 497–503.

9 Myers MP, Andersen JN, Cheng A, Tremblay ML, Horvath CM, Parisien JP, Salmeen A, Barford D & Tonks NK (2001) TYK2 and JAK2 are substrates of protein-tyrosine phosphatase 1B. *J Biol Chem* **276**, 47771–47774.

10 Zabolotny JM, Bence-Hanulec KK, Stricker-Krongrad A, Haj F, Wang Y, Minokoshi Y, Kim YB, Elmquist JK, Tartaglia LA, Kahn BB *et al.* (2002) PTP1B regulates leptin signal transduction *in vivo*. *Dev Cell* **2**, 489–495.

11 Julien SG, Dube N, Read M, Penney J, Paquet M, Han Y, Kennedy BP, Muller WJ & Tremblay ML (2007) Protein tyrosine phosphatase 1B deficiency or inhibition delays ErbB2-induced mammary tumorigenesis and protects from lung metastasis. *Nat Genet* **39**, 338–346.

12 Wiede F, Shields BJ, Chew SH, Kyparissoudis K, van Vliet C, Galic S, Tremblay ML, Russell SM, Godfrey DI & Tiganis T (2011) T cell protein tyrosine phosphatase attenuates T cell signaling to maintain tolerance in mice. *J Clin Invest* **121**, 4758–4774.

13 Higashi H, Tsutsumi R, Muto S, Sugiyama T, Azuma T, Asaka M & Hatakeyama M (2002) SHP-2 tyrosine phosphatase as an intracellular target of *Helicobacter pylori* CagA protein. *Science* **295**, 683–686.

14 Tartaglia M, Mehler EL, Goldberg R, Zampino G, Brunner HG, Kremer H, van der Burgt I, Crosby AH, Ion A, Jeffery S *et al.* (2001) Mutations in PTPN11, encoding the protein tyrosine phosphatase SHP-2, cause Noonan syndrome. *Nat Genet* **29**, 465–468.

15 Sun W, Shen YH, Qi DW, Xiang ZH & Zhang Z (2012) Molecular cloning and characterization of Ecdysone oxidase and 3-dehydroecdysone-3alpha-reductase involved in the ecdysone inactivation pathway of silkworm, *Bombyx mori*. *Int J Biol Sci* **8**, 125–138.

16 Stewart RA, Sanda T, Widlund HR, Zhu S, Swanson KD, Hurley AD, Bentires-Alj M, Fisher DE, Kontaridis MI, Look AT *et al.* (2010) Phosphatase-dependent and -independent functions of Shp2 in neural crest cells underlie LEOPARD syndrome pathogenesis. *Dev Cell* **18**, 750–762.

17 Uetani N, Chagnon MJ, Kennedy TE, Iwakura Y & Tremblay ML (2006) Mammalian motoneuron axon targeting requires receptor protein tyrosine phosphatases sigma and delta. *J Neurosci* **26**, 5872–5880.

18 Thompson KM, Uetani N, Manitt C, Elchebly M, Tremblay ML & Kennedy TE (2003) Receptor protein tyrosine phosphatase sigma inhibits axonal regeneration and the rate of axon extension. *Mol Cell Neurosci* **23**, 681–692.

19 Sapieha PS, Duplan L, Uetani N, Joly S, Tremblay ML, Kennedy TE & Di Polo A (2005) Receptor protein tyrosine phosphatase sigma inhibits axon regrowth in the adult injured CNS. *Mol Cell Neurosci* **28**, 625–635.

20 Bartscherer K, Pelte N, Ingelfinger D & Boutros M (2006) Secretion of Wnt ligands requires Evi, a conserved transmembrane protein. *Cell* **125**, 523–533.

21 Muller P, Kuttenkeuler D, Gesellchen V, Zeidler MP & Boutros M (2005) Identification of JAK/STAT signalling components by genome-wide RNA interference. *Nature* **436**, 871–875.

22 Puig O, Marr MT, Ruhf ML & Tjian R (2003) Control of cell number by *Drosophila* FOXO: downstream and feedback regulation of the insulin receptor pathway. *Genes Dev* **17**, 2006–2020.

23 Bier E (2005) *Drosophila*, the golden bug, emerges as a tool for human genetics. *Nat Rev Genet* **6**, 9–23.

24 Kaletta T & Hengartner MO (2006) Finding function in novel targets: *C. elegans* as a model organism. *Nat Rev Drug Disc* **5**, 387–398.

25 Reiter LT, Potocki L, Chien S, Gribskov M & Bier E (2001) A systematic analysis of human disease-associ-

ated gene sequences in *Drosophila melanogaster*. *Genome Res* **11**, 1114–1125.
26 Andersen JN, Del Vecchio RL, Kannan N, Gergel J, Neuwald AF & Tonks NK (2005) Computational analysis of protein tyrosine phosphatases: practical guide to bioinformatics and data resources. *Methods* **35**, 90–114.
27 Desai CJ, Krueger NX, Saito H & Zinn K (1997) Competition and cooperation among receptor tyrosine phosphatases control motoneuron growth cone guidance in *Drosophila*. *Development* **124**, 1941–1952.
28 Johnson KG & Van Vactor D (2003) Receptor protein tyrosine phosphatases in nervous system development. *Physiol Rev* **83**, 1–24.
29 Van Vactor D (1998) Protein tyrosine phosphatases in the developing nervous system. *Curr Opin Cell Biol* **10**, 174–181.
30 Van Vactor D, O'Reilly AM & Neel BG (1998) Genetic analysis of protein tyrosine phosphatases. *Curr Opin Genet Dev* **8**, 112–126.
31 Burridge K & Nelson A (1995) An in-gel assay for protein tyrosine phosphatase activity: detection of widespread distribution in cells and tissues. *Analytic Biochem* **232**, 56–64.
32 Meng TC, Hsu SF & Tonks NK (2005) Development of a modified in-gel assay to identify protein tyrosine phosphatases that are oxidized and inactivated *in vivo*. *Methods* **35**, 28–36.
33 Elsner M & Mak HC (2011) A modENCODE snapshot. *Nat Biotechnol* **29**, 238–240.
34 Graveley BR, Brooks AN, Carlson JW, Duff MO, Landolin JM, Yang L, Artieri CG, van Baren MJ, Boley N, Booth BW *et al*. (2011) The developmental transcriptome of *Drosophila melanogaster*. *Nature* **471**, 473–479.
35 Jeon M, Nguyen H, Bahri S & Zinn K (2008) Redundancy and compensation in axon guidance: genetic analysis of the *Drosophila* Ptp10D/Ptp4E receptor tyrosine phosphatase subfamily. *Neural Dev* **3**, 3.
36 Talbot WS, Swyryd EA & Hogness DS (1993) *Drosophila* tissues with different metamorphic responses to ecdysone express different ecdysone receptor isoforms. *Cell* **73**, 1323–1337.
37 Chintapalli VR, Wang J & Dow JA (2007) Using FlyAtlas to identify better *Drosophila melanogaster* models of human disease. *Nat Genet* **39**, 715–720.
38 Schindelholz B, Knirr M, Warrior R & Zinn K (2001) Regulation of CNS and motor axon guidance in *Drosophila* by the receptor tyrosine phosphatase DPTP52F. *Development* **128**, 4371–4382.
39 Ku HY, Wu CL, Rabinow L, Chen GC & Meng TC (2009) Organization of F-actin via concerted regulation of Kette by PTP61F and dAbl. *Mol Cell Biol* **29**, 3623–3632.
40 Li TR & White KP (2003) Tissue-specific gene expression and ecdysone-regulated genomic networks in *Drosophila*. *Dev Cell* **5**, 59–72.
41 Bugga L, Ratnaparkhi A & Zinn K (2009) The cell surface receptor Tartan is a potential *in vivo* substrate for the receptor tyrosine phosphatase Ptp52F. *Mol Cell Biol* **29**, 3390–3400.
42 Jeon M & Zinn K (2009) Receptor tyrosine phosphatases control tracheal tube geometries through negative regulation of Egfr signaling. *Development* **136**, 3121–3129.
43 Krause C, Wolf C, Hemphala J, Samakovlis C & Schuh R (2006) Distinct functions of the leucine-rich repeat transmembrane proteins capricious and tartan in the *Drosophila* tracheal morphogenesis. *Dev Biol* **296**, 253–264.
44 Broadus J, McCabe JR, Endrizzi B, Thummel CS & Woodard CT (1999) The *Drosophila* beta FTZ-F1 orphan nuclear receptor provides competence for stage-specific responses to the steroid hormone ecdysone. *Mol Cell* **3**, 143–149.
45 Davis MB, Carney GE, Robertson AE & Bender M (2005) Phenotypic analysis of EcR-A mutants suggests that EcR isoforms have unique functions during *Drosophila* development. *Dev Biol* **282**, 385–396.
46 Cakouros D, Daish TJ & Kumar S (2004) Ecdysone receptor directly binds the promoter of the Drosophila caspase dronc, regulating its expression in specific tissues. *J Cell Biol* **165**, 631–640.
47 Cherbas L, Lee K & Cherbas P (1991) Identification of ecdysone response elements by analysis of the Drosophila Eip28/29 gene. *Genes Dev* **5**, 120–131.
48 Matozaki T, Murata Y, Mori M, Kotani T, Okazawa H & Ohnishi H (2010) Expression, localization, and biological function of the R3 subtype of receptor-type protein tyrosine phosphatases in mammals. *Cell Signal* **22**, 1811–1817.
49 Hsu MF & Meng TC (2010) Enhancement of insulin responsiveness by nitric oxide-mediated inactivation of protein-tyrosine phosphatases. *J Biol Chem* **285**, 7919–7928.
50 Elliott DA & Brand AH (2008) The GAL4 system: a versatile system for the expression of genes. *Methods Mol Biol* **420**, 79–95.
51 Yin VP & Thummel CS (2004) A balance between the diap1 death inhibitor and reaper and hid death inducers controls steroid-triggered cell death in *Drosophila*. *Proc Natl Acad Sci USA* **101**, 8022–8027.

Supporting information

The following supplementary material is available:
Fig. S1. Tyrosine phosphatase activity and plasma membrane localization of PTP52F.
Fig. S2. Immunofluorescence staining of salivary gland with PTP52F antibody.
Fig. S3. Genetic interaction between EcR and PTP52F.

Fig. S4. Identification of potential ecdysone response elements in the promoter region of *Ptp52F* gene.

This supplementary material can be found in the online version of this article.

Please note: As a service to our authors and readers, this journal provides supporting information supplied by the authors. Such materials are peer-reviewed and may be reorganized for online delivery, but are not copy-edited or typeset. Technical support issues arising from supporting information (other than missing files) should be addressed to the authors.